# MOLECULAR MECHANISMS OF RESISTANCE OF PANCREATIC DUCTAL ADENOCARCINOMA CELLS TO ONCOLYTIC VESICULAR STOMATITIS VIRUS

by

Sébastien Alexandre Felt

A dissertation submitted to the faculty of
The University of North Carolina at Charlotte
in partial fulfillment of the requirements
for the degree of Doctor of Philosophy in
Biology

Charlotte

2017

Approved by:

_____
Dr. Valery Grdzelishvili

_____
Dr. Didier Dréau

_____
Dr. Ian Marriott

_____
Dr. Christine Richardson

_____
Dr. Jennifer Weller

# ABSTRACT

SÉBASTIEN ALEXANDRE FELT. Molecular mechanisms of resistance of pancreatic ductal adenocarcinoma cells to oncolytic vesicular stomatitis virus. (Under the direction of DR. VALERY Z. GRDZELISHVILI)

Oncolytic virus (OV) therapy is an anticancer therapy using replication-competent viruses selectively infecting, replicating in and killing cancer cells. Human pancreatic ductal adenocarcinoma (PDAC) cell lines are highly heterogeneous in their permissiveness to oncolytic vesicular stomatitis virus (VSV), in part due to differences in antiviral interferon (IFN) signaling. VSV-resistant PDACs were shown to constitutively express high levels of several IFN-stimulated genes (ISGs). This work identified two additional defects in VSV-resistant PDACs, apoptosis (Chapter 2) and cell attachment (Chapter 3). In Chapter 2, we discovered that three cell lines constitutively expressing high levels of several ISGs were also resistant to VSV-mediated apoptosis under most experimental conditions, even when VSV replication was improved by JAK Inhibitor I treatment. Two of these cell lines also poorly activated apoptosis when treated with Fas activating antibody, suggesting a general defect in apoptosis. In Chapter 3, we showed a dramatically weaker attachment of VSV in the most resistant PDAC cell line, HPAF-II. Although sequence analysis of the VSV receptor, low density lipoprotein receptor (LDLR), did not reveal any amino acid substitutions, HPAF-II cells displayed the lowest level of LDLR expression and LDLR activity. Treatment of cells with statins (HMG-CoA reductase inhibitors) strongly increased LDLR expression levels, but did not improve VSV attachment. However, LDLR-independent attachment of VSV to HPAF-II cells was dramatically improved by treating cells with polycations like polybrene or DEAE-dextran. Moreover, we successfully used a novel triple combination treatment to break

the resistance of HPAF-II *in vitro* to VSV by combining VSV with polybrene or DEAE-dextran and ruxolitinib (JAK 1/2 inhibitor), thus simultaneously improving VSV attachment and replication.

# DEDICATION

*To my parents*

*and*

*my wife, Andrea.*

# ACKNOWLEDGEMENTS

This work was made possible by the guidance and support of Dr. Valery Grdzelishvili. Thank you for the opportunity to work in your lab and your mentorship. I would like to thank my committee: Dr. Didier Dréau, Dr. Ian Marriott, Dr. Christine Richardson, and Dr. Jennifer Weller for their important feedback and support. Thank you to the members of the Grdzelishvili lab, Megan Moerdyk-Schauwecker, Dr. Nirav Shah, Dr. Eric Hastie, Dr. Marcela Cataldi and Gaith Droby for their assistance and friendship throughout my graduate career. Thank you to Dr. Pinku Mukherjee and her laboratory for providing materials and expertise in pancreatic cancer. I would like to thank The University of North Carolina at Charlotte Graduate School for the Graduate Assistant Support award for funding my graduate education. Lastly, I would like to acknowledge my parents, wife and friends for the patience and support. Thank you.

TABLE OF CONTENTS

# LIST OF FIGURES

# LIST OF TABLES

# LIST OF ABREVIATIONS

| | |
|---|---|
| ds | double-stranded |
| FACS | fluorescence-activated cell sorting |
| G | glycoprotein |
| GFP | green fluorescent protein |
| HMG-CoA | hydroxymethylglutaryl-CoA |
| IFN | interferon |
| ISG | interferon stimulated gene |
| L | large polymerase |
| LDLR | low density lipoprotein receptor |
| M | matrix protein |
| M51 | deletion of the methionine at position 51 |
| MOI | multiplicity of infection |
| MTT | methylthiazolydiphenyl-tetrazolium |
| MXa/MX1 | MX Dynamin-Like GTPase 1 |
| N | Nucleocapsid protein |
| OAS | 2'-5'-Oligoadenylate Synthetase |
| ORF | open reading frame |
| OV | oncolytic virus |
| PDAC | pancreatic ductal adenocarcinoma |
| P | phosphoprotein |
| PCSK9 | proprotein convertase subtilisin/kexin type 9 |

| | |
|---|---|
| PFU | plaque forming units |
| RdRP | RNA-dependent RNA polymerase |
| RNP | ribonucleoprotein |
| sLDLR | soluble LDLR |
| ss | single-stranded |
| TRAIL | TNF-related apoptosis-inducing ligand |
| VSV | vesicular stomatitis virus |
| WT | wild type |

# CHAPTER 1: INTRODUCTION

Viruses are submicroscopic, obligate intracellular parasites, which consist of a nucleic acid genome packaged in a protein coat. They are very prevalent in the environment and have been shown to infect all life forms (e.g. humans, other vertebrates, invertebrates, plants, fungi and bacteria). Viruses are important disease-causing agents (e.g. AIDS, cervical carcinoma, hemorrhagic fevers). However, viruses are also beneficial to us as studying them has led to numerous discoveries in molecular and cell biology and viruses are also used today as therapeutic agents for vaccines, gene therapy and cancer therapy (Draper and Heeney, 2010; Russell et al., 2012; Verma and Weitzman, 2005).

Many naturally occurring viruses preferentially infect, replicate in and kill cancer cells without causing harm to normal cells. Cancer cells are generally more permissive to viruses due to their defects in type I interferon (IFN)-mediated antiviral responses compared to non-malignant cells (Russell et al., 2012). Viruses can also be engineered to exploit these and other unique cancer-specific features (Naik and Russell, 2009). These naturally occurring and engineered viruses used in cancer therapy have been named oncolytic viruses (OVs). OVs have been of interest in cancer therapy for a long time. In the 19$^{th}$ century, naturally acquired virus infections have been described to cause tumor regression. Later, in the 1950s and 1960s, many viruses were tested but with limited success. This led to many scientists to leave the field. It is the ability of engineering viruses by reverse genetics to improve oncoselectivity and oncotoxicity that revived the

field and in the past 15 years almost every major group of animal viruses has been tested as a potential OV (Hammill et al., 2010; Kelly and Russell, 2007). Numerous preclinical and clinical successes have already been reported (Aghi and Martuza, 2005; Liu TC et al., 2007; Russell et al., 2012). Currently, three OVs are approved for clinical use: herpes simplex virus 1 based T-VEC for melanoma, approved in the U.S. (Orloff, 2016) and later in the European Union (Rehman et al., 2016), enteric cytopathic human orphan virus 7 based RIGVIR for melanoma, approved in Latvia, Georgia and Armenia (Donina et al., 2015), and adenovirus type 5 based Gendicine and Oncorine for head and neck squamous cell carcinoma in China (Garber, 2006).

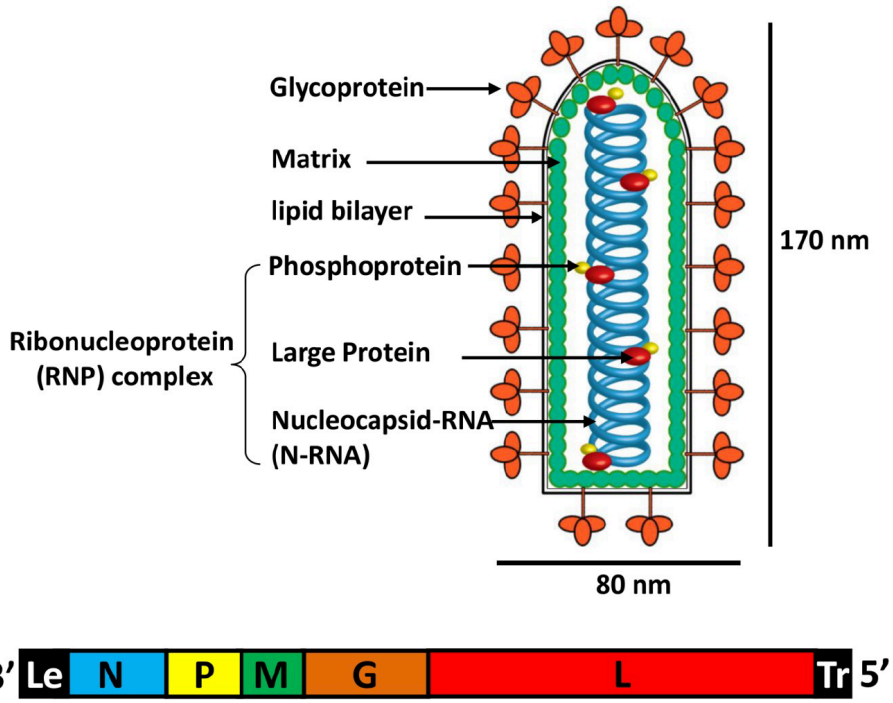


Figure1: VSV virion structure and genome organization. The genome of VSV is encapsidated with the N protein to form a nuclease resistant helical N-RNA complex. The N-RNA complex is tightly associated with the viral RNA-dependent RNA polymerase (RdRp), which consists of the L protein and P protein. Together, this structure is called the viral ribonucleoprotein (RNP) complex. The RNP complex is surrounded by the M protein and the transmembrane G protein is anchored in the viral envelope. Adapted from Jianrong Li and Yu Zhang (2012).

Based on the type of viral genetic material (DNA or RNA) and its replication mechanism, viruses are classified into seven groups according to a system designed by David Baltimore (Baltimore, 1971). The groups are group I (double-stranded (ds) DNA genome), group II (single-stranded (ss) DNA genome), group III (dsRNA genome), group IV (ssRNA positive-strand genome), group V (ssRNA negative-strand genome), group VI (ssRNA positive-strand genome; reverse transcriptase) and group VII (dsDNA; reverse transcriptase) (Baltimore, 1971). This work focuses on one of the promising OVs, vesicular stomatitis virus (VSV). VSV has a non-segmented negative-strand ssRNA genome (Baltimore group V, order *Mononegavirales*, family *Rhabdoviridae*). A small 11-kb VSV genome encodes 5 genes (Fig. 1): nucleocapsid protein (N), phosphoprotein (P), matrix protein (M), glycoprotein (G), and large polymerase (L). The steps of VSV life cycle are (Fig. 2): attachment, endocytosis, uncoating, mRNA transcription, viral protein translation, genome replication, viral assembly, and budding. Natural hosts of VSV include horses, cattle, pigs, and a range of other mammals and their insect vectors (Hastie et al., 2013b; Hastie and Grdzelishvili, 2012). Wild type (WT) VSV infections in livestock are non-lethal and cause fever and blister-like lesions on the oral cavity, feet, and teats. WT VSV infection in humans is generally asymptomatic and is limited to agricultural and laboratory workers (Hastie et al., 2013b; Hastie and Grdzelishvili, 2012). Only one case of WT VSV-mediated encephalitis has been reported in a 3-year-old Panamanian boy (Quiroz E et al., 1988).

VSV is a prototypic member of the order *Mononegavirales*, which includes many important human, animal, and plant pathogens such as rabies virus, Ebola and Marburg viruses, measles, mumps and respiratory syncytial virus. Most of our current

understanding of the biology of *Mononegavirales* derives from studying VSV. There are several advantages of using VSV as a research model for the members of this order including: i) the ability to safely study it in the laboratory; ii) its simple genome structure; iii) its ability to replicate in a wide range of cell types; and iv) available reverse genetic systems (Lyles DS, 2007). Furthermore, VSV has shown promise in many therapeutical applications including oncolytic virotherapy, vaccine development and gene therapy (Bukreyev et al., 2006; Finke and Conzelmann, 2005; von Messling V and Cattaneo, 2004).

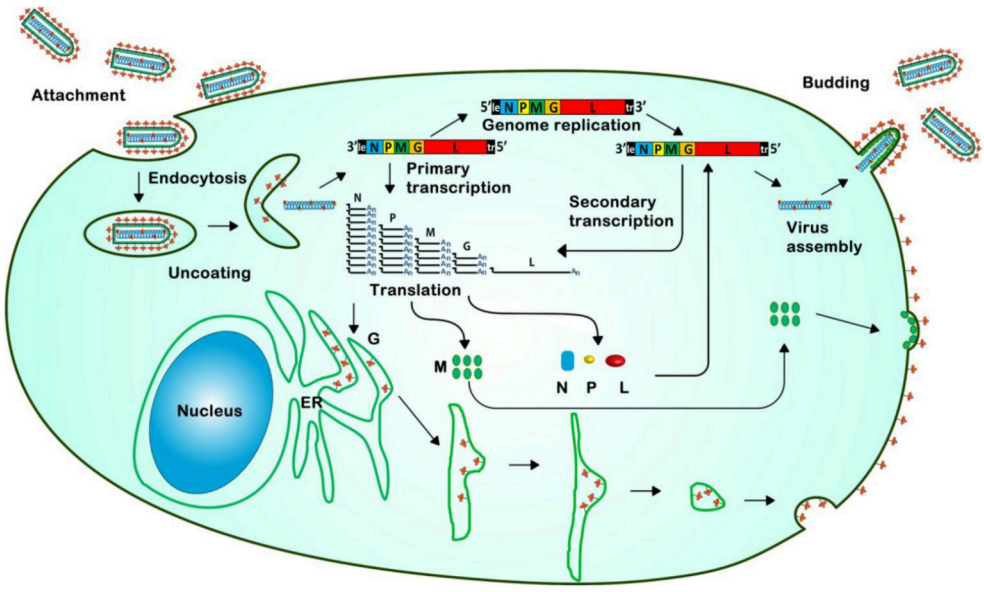


Figure 2: Overview diagram of VSV life cycle. The VSV life cycle starts with attachment and entrance via receptor mediated endocytosis. Decrease in pH triggers uncoating, which leads to the release of the RNP complex into the cytoplasm. Primary transcription then occurs, which involves RdRP transcribing the N-RNA template. The mature mRNAs are then translated to yield viral proteins that are required for viral genome replication. During viral genome replication RdRp synthesizes a full-length complementary antigenome that is then used as a template for synthesis of full length progeny genomes. The latter can then be utilized as templates for secondary transcription, or assembled into infectious particles, which then exit the cell. Adapted from Jianrong Li and Yu Zhang (2012).

The oncoselectivity of VSV is generally based on the type I IFN associated antiviral potential of a target cell. Although VSV cannot distinguish non-malignant ("normal") cells from cancer cells based on their receptor profile or cell cycle, there is a big difference between normal and cancer cells in their abilities to sense and respond to viral infection (Hastie et al., 2013b). When normal cells are infected with VSV, viral infection is sensed by normal cells and production of type I IFNs is triggered to impede viral replication and spread via the induction of antiviral state in the infected cells as well as the non-infected tissue surrounding the IFN-producing cells. In contrast to normal cells, it is observed that a majority of tumors have defective or inhibited type I IFN signaling (Barber, 2004; Lichty BD et al., 2004; Stojdl DF et al., 2003; Stojdl et al., 2000), likely because many IFN responses are anti-proliferative, anti-angiogenic, and pro-apoptotic (Wang et al., 2011). As VSV is highly sensitive to type I IFN responses, it preferentially replicates in cancer cells. The oncoselectivity of WT VSV is not sufficient, as it is able to inhibit type I IFN signaling through one of the functions of the VSV M protein, which localizes to the nuclear envelope and inhibits nucleocytoplasmic trafficking of cellular mRNAs, thus impeding antiviral gene expression not only in cancer, but also normal cells (Petersen et al., 2000). As a result, WT VSV exhibits unacceptable toxicity, most notably neurotoxicity (Hastie et al., 2013b). Thus, an intranasal administration of VSV in rodents can result in fatal infection of the CNS (Clarke DK, 2007), and in non-human primates an intrathalamic administration results in severe neurological disease (Johnson JE et al., 2007). To address this safety issue, various recombinant VSVs have been generated with a dramatically improved safety and oncoselectivity profile (Hastie and Grdzelishvili, 2012). VSV recombinants have been shown in several studies *in vitro* and *in vivo* to be

promising OV agents against a variety of cancers (Hastie and Grdzelishvili, 2012). A recent study tested a VSV recombinant, VSV-IFNβ, on rhesus macaques via intrahepatic injection and no neurological signs were observed at any time point (Johnson JE et al., 2007). As a result, VSV-IFNβ is currently in a phase I clinical trial against refractory solid tumors (ClinicalTrials.gov Identifier: NCT02923466).

Several factors make VSV a promising OV for clinical use: a small and easily manipulated genome, cytoplasmic replication without risk of host cell transformation, relative independence of cell cycle, and lack of pre-existing human immunity against VSV (Hastie and Grdzelishvili, 2012). Furthermore, one of the distinctive features of VSV as an OV is its pantropism (Hastie et al., 2013b), with several ubiquitously expressed cell-surface molecules, such as the low-density lipoprotein receptor (LDLR) (Finkelshtein et al., 2013b), phosphatidylserine (Carneiro et al., 2006; Coil and Miller, 2004; Schlegel et al., 1983) and sialoglycolipids (Schloemer and Wagner, 1975) and heparan sulfate (Guibinga et al., 2002) suggested to play a role in VSV attachment to host cells. While such pantropism does not allow VSV to distinguish normal cells from cancer cells based on their differential receptor expression profiles, the relative independence of VSV from one single receptor can be an advantage, allowing VSV-based OVs to target a wide range of tumor types. In contrast, other OVs could be limited by the expression of their receptor, such as the coxsackievirus and adenovirus receptor, required for efficient entry of the widely used adenovirus 5 based OVs (Pearson et al., 1999).

This work focuses mainly on VSV-ΔM51, which is one of the best performing oncolytic VSVs with replacement or deletion of the methionine at amino acid position 51 (M51) of the VSV M protein. The ΔM51 mutation ablates WT M protein's ability to

inhibit cellular antiviral gene expression (Ahmed et al., 2003; Kopecky et al., 2001; Stojdl DF et al., 2003), while still allowing VSV to replicate in and kill cancer cells, as many cancers have defective type I IFN antiviral responses. Importantly, the ΔM51 mutation also strongly inhibits neurotoxicity associated with WT VSV, and VSVs with different ΔM51 mutations have been explored extensively (Bell and McFadden, 2014; Hastie and Grdzelishvili, 2012; Turnbull et al., 2015).

Pancreatic cancer is the fourth leading cause of cancer-related deaths worldwide (Kamisawa et al., 2016) and expected to become the second leading cause of cancer-related death in the U.S. by the year 2030 (Rahib et al., 2014). Pancreatic ductal adenocarcinoma (PDAC) is the most common pancreatic neoplasm, which comprise about 95% of pancreatic cancers (Stathis A and Moore, 2010). Lack of early detection, aggressive local metastases, and limited treatment options means PDAC diagnosis closely mirrors mortality. Surgical removal of tumors is possible in less than 20 percent of patients and current chemo or radiation-based therapies fail to significantly extend life expectancy (Lowery and O'Reilly, 2015). Various OVs have been tested against PDAC *in vitro* and *in vivo* with limited efficacy (Wennier et al., 2011). An understanding of the cellular factors that prevent or allow success is lacking.

Our recent studies demonstrated that VSV-ΔM51 is effective against the majority of human PDAC cell lines, both *in vitro* and *in vivo* (Murphy et al., 2012). However, while VSV-ΔM51 kills a majority of human PDAC cell lines *in vitro*, resistance of some cell lines to this virus needs to be addressed (Moerdyk-Schauwecker et al., 2013; Murphy et al., 2012). Cellular factors that inhibit infection, replication, or oncolysis can lead to resistance against VSV therapy. Our previous studies showed that not only resistant but

many permissive PDAC cell lines are able to mount type I IFN responses, producing type I IFNs and IFN-stimulated genes (ISGs) in response to VSV-ΔM51 infection (Moerdyk-Schauwecker et al., 2013; Murphy et al., 2012). However, only resistant cell lines showed high-level constitutive expression of several ISGs, including MX Dynamin-Like GTPase 1 (MX1) and 2'-5'-Oligoadenylate Synthetase 2 (OAS2) (Cataldi et al., 2015; Hastie et al., 2016; Moerdyk-Schauwecker et al., 2013). We also demonstrated that resistance of PDAC cell lines to VSV-ΔM51 replication can be overcome by combining virus with IFN signaling inhibitors such as JAK Inhibitor I and ruxolitinib (Cataldi et al., 2015; Moerdyk-Schauwecker et al., 2013). In addition, we showed a similar effect for TPCA-1 (Cataldi et al., 2015), which had previously been described as a direct inhibitor of IKK-β (Birrell et al., 2005; Birrell et al., 2006; Podolin et al., 2005). Our study (Cataldi et al., 2015) demonstrated pleiotropy for TPCA-1, which inhibited not only IKK-β (Birrell et al., 2005; Birrell et al., 2006; Podolin et al., 2005), but also JAK1 kinase activity (Cataldi et al., 2015). Taken together, upregulated type I IFN signaling plays a major role in resistance of pancreatic cancer cells to oncolytic viruses.

This dissertation examined whether resistant PDAC cell lines, in addition to inhibiting VSV replication, also inhibit VSV-mediated apoptosis (Chapter 2) and VSV attachment *in vitro* (Chapter 3). To define PDAC cellular factors that impact the success of VSV therapy is critical. This knowledge will further our understanding of basic mechanisms of controlling viral infection, enhance the efficacy of VSV, and broaden the spectrum of PDAC successfully treated. Moreover, these cellular factors may be used as prognostic biomarkers to select patients for VSV-based virotherapy. While this work

focused on VSV and PDAC, it likely defined cellular factors affecting other OVs and tumor systems as well.

# CHAPTER 2: INDUCTION OF APOPTOSIS IN PANCREATIC CANCER CELLS BY VESICULAR STOMATITIS VIRUS

## 2.1 Introduction

Effective oncolytic virus (OV) therapy depends not only on the ability of OVs to infect and replicate in cancer cells, but also to kill them. In our previous publication we have shown that some pancreatic ductal adenocarcinoma (PDAC) cell lines are resistant to vesicular stomatitis virus (VSV)-mediated cell death (Murphy et al., 2012). VSV kills infected cells primarily via induction of apoptosis (Balachandran et al., 2001; Balachandran et al., 2000; Cary et al., 2011; Gadaleta et al., 2005; Gaddy DF and and Lyles, 2005; Gaddy DF, 2007; Kopecky and Lyles, 2003; Kopecky et al., 2001). The specific mechanism of apoptosis in response to VSV infection depends on both virus and cell type, and apoptosis induction has never been studied in any pancreatic cancer cells in response to VSV. Thus, the goals of the first study (Chapter 2) were (1) to investigate the mechanism of apoptosis induction in PDAC cell lines *in vitro* by three different viruses: wild type (WT)-like VSV (VSV-GFP) and VSV attenuated by M dependent and independent mechanisms (VSV-ΔM51-GFP and VSV-P1-GFP respectively); and (2) to examine whether dysregulation of apoptosis, a hallmark of PDACs as well as other cancers (Hamacher et al., 2008; Neesse et al., 2012; Roder et al., 2011), contributes to the resistance of some PDACs to VSV-mediated oncolysis. The use of a VSV recombinant

with the M51 deletion in the M protein (unable to evade type I interferon (IFN) responses), and two VSV recombinants with WT M protein revealed possible links between apoptosis and type I IFN signaling in PDAC cell lines. Moreover, the ability of PDAC cells to undergo apoptosis following non-viral stimuli was also examined. Finally, as apoptosis activation may reduce viral replication (and potentially reduce oncolytic virus efficiency), as has been reported for many viruses (Galluzzi et al., 2008; O'Brien, 1998) including, in some instances, VSV (Chattopadhyay et al., 2011; Desforges et al., 2002; Sharif-Askari et al., 2007), the effect of apoptosis activation on VSV replication in PDAC cells was examined. Revealing mechanisms of VSV-mediated apoptosis in PDAC cells is important for understanding virus-host interactions in cancer cells.

## 2.2 Materials and Methods

### Viruses

VSV-ΔM51-GFP and VSV-p1-GFP viruses were kindly provided by Jack Rose (Yale University), and VSV-GFP virus was kindly provided by Asit Pattnaik (University of Nebraska). All 3 VSV recombinants are based on the same full-length VSV (Indiana serotype) cDNA clone (Lawson et al., 1995), which contains the L gene and the N-terminal 49 residues of the N gene from the Mudd-Summers strain, the remainder of the genome from the San Juan strain (both belonging to the Indiana serotype). VSV-ΔM51-GFP has a deletion of methionine at amino acid position 51 of the M protein and the green fluorescent protein (GFP) ORF inserted at position 5 of the viral genome (Wollmann G et al., 2010). VSV-GFP is similar to VSV-ΔM51-GFP, but has WT M (Das et al., 2006). VSV-p1-GFP also has WT M but GFP is inserted in position 1 (Wollmann G et al., 2010). Viruses were grown in BHK-21. Viral titers were determined by a

standard plaque assay on BHK-21 cells and expressed as plaque forming units (PFU) per ml.

## Cell lines

The human PDAC cell lines used in this study were kindly provided by the following individuals in Fall 2010: David McConkey (M. D. Anderson Cancer Center): CFPAC-1 and Hs766T cells; Randall Kimple (UNC-Chapel Hill): Capan-2 and T3M4 cells; Timothy Wang (Columbia University): AsPC-1 cells; Andrei Ivanov (University of Rochester Medical School): HPAF-II cells; Michael Hollingsworth (University of Nebraska Medical Center): Suit2 cells; Emmanuel Zervos (Tampa General Hospital): HPAC cells; Pinku Mukherjee (University of North Carolina at Charlotte): Capan-1, MIA PaCa-2 and Panc-1 cells. Cells were maintained as previously described (Moerdyk-Schauwecker et al., 2013). After receipt, the human origin of all cell lines was confirmed by partial sequencing of KRAS and actin. As expected, all PDAC cell lines had a mutation in KRAS, as is typical for PDACs (Hastie et al., 2016).

## Drugs

The following drugs were used in this study: recombinant carrier-free human TNF-α (R&D Systems); recombinant human TNF-related apoptosis-inducing ligand (TRAIL) (Millipore); Fas activating antibody (Millipore, clone CH11); caspase-8 inhibitor Z-IETD-FMK (R&D Systems); pan-caspase inhibitor Z-VAD-FMK (R&D Systems) and JAK Inhibitor I (“InSolution”, Calbiochem).

## Western Blot

Cellular lysates and western blots were prepared as previously described (Moerdyk-Schauwecker et al., 2013). Cell lysates were collected at 17 hours (h) post infection (p.i.)

following infection at multiplicity of infection (MOI) 15 (based on BHK-21 titer). Due to a limited amount of total protein isolated from T3M4 and HPAC cells, the following exceptions were made: for PKR T3M4 sample, no protein was loaded for uninfected T3M4 cells; for caspase 3 and FADD in HPAC cells 15 µg (half the amount) was loaded. The following primary antibodies were used in TBS-T with 5% BSA or milk and 0.02% sodium azide: 1:10,000 rabbit polyclonal anti-VSV antibodies (raised against VSV virion proteins), 1:1000 anti-MxA (clone 631-645) antibodies from Sigma, and the following antibodies from Cell Signaling Technology (1:1000 or 1:500): caspase 3, caspase 8 (clone 1C12), caspase 9, Bak, Bax (clone D2E11), BID, Bcl-2 (clone 50E3), Bcl-xL (clone 54H6), Daxx (clone 25C12), FADD, Fas (clone 4C3), Mcl-1 (clone D35A5). The following horseradish peroxidase-conjugated secondary antibodies were used: 1:2000 goat anti-mouse and 1:2000 goat anti-rabbit (Jackson-ImmunoResearch). The Amersham ECL Western Blotting Detection Kit (GE Healthcare) or Pierce SuperSignal West Pico Detection Kit (Thermo Scientific) was used for detection. Membranes were (Moyer et al., 1986) Coomassie blue stained to verify sample loading. When JAK Inhibitor I treatment was used, 6-well plates were seeded such that they were approximately 80% confluent at the time of inhibitor treatment. Cells were treated with 2.5 µM JAK Inhibitor I or vehicle (DMSO) only in cell culture media with 5% FBS for 48 h prior to infection (media was removed and replaced with fresh drug/vehicle containing media after the first 24 h). Cells were then mock infected or infected with VSV-ΔM51-GFP in DMEM without FBS at an MOI of 15 (based on BHK-21 titer). Following a 1 h absorption period, the virus containing media was aspirated and replaced with growth media with 5% FBS containing

either 2.5 μM JAK Inhibitor I or vehicle. At 17 h p.i., cells were collected and used to prepare cellular lysates for western blotting as described above.

Cell based apoptosis detection

For detection of apoptosis induction following virus infection, cells were seeded in 96-well plates such that they were approximately 80% confluent at the time of treatment. Cells were then mock- or virus-infected at an MOI of 15 (based on BHK-21 titer). Following a 1 h absorption period, the virus containing media was aspirated and replaced with growth media containing 5% FBS. At 24 h p.i., apoptosis activation was assessed using the Caspase Glow 3/7 assay (Promega) in accordance with manufacturer instructions. When inhibitors of apoptosis were used, cells were pretreated with 100 μM caspase-8 inhibitor Z-IETD-FMK, 100 μM pan-caspase inhibitor Z-VAD-FMK or vehicle only (DMSO diluted in PBS) in growth media for 1 h prior to infection. Cells were then mock infected or infected with VSV-ΔM51-GFP at an MOI of 15 (based on BHK-21 titer), or treated with 1μg/ml Fas activating antibody, 1μg/ml TRAIL, or 25ng/ml TNF-α in the continued presence of either inhibitor or vehicle. Following a 1 h absorption period, the virus containing media was aspirated and replaced with growth media with 5% FBS (experiments using only virus) or no FBS (experiments also utilizing other drugs) containing either inhibitor or vehicle. At 17 h p.i., apoptosis activation was assessed using the Cleaved Caspase-3 In-Cell ELISA (Thermo Scientific), in accordance with manufacturer instructions. Alternatively, cells were infected at a cell line specific MOI of 2 to ensure one-step growth kinetics, and then treated with inhibitors of apoptosis as above. At the indicated time points, virus replication was monitored by measuring virus-directed GFP fluorescence in live cells [CytoFluor Series 4000 (Perseptive

Biosystems), with excitation filter of 485/20 nm, emission filter of 530/25 nm and gain=50] and by collecting virus containing media for titration on BHK-21 cells.

### Statistical analysis

All statistical analyses were performed using GraphPad Prism, version 5.03 for Windows (GraphPad Software, San Diego, California). Caspase 3/7 activity and caspase 3 cleavage within a cell line were analyzed by one-way ANOVA with Bonferroni post-test for comparison to the control. Virus driven GFP expression and virus replication following caspase inhibitor treatment was analyzed by repeated measures two-way ANOVA with Bonferroni post-test, following log transformation of replication values to normalize data.

## 2.3 Results

### Human PDAC cells are highly heterogeneous in their abilities to activate apoptosis following VSV infection

Effective OV therapy is dependent on the ability of a replication-competent virus to kill infected cancer cells. Although VSV mediated apoptosis was studied in other systems (Balachandran et al., 2001; Balachandran et al., 2000; Cary et al., 2011; Gadaleta et al., 2005; Gaddy DF and and Lyles, 2005; Gaddy DF, 2007; Sharif-Askari et al., 2007), the mechanism of apoptosis induction by VSV in pancreatic cancer cells has never been examined.

Our major focus is the commonly used VSV recombinant with the ΔM51 mutation in the M gene (Brown et al., 2009; Ebert O et al., 2005; Stojdl DF et al., 2003; Wollmann G et al., 2010). The recombinant VSV-ΔM51-GFP used in this study also contains the GFP ORF at position 5 of the viral genome (between G and L) (Fig. 3), which only marginally affects VSV replication, but allows for monitoring of VSV infection, replication, and

spread, based on virus-driven GFP expression (Wollmann G et al., 2010). Several experiments also utilized two VSV recombinants encoding the WT M gene: VSV-GFP and VSV-p1-GFP (Fig. 3). VSV-GFP has the same GFP insertion as VSV-ΔM51-GFP but WT M gene, allowing study of the role of M protein in apoptosis induction. VSV-p1-GFP, also has the WT M gene, but insertion of the GFP ORF at position 1 of the VSV genome results in slower viral replication kinetics (Ramsburg et al., 2005; Wollmann G et al., 2010), allowing for examination of the role of M protein independent virus attenuation in apoptosis induction(Ramsburg et al., 2005; Wollmann G et al., 2010).

To examine the ability of VSV recombinants to induce apoptosis in PDAC cells, a panel of 10 clinically relevant human PDAC cell lines was used (Table 1). These cells have been characterized in our previous studies for their permissiveness to VSV as well as their type I IFN signaling status (Moerdyk-Schauwecker et al., 2013; Murphy et al., 2012) (summarized in Table 1). Importantly, two of these PDAC cell lines (MIA PaCa-2 and Capan-1, indicated in all figures using green font) are highly permissive to VSV and defective in antiviral signaling in response to VSV infection; four cell lines (Capan-2, AsPC-1, Suit2, and T3M4, black font) are permissive to VSV but have VSV-inducible IFN signaling; two cell lines (CFPAC-1 and HPAC, blue font) are moderately permissive to VSV (resistant only at low MOIs) and have VSV-inducible IFN signaling and constitutive expression of MxA and OAS; and two cell lines (HPAF-II and Hs766T, red font) are highly resistant to VSV (at all tested MOIs) and have VSV-inducible IFN signaling and constitutive expression of MxA and OAS.

Cells were mock-treated or infected at an MOI of 15 (based on virus titration on BHK-21 cells) with VSV-ΔM51-GFP, VSV-p1-GFP or VSV-GFP. Protein was isolated

at 17 h p.i. and western blotting performed to examine VSV replication, IFN-stimulated gene (ISG) expression and the presence or absence of cleaved caspases and other apoptosis related factors. Figure 4 outlines the different apoptotic pathways PDAC cell lines can undergo once infected and important proteins that regulate them.

In agreement with our previous studies (Moerdyk-Schauwecker et al., 2013; Murphy et al., 2012), most cell lines supported good VSV replication (Fig. 5A), with the exception of Hs766T and HPAF-II which are resistant to VSV even at high MOI infection. Also, in agreement with our previous study (Moerdyk-Schauwecker et al., 2013), CFPAC-1, HPAC, HPAF-II and Hs766T constitutively expressed MxA, while VSV-induced expression of this ISG was observed in most other PDACs. Although basal levels of another ISG, PKR, did not differ in most cell lines [as previously shown (Moerdyk-Schauwecker et al., 2013)], PKR protein levels were increased following VSV infection in most cell lines with VSV-inducible type IFN signaling.

In most PDAC cell lines, all 3 VSV recombinants induced caspase 3 cleavage following infection (Fig. 5B; cleaved products appear as a double band at p17/p19). However, all 3 viruses induced similar (and the highest) levels of caspase 3 cleavage only in Capan1 and MIA PaCa-2. Both cell lines are unable to induce Type I IFN responses to VSV (Moerdyk-Schauwecker et al., 2013; Murphy et al., 2012). In all cell lines with VSV-inducible Type I IFN responses, despite similar replication levels for the 3 tested VSVs, VSV-ΔM51-GFP induced more caspase 3 cleavage. This indicates a positive role for the ΔM51 mutation, and therefore host responses, in apoptosis induction, and is unlikely to be simply a result of virus attenuation as VSV-p1-GFP induced caspase cleavage similarly to VSV-GFP. In agreement with their general resistance to VSV

infection and replication (Moerdyk-Schauwecker et al., 2013; Murphy et al., 2012), Hs766T and HPAF-II showed the lowest levels of VSV protein accumulation in infected cells (Fig. 5A). However, while Hs766T had no detectable cleaved caspase 3, HPAF-II showed low but easily detectable caspase 3 cleavage in cells infected with VSV-ΔM51-GFP and VSV-GFP (Fig. 5B.). Surprisingly, HPAC cells, while supporting good levels of replication for all 3 tested VSVs, had no detectable cleaved caspase 3. This result shows that VSV replication is likely an important determinant of apoptosis, but it is not sufficient for apoptosis induction in PDAC cells.

The ability of VSV recombinants to induce apoptosis in PDAC cells was also analyzed by measuring the activity of effector caspases 3 and 7 (Fig. 6). Hs766T and HPAC, which showed no detectable cleaved caspase 3 (Fig. 5B), also showed the lowest caspase 3/7 activity (Fig. 6), again indicating a possible block(s) in apoptosis upstream of caspase 3/7. Also consistent with Figure 5B, only 2 PDAC cell lines (Capan-1 and MIA PaCa-2) showed similar caspase 3/7 activity when infected with any of the three VSV recombinants, while all other cell lines showed greater induction of apoptosis by VSV-ΔM51-GFP (Fig. 6).

## Apoptosis activation mechanism depends on both VSV M protein and PDAC cell line

Previous studies in other cell types demonstrated that VSV M51 mutants typically activate apoptosis via the caspase 8 dependent extrinsic pathway (Cary et al., 2011; Gaddy DF and and Lyles, 2005; Gaddy DF, 2007), with the Fas receptor appearing to play a key role (Gaddy DF, 2007). The extrinsic apoptotic pathway can be either type I, where caspase-8 cleavage is sufficient to activate effector caspases, or type II where the signal must be amplified through the intrinsic pathway via caspase-8 cleavage of Bid

(Barnhart et al., 2003; Scaffidi et al., 1998). In contrast to VSV M51 mutants, VSV encoding WT M protein typically activates apoptosis through the caspase 9 dependent intrinsic (mitochondrial) pathway (Balachandran et al., 2001; Balachandran et al., 2000; Gaddy DF and and Lyles, 2005)**.** VSV WT M protein likely plays an important role in apoptosis induction by inhibiting host gene expression (Kopecky and Lyles, 2003; Kopecky et al., 2001). However, the specific mechanism of apoptosis in response to VSV infection depends on both virus and cell type (Balachandran et al., 2001; Balachandran et al., 2000; Cary et al., 2011; Gaddy DF and and Lyles, 2005), and the mechanism of apoptosis induction by VSV has never been studied in PDAC cells.

As seen in Figure 5B for VSV-ΔM51-GFP infected cells, where cleavage of caspase 3 took place, cleavage of both caspase 8 and 9 was also detectable in all PDACs cell lines, except for HPAF-II, indicating that this virus induces both the extrinsic and intrinsic apoptosis pathways in most PDACs. Interestingly, in HPAF-II cells, VSV-ΔM51-GFP induced caspase 9 but not caspase 8 cleavage, suggesting that only the intrinsic pathway was induced.

For VSV-GFP and VSV-p1-GFP, a predominance of caspase 9 cleavage to caspase 8 cleavage was seen in Capan-2, AsPC-1 and HPAF-II compared to other PDACs, suggesting induction of apoptosis primarily through the intrinsic pathway as previously reported for WT M. However, in all other cell lines cleavage of both caspase 8 and caspase 9 was seen even upon infection with VSV expressing WT M (Fig. 5B).

Having demonstrated heterogeneity in the ability of PDAC cell lines to undergo apoptosis depending on both virus and cell, we examined whether expression of major apoptosis regulator(s) could account for these differences. Signaling through the Fas

death receptor has been shown to be required for VSV-M51R induced apoptosis (Gaddy DF, 2007). Interestingly, two PDAC cell lines, Hs766T and HPAF-II, most resistant to VSV replication and displaying no or low apoptosis induction in response to VSV, both showed low levels of Fas receptor (Fig. 5C) compared to most other PDAC cell lines, suggesting that low Fas levels could play a role in resistance of these cell lines to VSV-mediated apoptosis. However, two other PDAC cell lines (Capan-1 and Capan-2), also showed low levels of Fas expression despite the lack of resistance to VSV-mediated apoptosis. Another apoptosis-resistant PDAC cell line, HPAC, showed good levels of Fas receptor. FADD and Daxx have both been shown to play important roles in Fas signaling (Balachandran et al., 2000; Gaddy DF, 2007); however there were no major differences between PDAC cell lines.

Bcl-2 family members have been shown to be altered in PDACs, as well as other cancers, and to have predictive value for prognosis and treatment response to chemotherapy and radiotherapy (Frenzel et al., 2009; Westphal and Kalthoff, 2003). This family is part of the intrinsic pathway (and thus also the type II extrinsic pathway) and contains both pro- and anti-apoptotic members. As shown in Figure 5D, Mcl-1, an anti-apoptotic protein, was consistently expressed in all uninfected cell lines. However, Mcl-1 levels decreased in most VSV-sensitive cell lines in response to infection with one or more VSV recombinants, likely as part of the apoptosis initiation process (Schache et al., 2009). Production of Bcl-2, an anti-apoptotic protein, was highly variable and undetectable in a number of cell lines. Hs766T was the only apoptosis-resistant PDAC cell line where Bcl-2 was detectable, possibly explaining why it is more resistant to VSV mediated apoptosis than other cell lines. However, Capan-1 and MIA PaCa-2 cells, which

efficiently activate apoptosis in response to VSV infection, expressed Bcl-2 at equal or greater levels to Hs766T. The anti-apoptotic protein Bcl-xL was expressed evenly among all cell lines, indicating that this protein is probably not a key player in resistance to VSV induced apoptosis, as were the pro-apoptotic proteins Bak, Bax and Bid. Apoptosis-sensitive PDAC cell lines showed Bid cleavage when infected with VSV-ΔM51-GFP. While a potential biomarker of apoptosis resistance was not identified, it is known that the ratio rather than the absolute quantity of these pro- and anti-apoptotic proteins is important in the regulation of cell death (Wong, 2011). Further studies are needed to determine a role of these apoptotic regulators in the resistance of some PDACs to VSV induced apoptosis.

VSV-ΔM51 induces apoptosis in PDACs via the type II extrinsic pathway.

The major focus of this study was VSV-ΔM51-GFP. Therefore, the mechanism of apoptosis induction during VSV-ΔM51-GFP infection was studied in more detail. As shown in Figure 5B, where cleavage of caspase 3 took place, cleavage of both caspase 8 and 9 was also detectable in all VSV-ΔM51-GFP infected cells (except for HPAF-II). Cleavage of both caspases 8 and 9 can result from either activation of the type II extrinsic pathway (where caspase 8 is essential for the activation of caspases 9 and 3), independent activation of intrinsic and extrinsic pathways, or death receptor-independent activation of caspase 8 as part of a positive feedback loop following cleavage of caspase 3 after initial activation of the intrinsic pathway (Liu et al., 2011). As VSVs with M51 mutations frequently induce apoptosis via the extrinsic pathway (Gaddy DF and and Lyles, 2005; Gaddy DF, 2007) and pancreatic cells have been shown to utilize the type II extrinsic

pathway (Hinz et al., 2000), we hypothesized that VSV-ΔM51-GFP induced apoptosis in PDAC cells via this mechanism.

To test this hypothesis, infections with VSV-ΔM51-GFP at MOI 15 (based on BHK-21 titer) were conducted in the presence of Z-VAD-FMK, a pan-caspase inhibitor, or Z-IETD-FMK, a caspase 8 specific inhibitor. Following treatment, cleavage of caspase 3 was measured by ELISA at 17 h p.i. As shown in Figure 7, most PDAC cell lines showed a strong increase in caspase 3 cleavage following VSV-ΔM51-GFP infection in agreement with the western blot analysis (Fig. 5B) and the caspase activity assay (Fig. 6). The two PDAC cell lines (HPAC and Hs766T), which showed minimal caspase 3 activity and cleavage in the previous assays again showed low levels of cleaved caspase 3. Importantly, treatment with Z-IETD-FMK returned cleaved caspase 3 levels to near baseline in all cell lines, indicating caspase 8 is critical to apoptosis induction following VSV-ΔM51-GFP infection. As caspase 9 cleavage was also seen in all these PDAC cell lines (Fig. 5B), we concluded that apoptosis occurred through the type II extrinsic pathway. This mechanism is also consistent with the detection of cleaved Bid in many PDACs cell lines infected with VSV-ΔM51-GFP (Fig. 5D).

### Role of virus replication levels and type I interferon in apoptosis induction in PDAC cell lines

Under the experimental conditions shown in Figure 8 (MOI 15 infection), VSV replication was severely inhibited in HPAF-II and Hs766T. No (Hs766T) or low (HPAF-II) caspase 3 cleavage (Fig. 5B) could potentially be attributed to very low levels of virus replication in these two cell lines. However, HPAC cells, while supporting good levels of VSV replication, showed no detectable cleaved caspase 3, indicating that good VSV replication levels are not sufficient for apoptosis induction at least in some PDAC cells.

All three cell lines (HPAC, HPAF-II and Hs766T) as well as CFPAC-1 constitutively express some ISGs, including MxA [Fig. 8 and (Moerdyk-Schauwecker et al., 2013)]. Therefore, we conducted an experiment to test the hypothesis that resistance of PDAC cells to VSV-mediated apoptosis is the result of upregulated type I IFN signaling leading to low-level VSV replication and/or expression of one or more anti-apoptotic factors. As controls, we used MIA PaCa-2 cells, which are defective in type I IFN signaling, as well as CFPAC-1 cells, which are similar to HPAC cells in their constitutive expression of ISGs, but, unlike HPAC, undergo apoptosis following VSV infection.

Inhibition of type I IFN signaling and subsequent increase in VSV-ΔM51-GFP replication levels were achieved by treatment of cells with JAK Inh. I as in our previous study (Moerdyk-Schauwecker et al., 2013). Cell lines were mock-infected or infected at MOI 15 (based on BHK-21 titer) with VSV-ΔM51-GFP and protein was isolated at 17 h p.i. MxA protein was downregulated in all treated cell lines, confirming JAK Inh. I treatment was effective. Importantly, although JAK Inh. I treatment increased VSV-ΔM51-GFP replication in PDAC cell lines with constitutive ISG expression, it did not result in increased caspase 3 cleavage (Fig. 8). These results demonstrate that even when viral replication is increased and type I IFN signaling inhibited, HPAC and Hs766T cannot efficiently activate apoptosis. Therefore, there is no clear correlation between VSV-ΔM51-GFP replication levels or type I IFN signaling and apoptosis in these two cell lines. To not miss effects of JAK Inh. I treatment upstream of caspase 3, we looked also for changes in cleavage of caspases 8 and 9 and expression of extrinsic/intrinsic regulators and did not see any major changes (Fig. 8).

Activation of apoptosis by non-viral stimulators.

Since VSV-ΔM51-GFP was unable to effectively induce apoptosis in Hs766T and HPAC and weakly and variably induced apoptosis in HPAF-II, we wanted to know whether these cell lines resist only virus mediated apoptosis or if they have a more general defect in apoptosis. Therefore, we tested if the extrinsic apoptosis pathway could be induced using a virus independent method. Hs766T, HPAC, HPAF-II and MIA PaCa-2 were treated with Fas activating antibody CH11, TNF-α, TRAIL or VSV-ΔM51-GFP and tested for caspase-3 cleavage at 17 h p.i. All stimulators induced caspase 3 cleavage in MIA PaCa-2 but VSV-ΔM51-GFP appeared to do so most effectively (Fig. 9). TNF-α did not induce apoptosis in any of the PDAC cell lines resistant to VSV mediated apoptosis. Fas activating antibody CH11 more strongly induced caspase 3 cleavage in HPAC than in Hs766T and HPAF-II, consistent with Fas receptor levels (Fig. 5C and 8). Finally, consistent with previous data, VSV-ΔM51-GFP did not induce caspase 3 cleavage in HPAC, Hs766T and HPAF-II cells. Together, the data suggest that at least two of the three PDAC cell lines resistant to VSV mediated apoptosis have a more general defect in apoptosis.

Impact of apoptosis on VSV-ΔM51-GFP replication.

While strong inhibition of apoptosis in response to VSV-ΔM51-GFP infection can prevent oncolysis, rapid induction of apoptosis can potentially have an antiviral effect by destroying the infected cell before the virus reaches its maximum replication potential. As this could limit the effectiveness of VSV as an oncolytic virus, we examined the possible effects of apoptosis induction on VSV-ΔM51-GFP replication in PDAC cells. Two cell lines (VSV-permissive MIA PaCa-2 and VSV-resistant HPAF-II) were infected

with VSV-ΔM51-GFP in the presence or absence of Z-VAD-FMK (a pan-caspase inhibitor) or Z-IETD-FMK (a caspase 8 specific inhibitor). Cells were infected at a cell line specific MOI of 2 to ensure one-step growth kinetics, and virus replication was monitored by measuring virus-directed GFP fluorescence in live cells (Fig. 10A) and measuring new particle production by titration of media on BHK-21 cells (Fig. 10B). GFP expression only modestly (although statistically significant at most time points) increased in inhibitor-treated cells (Fig. 10A). However, no statistically significant increase in new particle production was seen in MIA PaCa-2 cells at any time point, and an increase was only seen in HPAF-II at 120 h p.i. (Fig. 10B). The tolerance of VSV replication to apoptosis in MIA PaCa-2 and HPAF-II is most likely due to VSV's relatively fast replication cycle, allowing it to outpace the apoptotic response (Koyama, 1995; Timm and Yin, 2012).

## 2.4 Conclusions

VSV-ΔM51-GFP primarily activated the type II extrinsic pathway in PDACs. Three of the tested cell lines that constitutively expressed high levels of IFN-stimulated genes (HPAF-II, Hs766T and HPAC) were resistant to apoptosis under most experimental conditions, even when VSV replication was restored by JAK Inh. I treatment. Two of these cell lines also poorly activated apoptosis when treated with Fas activating antibody, suggesting a general defect in apoptosis. These results will be further discussed in the dissertation summary (Chapter 4).

2.5 Figures

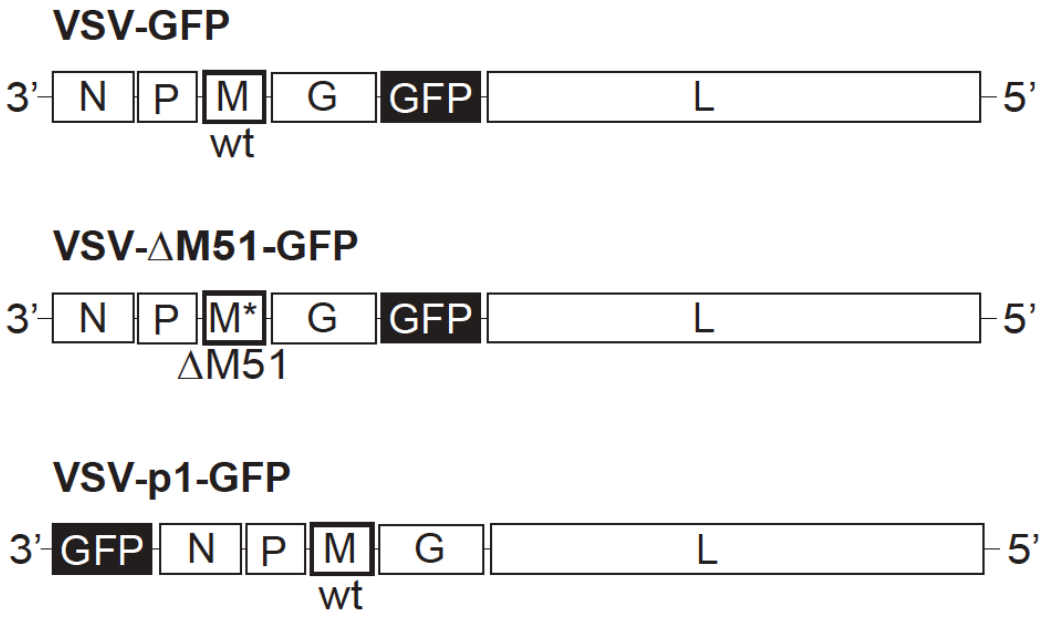


Figure 3: Viruses used in this study. The viruses used in this study were VSV-ΔM51-GFP, VSV-p1-GFP and VSV-GFP. VSV-ΔM51-GFP has a deletion of methionine at amino acid position 51 of the M protein and the green fluorescent protein (GFP) ORF inserted at position 5 of the viral genome. VSV-GFP is similar to VSV-ΔM51-GFP, but has WT M. VSV-p1-GFP also has WT M but GFP is inserted in position 1.

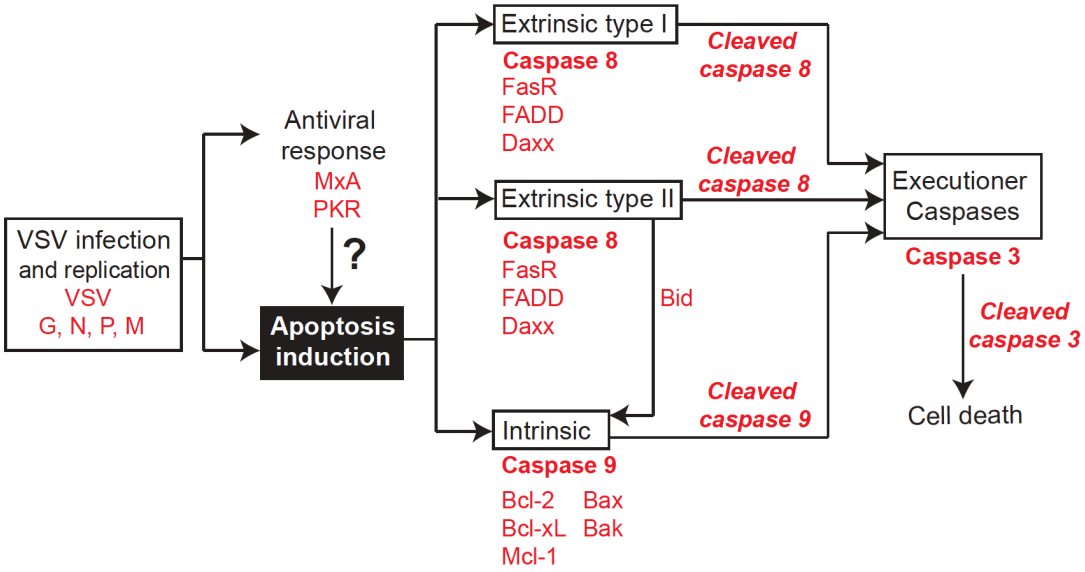


Figure 4: Pathways and proteins studied. Relationship between the apoptotic pathways. All proteins of interest for this study are in red.

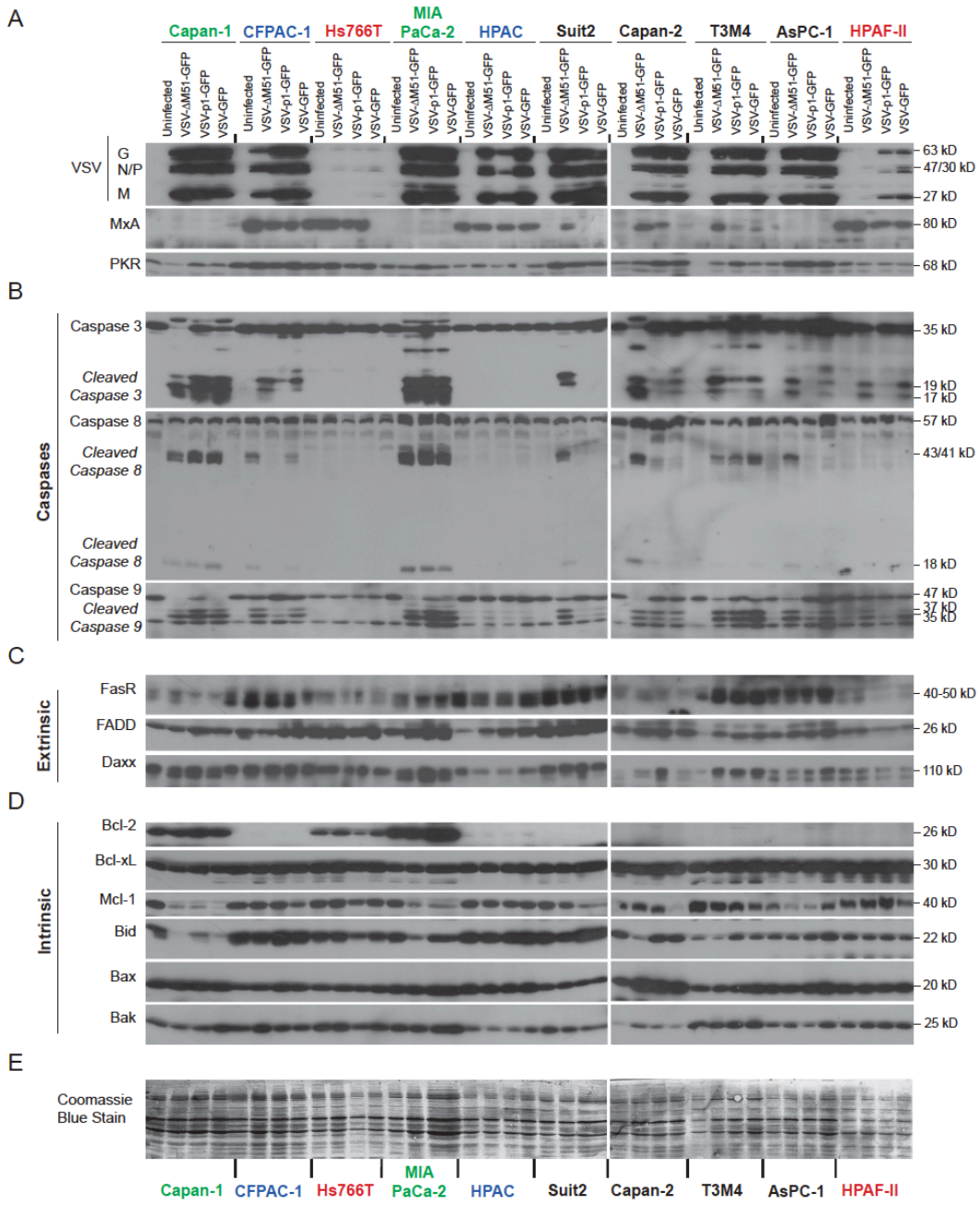


Figure 5: Protein levels of apoptosis related genes in PDAC cells following VSV-ΔM51-GFP infection. Cells were mock-infected or infected with VSV-ΔM51-GFP, VSV-p1-GFP or VSV-GFP at an MOI of 15 (based on BHK-21 titer). At 17 h p.i, cell lysates were prepared and analyzed by western blot for the indicated proteins associated with (A) virus replication and antiviral response, (B) caspase cleavage, (C) the extrinsic apoptosis pathway, (D) the intrinsic apoptosis pathway and (E) total protein staining. Protein (kDa) product sizes are indicated on the right. Due to a limited amount of total protein isolated from T3M4 and HPAC cells, the following exceptions were made: for PKR T3M4 sample, no protein was loaded for uninfected T3M4 cells; for caspase 3 and FADD in HPAC cells 15 µg (half the amount) was loaded.

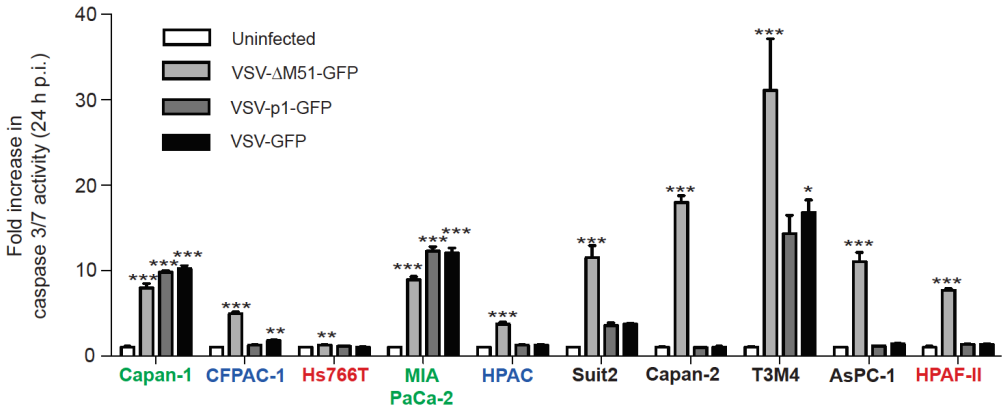


Figure 6: Caspase 3/7 activation in PDAC cells following VSV-ΔM51-GFP infection. Cells were mock- or virus-infected at an MOI of 15 (based on BHK-21 titer). At 24 h p.i., apoptosis activation was assessed using the Caspase Glow 3/7 assay. Caspase 3/7 activation is expressed as fold increase over mock treated, with the mock treated activity indicated as 1. Assay was done in triplicate and data represent the mean ± standard error of mean. Treatments were compared using a 1-way ANOVA followed by the Bonferroni posttest for comparison to the control. *, $p<0.05$; **, $p<0.01$; ***, $p<0.001$.

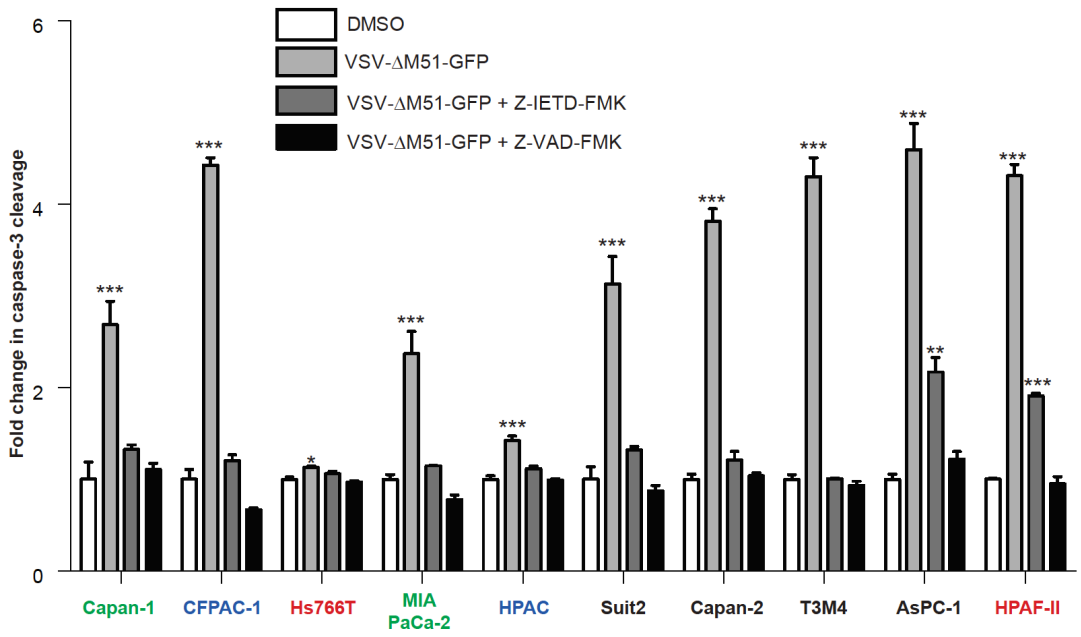


Figure 7: Effect of caspase inhibitors on caspase 3 cleavage. Cells were pretreated with 100 µM caspase-8 inhibitor Z-IETD-FMK, 100 µM general caspase inhibitor Z-VAD-FMK or vehicle only (DMSO) in growth media for 1 h prior to infection. Cells were then mock infected or infected with VSV-ΔM51-GFP at an MOI of 15 PFU/cell (based on BHK-21 titer) in the continued presence of either inhibitor or vehicle. At 17 h p.i., cleaved caspase 3 was analyzed by ELISA. Caspase 3 cleavage is expressed as fold increase over mock treated, with the mock treated level indicated as 1. Assay was done in triplicate and data represent the mean ± standard error of mean. Treatments were compared using a 1-way ANOVA followed by the Bonferroni posttest for comparison to the control. *, $p<0.05$; **, $P<0.01$; ***, $p<0.001$.

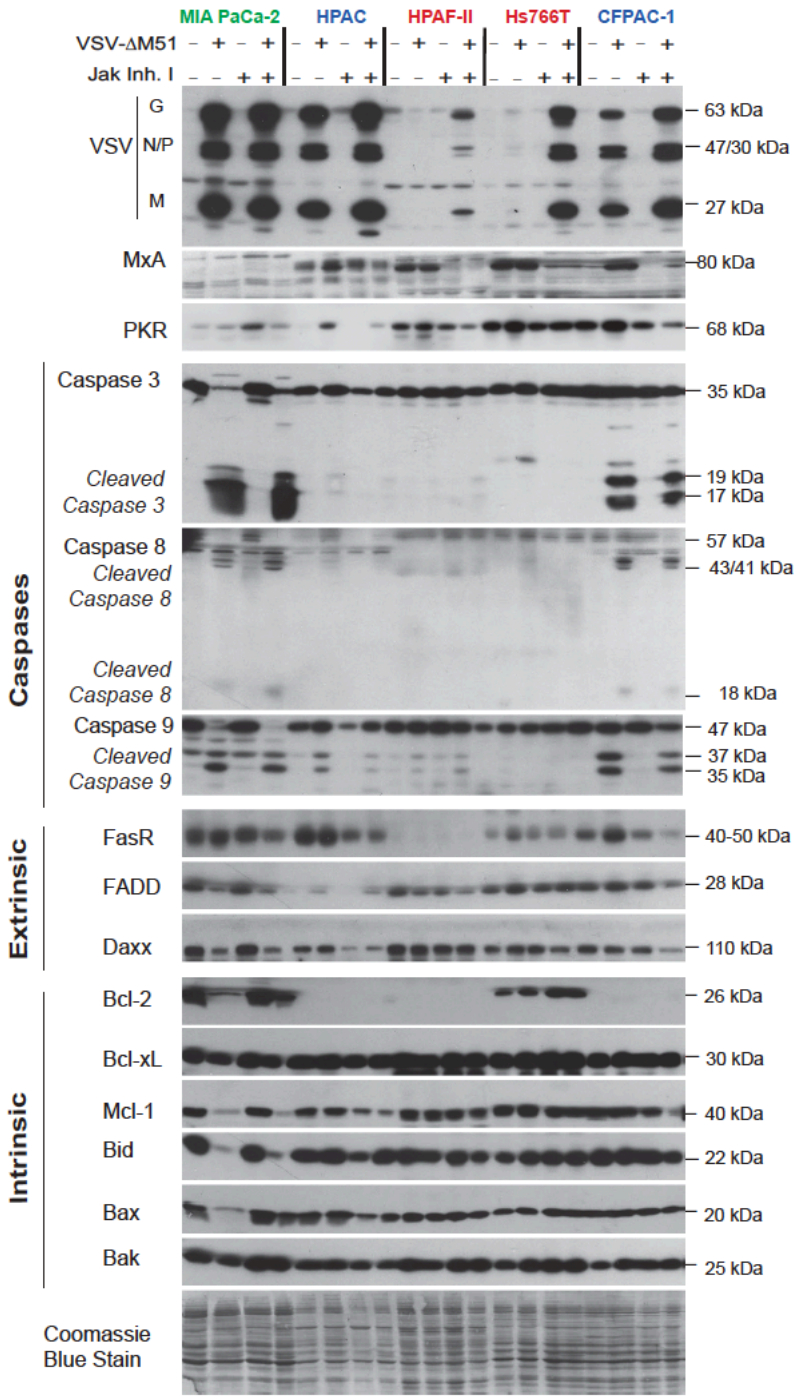


Figure 8: Effect of type I IFN signaling inhibition and increased VSV-ΔM51-GFP replication. Cells were mock (DMSO) treated or treated with 2.5 μM JAK Inh. I for 48 h prior to infection with VSV-ΔM51-GFP at MOI 15 PFU/cell. Cells were harvested at 17 h p.i. and cell lysates were prepared and analyzed by western blot for the indicated proteins. Protein (kDa) product sizes are indicated on the right.

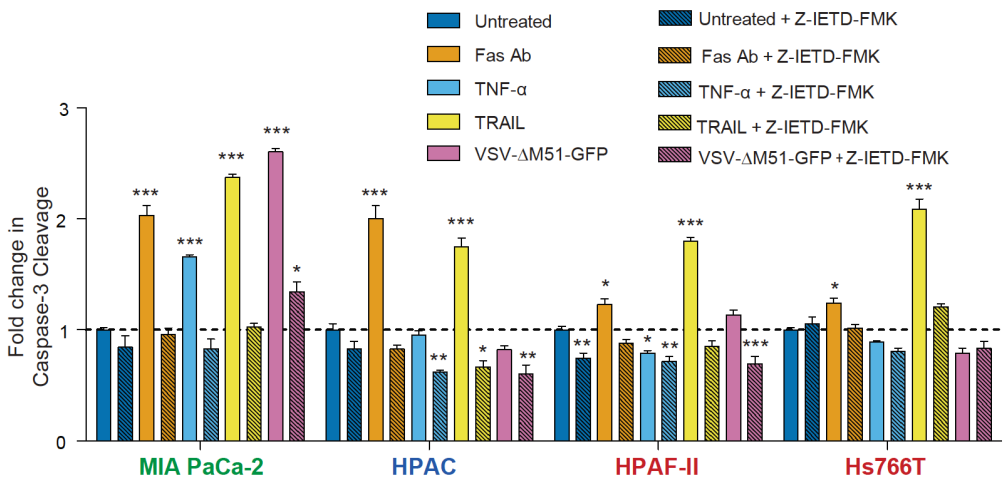


Figure 9: Effect of Fas antibody/TNF-alfa/TRAIL on caspase 3 cleavage. Cells were pretreated with 100 µM caspase-8 inhibitor Z-IETD-FMK or vehicle only (DMSO) in growth media for 1 h prior to treatment. Cells were then mock treated, treated with 1µg/ml Fas activating antibody, 1µg/ml TRAIL, or 25ng/ml TNF-α or infected with VSV-ΔM51-GFP at an MOI of 15 PFU/cell (based on BHK-21 titer) in the continued presence of either inhibitor or vehicle. At 17 h p.i., cleaved caspase 3 was analyzed by ELISA. Caspase 3 cleavage is expressed as fold increase over mock treated, with the mock treated level indicated as 1. Assays were done in triplicate and data represent the mean ± standard error of mean. Treatments were compared using a 1-way ANOVA followed by the Bonferroni posttest for comparison to the control. *, $p<0.05$; **, $p<0.01$; ***, $p<0.001$.

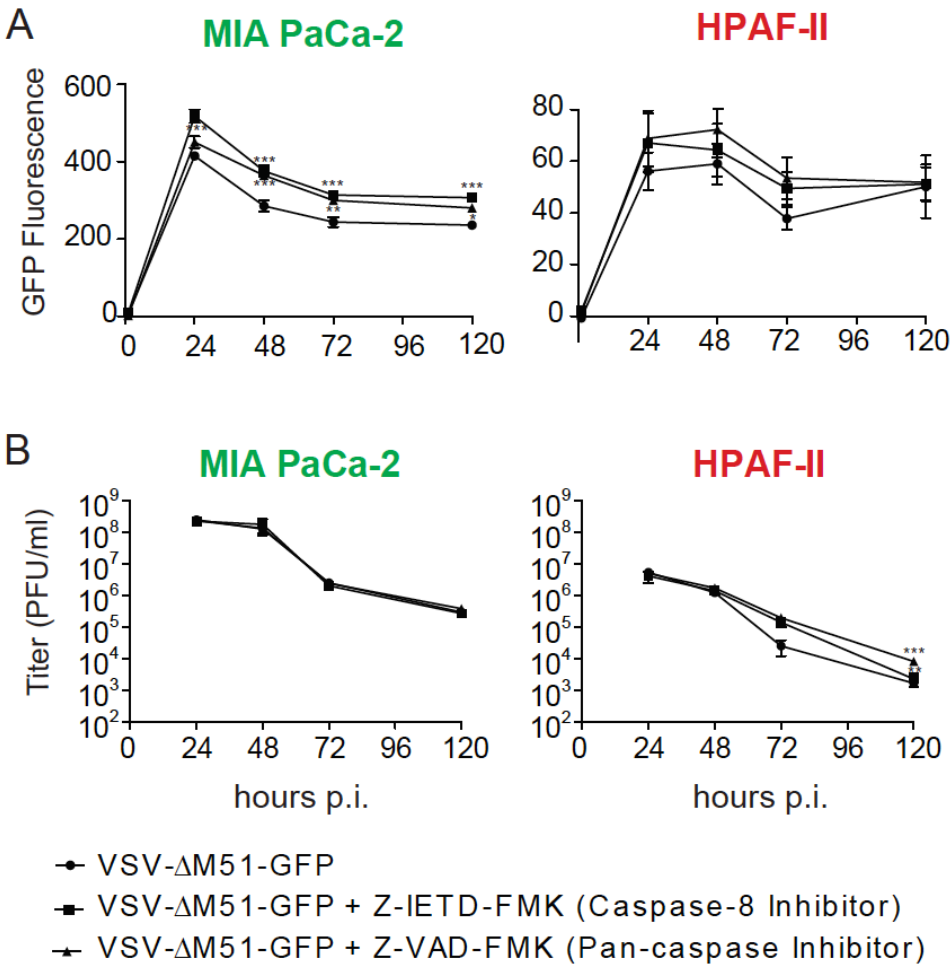


Figure 10: Effect of apoptosis inhibition on VSV-ΔM51-GFP replication. Cells were pretreated with 100 µM caspase-8 inhibitor Z-IETD-FMK, 100 µM general caspase inhibitor Z-VAD-FMK or vehicle only (DMSO diluted in PBS) in growth media for 1 h prior to infection. Cells were then mock infected or infected with VSV-ΔM51-GFP at an MOI of 2 PFU/cell (cell line specific titer) for the study of 1-step replication kinetics based on (A) virus driven GFP expression or (B) infectious particle production (limit of detection=2x102 PFU/ml) as determined at the indicated time points. Assays were performed in triplicate and values represent mean ± standard error of mean. Treatments were compared by two-way ANOVA with Bonferroni posttest for comparison of treatments to control. *, $p<0.05$; **, $p<0.01$; ***, $p<0.001$.

**Table 1**

Relationship between apoptosis induction and IFN status of PDA cells.

| Human cell line | Origin | VSV-induced caspase 3 cleavage | | | VSV-induced caspase 8 cleavage* | | | VSV-induced caspase 9 cleavage | | | ** VSV-induced IFN-β mRNA | ** VSV-induced or constit. IFN-α mRNA | ** Constit. MxA and OAS | ** Resist to VSV-ΔM51 at low MOI | ** Resist to VSV-ΔM51 at high MOI |
|---|---|---|---|---|---|---|---|---|---|---|---|---|---|---|---|
| | | M51 | P1 | WT | M51 | P1 | WT | M51 | P1 | WT | | | | | |
| Capan-1 | liver metastasis | ++ | ++ | ++ | ++ | ++ | ++ | ++ | ++ | ++ | N | N | N | N | N |
| MIA PaCa-2 | primary PDA | ++ | ++ | ++ | ++ | ++ | ++ | ++ | ++ | ++ | N | N | N | N | N |
| Capan-2 | primary PDA | ++ | + | + | ++ | + | + | ++ | ++ | ++ | Y | Y | N | N | N |
| AsPC-1 | ascites | ++ | – | + | ++ | – | – | ++ | + | ++ | Y | Y | N | N | N |
| Suit2 | liver metastasis | ++ | – | – | ++ | – | – | ++ | – | – | Y | Y | N | N | N |
| T3M4 | lymph node metastasis | ++ | + | + | + | + | + | ++ | ++ | ++ | Y | Y | N | N | N |
| CFPAC-1 | primary PDA | ++ | – | + | ++ | – | ++ | ++ | + | ++ | Y | Y | Y | Y | N |
| HPAC | primary PDA | – | – | – | – | – | – | – | – | – | Y | Y | Y | Y | N |
| HPAF-II | primary PDA | + | – | + | – | – | – | + | – | + | Y | Y | Y | Y | Y |
| Hs766T | lymph node metastasis | – | – | – | – | – | – | – | – | – | Y | Y | Y | Y | Y |

"M51" - VSV-ΔM51-GFP; "P1" - VSV-p1-GFP; "WT" - VSV-GFP; "Y" – yes; "N" – no.

– Low/not detectable levels

+ Intermediate levels

++ High levels

* ++ Cleaved Caspase 8 p43/41 and p18 are detected, + Cleaved Caspase 8 p 43/41 only is detected

** Summarized from our previous studies (Moerdyk-Schauwecker et al., 2013; Murphy et al., 2012)

# CHAPTER 3: MULTIPLE MECHANISMS DETERMINE RESISTANCE OF PANCREATIC CANCER CELLS TO ONCOLYTIC VESICULAR STOMATITIS VIRUS

## 3.1 Introduction

Although vesicular stomatitis virus (VSV) is effective against a majority of pancreatic ductal adenocarcinoma (PDAC) cell lines, some PDAC cell lines are highly resistant to VSV, and the mechanisms of the resistance are still unclear. We have previously shown that treating resistant PDAC cell lines with type I interferon inhibitors, such as JAK Inhibitor I (a pan-JAK inhibitor) or ruxolitinib (a specific JAK1/2 inhibitor), significantly improved permissiveness of the cells to VSV (Cataldi et al., 2015; Hastie et al., 2016; Moerdyk-Schauwecker et al., 2013). However, this approach only moderately improved susceptibility of resistant cells to VSV initial infection, and overall VSV replication never reached the level of VSV-permissive PDAC cell lines (Cataldi et al., 2015; Hastie et al., 2016; Moerdyk-Schauwecker et al., 2013). In agreement with this observation, pre-treatment of cells with ruxolitinib (compared to post-treatment only) did not change the kinetics of VSV replication, with a significant increase in VSV replication that could be seen only 48 hours (h) post infection (p.i) even in cells pretreated with ruxolitinib for up to 48 h, suggesting that ruxolitinib did not improve the rate of initial infection but rather facilitated secondary infection via inhibition of antiviral signaling in PDAC cells (Cataldi et al., 2015; Hastie et al., 2016). Together, our previous studies suggest that resistant PDAC cell lines may have an additional block at an early stage of VSV infection that

could not be removed via JAK inhibition. In this study, we examined the role of VSV attachment in resistance of PDAC cells to VSV, as it is the first critical stage for a successful VSV infection. We showed that inefficient VSV attachment can contribute to resistance of PDACs to VSV. Moreover, we successfully used a novel approach to break the multiple mechanisms of resistance of PDAC cells *in vitro* to VSV by combining the virus with polycations and ruxolitinib to simultaneously improve VSV attachment and virus replication.

## 3.2 Materials and Methods

### Viruses and cell lines

The recombinant VSV-ΔM51-eqFP650 (Hastie et al., 2015) or VSV-ΔM51-GFP (Wollmann G et al., 2010) have been described previously. VSV-ΔM51 has a deletion of the methionine at amino acid position 51 of the matrix (M) protein. In addition, VSV-ΔM51-eqFP650 has the near-infrared fluorescent protein open reading frame (ORF) (Hastie et al., 2015) and VSV-ΔM51-GFP has the green fluorescent protein (GFP) ORF (Wollmann G et al., 2010) inserted between the VSV G and L genes. For attachment assay, viruses were ultra-purified exactly as previously described (Moerdyk-Schauwecker et al., 2014). The following human PDAC cell lines were used in this study: HPAF-II (ATCC CRL-1997), Hs766T (ATCC HTB-134), MIA PaCa-2 (ATCC CRL-1420), and Suit2 (Iwamura T et al., 1987). The human origin of all these PDAC cell lines was confirmed by partial sequencing of KRAS and actin. As expected, all PDAC cell lines had a mutation in KRAS, as is typical for PDACs (Cataldi et al., 2015; Hastie et al., 2016). The baby hamster kidney BHK-21 fibroblast cell line (ATCC CCL-10) was used to grow viruses and determine their titers. MIA PaCa-2, Hs766T, and Suit2 cells were

maintained in Dulbecco's modified Eagle's medium (DMEM, Cellgro, 10-013-CV), while HPAF-II and BHK-21 in modified Eagle's medium (MEM, Cellgro, 10-010-CV). All cell growth media were supplemented with 9% fetal bovine serum (FBS, Gibco), 3.4 mM L-glutamine, 900 U/ml penicillin and 900 µg/ml streptomycin (HyClone). MEM was additionally supplemented with 0.3% glucose (w/v). Cells were kept in a 5% $CO_2$ atmosphere at 37°C. For all experiments, PDAC cell lines were passaged no more than 15 times.

VSV attachment assay

VSV-ΔM51-eqFP650 was used for all attachment assays. To assay for VSV attachment to cells in suspension, adherent cells were washed one time with PBS and then treated with PBS with 0.2% EDTA or 0.05% trypsin for 30 minutes (min) to detach them from the surface. DMEM with 10% FBS was then added for trypsin neutralization, and cells then were washed one time with PBS. 400,000 cells in 100 µl DMEM (without FBS) were then incubated for 1 h at 4 °C (the rest of the procedure is done at 4 °C) for VSV attachment. After the incubation, cells were washed 3 times with PBS to remove any unbound virus. Cells were resuspended in PBS with 2% BSA and blocked for 10 min, followed by a 1 h incubation with 1:1000 VSV-G antibody [Kerafast, 8G5F11] and a 30 min incubation with 1:10 Mouse F(ab)2 IgG (H+L) APC-conjugated antibody (R&D, F0101B). Cells were collected using the LSR Fortessa cell analyser (BD Bioscience), and were analyzed using FlowJo software (Treestar). To assay for VSV attachment to the cell monolayer, cells were seeded in a 6-well or 12-well plate such that confluency was at 80% the next day. Media was then removed, and cells were washed one time with PBS. Virus in DMEM (without FBS) then was added, and cells were

incubated on a rocker for 1 h at 4°C. After incubation, wells were washed 3 times with PBS to remove any unbound virus. Protein isolation buffer was added and western blot analysis was performed (as described below).

Protein Isolation and western blot analysis

Cells were seeded in a 6-well or 12-well plate and treated as described above. Media was removed and cells were lysed in non-reducing conditions with lysis buffer containing 0.0625 M Tris-HCl (pH 6.8), 10% glycerol, 2% SDS and 0.02% (w/v) bromophenol blue. We used non-reducing conditions, as reduction of disulfide bridges in the low-density lipoprotein receptor (LDLR) from the medium has been reported to prevent the binding of both LDL and the well-characterized LDLR antibodies (Beisiegel et al., 1982; Nguyen et al., 2006; van Driel et al., 1987). Total protein was separated by electrophoresis on SDS-PAGE gels and electroblotted to polyvinylidene difluoride membranes. Membranes were blocked using 5% non-fat powdered milk in TBS-T [0.5 M NaCl, 20 mM Tris (pH 7.5), 0.1% Tween20]. Membranes were incubated with 1:5000 rabbit polyclonal anti-VSV antibodies (raised against VSV virions), 1:2000 anti-LDLR (R&D Systems, AF2148) or 1:1000 anti-MX1 (Sigma-Aldrich, 631-645) in TBS-T with 5% BSA or 5% milk with 0.02% sodium azide. The goat anti-mouse or goat anti-rabbit or chicken anti-goat horseradish peroxidase-conjugated secondary antibodies (Jackson-ImmunoResearch) were used. The Amersham ECL Western Blotting Detection Kit (GE Healthcare) was used for detection. To verify total protein in each loaded sample, membranes were re-probed with rabbit 1:1000 anti-GAPDH antibody (Santa Cruz, sc-25778) or stained with Coomassie blue R-250.

## ELISA

Cells were seeded in a 96-well plate with appropriate media (9% FBS) so that they were 80% confluent the next day. The wells were then aspirated, washed one time with PBS and replaced with appropriate media (0% FBS) and treatment. The treatments consisted of DMSO only, IFN (Calbiochem 407294-5MU) (5000 U/ml), ruxolitinib (INCB018424, trade names Jakafi and Jakavi) (2.5 μM) and IFN (5000 U/ml) / ruxolitinib (2.5 μM) mixture in appropriate media with 0% FBS. All conditions contained 0.1% DMSO. Cell culture lysates and supernates were isolated 24 h later and analyzed by ELISA for cellular LDLR and soluble LDLR (sLDLR), respectively, according to manufacturer's instructions (Human LDL R Quantikine ELISA kit, R&D Systems).

## Fluorescence-activated cell sorting (FACS) analysis of LDLR cell surface expression

For the LDLR cell surface expression experiment, cells were washed one time with PBS and then incubated with 0.2% EDTA in PBS (to retain LDLR on the cell surface). When the adherent cells detached, cells were counted with hemocytometer, and 1 million cells were used per condition. Three conditions were used for each cell line: cells alone, cells with secondary antibody (indicated as "control" in the figures) and cells with primary and secondary antibody (indicated as "LDLR" in the figures). Cells were first blocked in 2% BSA for 10 min, then incubated with 1:10 primary antibody against human LDLR (R&D Systems, AF2148) for 30 min and then incubated with 1:10 secondary antibody (Goat IgG (H+L) APC-conjugated antibody; R&D Systems, F0108) for 15 min. Cells were washed with PBS one time after incubation with the primary antibody and six times after secondary antibody. Cells were analyzed on a LSR Fortessa

cell analyser (BD Bioscience), and the data were analyzed with FlowJo software (Treestar).

### LDL uptake assay

For the LDL uptake assay, cells were seeded in 6-well plates so that they were 80% confluent the next day. Media was then aspirated, wells were washed one time with PBS, and then DMEM with 0% FBS was added. Fluorescently labeled LDL from human plasma (Molecular Probes, L3482) was then added at the concentration of 3 μg/ml to the media for 4 h at 37°C. Media was then aspirated and cells were washed 3 times with PBS to remove unbound LDL. Cells were then incubated with 0.05% trypsin in PBS to eliminate LDL that bound but did not enter into the cells. Cells were analyzed using the LSR Fortessa cell analyser (BD Bioscience), and the data were analyzed with FlowJo software (Treestar).

### VSV infection inhibition by soluble LDLR

To analyze the effect of soluble sLDLR on VSV infectivity, cells were seeded in 12-well plates so that they were 80% confluent the next day. Media was then aspirated, wells were washed one time with PBS and then DMEM with 0% FBS was added. First, sLDLR (R&D Systems, 2148-LD-025) was added at a concentration of 1 μg/ml and then VSV-ΔM51-eqFP650 was added. Cells were incubated with the mixture for 30 min at 37°C. Then cells were washed 3 times with PBS, and overlaid with 0.5% agar containing DMEM (5% FBS). Plaques were counted 16 h later to determine the titer.

### Effect of statins and PCSK9 antagonist on VSV attachment and LDL uptake

Atorvastatin Calcium (S2077), Fluvastatin Sodium (S1909), Rosuvastatin Calcium (S2169), Simvastatin (S1792) and SBC-115076 (S7976, a PCSK9 antagonist) were

purchased from Selleck Chemicals. Cells were seeded in 12-well plate so that they were 80% confluent the next day. Media was then aspirated, washed one time with PBS and then statins or a SBC-115076 were added at appropriate concentration in DMEM with 5% FBS for 24 hours. VSV attachment (monolayer) or LDL uptake assays were performed as described above.

RNA RT-PCR analysis

Cells were seeded in 12-well plates so that they reached approximately 80% confluence at 24 h. Cellular RNA was extracted with TRIzol (Life Technologies) per the manufacturer protocol. 0.5 μg of total RNA per reverse transcription (RT) reaction using random hexamer primers and SMART-Scribe reverse transcriptase (Clontech) was used for the cDNA synthesis as per manufacturer's protocol. PCR was carried out on cDNA using the following conditions: denaturation at 95°C for 30 seconds (s), annealing at 60°C for 30 s, and extension at 72°C for 60s for 40 cycles. Human LDLR specific primers were previously described (Tveten et al., 2006). The following primers were used to amplify cDNA using PCR: GGGCCCTGGGGCTGGAAATT (forward primer, LDLR Exon 1) and CTGGCTGCAGGTGTCGGGAT (reverse primer, LDLR Exon 8); ACCTGCAAATCCGGGGACTT (forward primer, LDLR Exon 3) and GTCATAGGAAGAGACGCCGT (reverse primer, LDLR Exon 10); GCTGTTCCCACGTCTGCAAT (forward primer, LDLR Exon 7) and AGATACTGGCAGCCGCCATT (reverse primer, LDLR Exon 14); GATGGGGAACTCCCGCCAA (forward primer, LDLR Exon 11) and GACCCCCAGGCAAAGGAAGA (reverse primer, LDLR Exon 17); TCAGTGCCAACCGCCTCACA (forward primer, LDLR Exon 13) and

GCCACGTCATCCTCCAGACT (reverse primer, LDLR Exon 18). PCR products were electrophoresed on a 1% agarose gel with ethidium bromide, PCR bands were isolated and DNA was analyzed by Sanger sequencing from both directions (Eurofins Genomics). DNA sequence analysis was conducted using SnapGene software (GSL Biotech) by comparing cDNA sequences of PDAC cells to the "WT" LDLR ORF (NCBI Reference Sequence: NM_000527.3). To identify possible alternatively spliced variants of LDLR mRNA, PCR products were analyzed using a high-resolution Criterion 5% TBE gels (BIO-RAD) electrophoresis, as described previously (Tveten et al., 2006). The Quick-Load 2-Log DNA Ladder (0.1-10.0 kb, New England Biolabs) was used.

Effect of polycations and pH on VSV infectivity and cell viability

HPAF-II cells were seeded in a 96-well plate such that they were approximately 90% confluent at the time of treatment. Cells were washed once with PBS. For each test condition, 35 μL of various concentrations of DEAE-dextran (Alfa Aesar J63781) or polybrene (Millipore TR-1003-G) and protons in MEM without FBS was added to cells. For control wells, 35 μL of MEM without FBS was added. The plate was incubated at 37°C for 30 min during which it was rocked every 5 min. 15 μL of VSV-ΔM51-GFP in MEM without FBS at multiplicity of infection (MOI) 0.1 based on HPAF-II cells was added and incubated for 1 h with rocking every 10 min. The 50 μL mixture was aspirated, wells washed 3 times with PBS, MEM with 5% FBS was added to wells, and cells were incubated at 37°C. GFP fluorescence was measured at regular intervals (CytoFluor Series 4000, excitation filter of 485/20 nm, emission 530/25 nm, gain=63; Applied Biosystems). 5 days post infection, cell viability was determined by methylthiazolydiphenyl-tetrazolium (MTT) cell viability assay (Biotium).

## Effects of combination of polycations and ruxolitinib on VSV infectivity, replication and cell viability

HPAF-II cells were seeded in a 96-well plate such that they were approximately 80% confluent at the time of treatment. Cells were washed once with PBS. For each test condition, 35 µL of polybrene or DEAE-dextran in MEM without FBS was added to cells. For control and ruxolitinib wells, 35 µL of MEM without FBS was added. The plate was incubated at 37°C for 30 min during which it was rocked every 5 min. 15 µL of VSV-ΔM51-GFP in MEM without FBS at MOI 0.001 based on HPAF-II cells was added and the plate was incubated for 1 h with rocking every 10 min. The 50 µL mixture was aspirated and wells washed 3 times with PBS. For ruxolitinib-treated wells, 100 µL of MEM with 5% FBS, 0.1% DMSO and 2.5 µM ruxolitinib was added. For wells without ruxolitinib treatment, 100 µL of MEM with 5% FBS and 0.1% DMSO was added. The plate was incubated at 37°C. GFP fluorescence was measured at regular intervals (CytoFluor Series 4000, excitation filter of 485/20 nm, emission 530/25 nm, gain=63; Applied Biosystems). Cell viability assay (MTT) was performed 3 days p.i. To examine the effects of polycations on VSV infectivity by FACS analysis, HPAF-II cells were seeded in a 6-well plate such that they were approximately 80% confluent at the time of treatment. Cells were washed once with PBS. For each test condition, 350 µL of DEAE-dextran or polybrene in MEM without FBS was dispensed appropriately. For control and ruxolitinib wells, 350 µL of MEM without FBS was added. The plate was incubated at 37 °C for 30 min during which it was rocked every 5 min. 150 µL of VSV-ΔM51-GFP in MEM without FBS at MOI 0.001 was added and incubated for 1 h with rocking every 10 min. The 500 µL mixture was aspirated and wells were washed 3 times with PBS. For ruxolitinib-treated wells, 2000 µL of MEM with 5% FBS, 0.1% DMSO and 2.5 µM

ruxolitinib was added. For wells without ruxolitinib treatment, 2000 µL of MEM with 5% FBS and 0.1% DMSO was added. Wells were incubated at 37 °C. At 18 h p.i., cells were washed once with PBS, then trypsinized and resuspended in MEM with 10% FBS. The mixture was transferred to flow cytometry tubes and spun at 2000 rpm for 2 min. The supernatant was aspirated and pellet was washed with PBS, then spun again at 2000 rpm for 2 min. The pellet was fixed with 500 µL of 4% paraformaldehyde and kept on ice for 15 min. After another round of centrifugation, the pellet was re-suspended in PBS and kept on ice. Cells were analyzed on a LSR Fortessa cell analyser (BD Bioscience), and the data were analyzed with FlowJo software (Treestar).

### Statistical analysis

All statistical analyses were performed using GraphPad Prism, version 7.0a for Mac OS X (GraphPad Software, San Diego, CA).

## 3.3 Results

### VSV attachment to HPAF-II is impaired

The human PDAC cell line HPAF-II, which showed the highest level of resistance to VSV in our previous studies, was the main focus of this study (Cataldi et al., 2015; Felt et al., 2015; Hastie et al., 2016; Moerdyk-Schauwecker et al., 2013; Murphy et al., 2012). In addition, many experiments included Hs766T, another VSV-resistant human PDAC cell line, as well as two VSV-permissive human PDAC cell lines, MIA PaCa-2 and Suit2. This work focuses on one of the most commonly used VSV-based oncolytic recombinants, VSV-ΔM51 (hereafter called VSV; Figure legends and Materials and Methods indicate the specific VSV recombinant used in each experiment), which has a deletion of a methionine at position 51 in the M protein (Wollmann G et al., 2010). This

mutation causes ablation of wild type (WT) M protein's ability to inhibit cellular antiviral gene expression. As many cancers have defective type I interferon antiviral signaling, VSV-ΔM51 can still replicate in and kill cancer cells (Ahmed et al., 2003; Kopecky et al., 2001). In addition, to facilitate visualization of viral infection, VSV recombinants used in this study encode either the near-infrared RFP (Hastie et al., 2015) or GFP (Wollmann G et al., 2010) ORF inserted between the VSV G and L genes.

We used two different approaches to examine the efficacy of VSV attachment to PDAC cells. For FACS analysis, virus attachment was examined using cells in suspension (Fig. 11). Adherent cells were treated with EDTA to detach them from plastic surfaces, incubated with different amounts of VSV (MOI 1.25, 12.5, or 125 based on VSV titer on MIA PaCa-2 cells) for 1 h at 4°C, washed to remove any unbound virus, and analyzed for cell-bound VSV using VSV-G antibody and FACS analysis. EDTA, rather than trypsin, was used to retain protein receptors of VSV (such as LDLR) on the cell surface. We also assayed VSV attachment using an alternative approach, where VSV attachment to cell monolayers was examined. Cells were incubated with different amounts of VSV (MOI 0.1 to 250 based on MIA PaCa-2) for 1 h at 4°C, then washed to remove any unbound virus, and analyzed for cell-bound VSV using western blot analysis of the total cell lysates (Fig. 12). As our study focuses on attachment, in both approaches virus-cell incubations were conducted at 4°C to prevent virus entry. To confirm that VSV did not penetrate cells under these conditions, cells were incubated with VSV for 1 h at 4°C, trypsinized to remove all surface proteins, and analyzed for the presence of VSV. As expected, no VSV products could be detected after trypsinization, indicating that VSV was only bound to the cell surface (Fig. 13).

As shown in Fig. 11 for VSV attachment to cells in suspension, the lowest level of VSV attachment was observed in HPAF-II under all tested conditions (MOIs). For example, at MOI 12.5, only 10% of HPAF-II were VSV-positive, compared to 57.4% of Hs766T, 31.9% of MIA PaCa-2 and 46.5% of Suit2. And even at MOI 125, only 57.4% of HPAF-II were VSV-positive, while all other cell lines were close to 100%. In agreement with these data, we also observed lower VSV attachment to HPAF-II cell monolayers (Fig. 12, "Attachment"). Based on the serial dilutions of virus and comparing VSV protein bands of similar intensity for each cell line, VSV was attaching to HPAF-II cells at least 12-fold less efficiently than to MIA PaCa-2 and Hs766T cells, and 3.5-fold less efficiently compared to Suit2 cells (Fig. 12, "Attachment"). While examining VSV attachment to cell monolayers, a duplicate set of samples was incubated for an extra 8 h at 37°C to determine relative VSV replication levels and confirm the status of PDAC cell lines in regard to their resistance/permissiveness to VSV. As shown in Fig. 1B ("Replication"), MIA PaCa-2 and Suit2 are highly permissive to VSV, illustrated by high levels of VSV replication at 8 h p.i., and that HPAF-II and Hs766T are resistant, with HPAF-II showing the highest level of resistance (Fig. 12, "Replication"). Interestingly, even though Hs766T had a similar level of VSV attachment as MIA PaCa-2 and even higher level than Suit2 (about 3.5-fold higher based on serial dilution of virus in Fig. 12), Hs766T showed dramatically lower levels of VSV replication, compared to both MIA PaCa-2 and Suit2. This result suggests that Hs766T is not defective in VSV attachment. In contrast, HPAF-II showed not only the lowest levels of VSV replication, but also the lowest levels of VSV attachment, suggesting that the impaired VSV attachment contributes to the resistance of HPAF-II to VSV.

In the experiments shown in Fig. 11 and 12, VSV was incubated with cells for 1 h. To examine relative kinetics of VSV attachment to different PDAC cell lines, we performed the VSV monolayer attachment assay at 4°C for 15 min, 30 min, and 60 min (Fig. 14). VSV attachment kinetics pattern was very similar in PDAC cell lines with most virus particles already attaching in the first 30 min p.i. Again, HPAF-II showed the lowest VSV attachment levels at all three time points.

LDLR expression and LDL uptake are lower in HPAF-II cells

Recently, LDLR has been proposed as one of the receptors for VSV (Amirache et al., 2014; Ammayappan et al., 2013; Finkelshtein et al., 2013a). As a high variation in LDLR expression was shown between different cell lines of pancreatic origin (Guillaumond et al., 2015), we hypothesized that HPAF-II could have a defect in LDLR expression, which could explain ineffective VSV attachment.

Three different approaches, ELISA, western blot, and FACS analysis were used to determine relative levels of LDLR expression in the four PDAC cell lines. First, using an LDLR ELISA assay, cell lysates were examined for cell-associated total LDLR levels in PDAC cell lines. As shown in Fig. 15, although all four tested cell lines showed detectable levels of LDLR, the lowest level was in HPAF-II cells, with somewhat higher levels in MIA PaCa-2 and Suit2, and the highest level in Hs766T. When cell lysates were analyzed by western blot, Hs766T also showed the highest levels of LDLR (Fig. 16). Interestingly, although this analysis showed similar levels of LDLR in HPAF-II, MIA PaCa-2, and Suit2 cells, HPAF-II was the only cell line with an extra band underneath the main LDLR band (Fig. 16). This band generally represents an unglycosylated inactive form of LDLR, and is often indicative of an abnormal LDLR processing in the cells

(Maxwell et al., 2005; Tolleshaug et al., 1982; Tolleshaug et al., 1983). Because only cell surface LDLR could be utilized by virus for attachment, LDLR cell surface expression was examined by FACS analysis using a primary antibody against LDLR. Again, EDTA, rather than trypsin, was used to retain LDLR on the cell surface. Importantly, cells were not fixed or permeabilized, and were incubated at 4°C during the entire procedure to ensure that only cell surface LDLR expression is detected. As shown in Fig. 17, although all 4 cell lines expressed LDLR at the cell surface, the lowest levels were in HPAF-II. This could be due to HPAF-II expressing the unglycosylated inactive form of LDLR (Fig. 16) that is not expressed on the cell surface (Maxwell et al., 2005; Tolleshaug et al., 1982; Tolleshaug et al., 1983).

Next, we wanted to examine LDLR functionality, which is normally done by examining the uptake of low density lipoprotein (LDL), the ligand of LDLR. Importantly, LDL has been previously shown to compete with VSV for LDLR (Finkelshtein et al., 2013b). Therefore, the ability of LDLR to uptake LDL could be used not only to examine LDLR functionality as an LDL receptor, but also as a VSV receptor. To assay for LDLR functionality, PDAC cell lines were compared for their abilities to uptake an exogenous fluorescently-labeled LDL. PDAC cells were incubated with DiI-LDL (3,3'-dioctadecylindocarbocyanine-LDL) for 4 h, and then analyzed for the levels of the internalized LDL by FACS. As shown in Fig. 18, LDL uptake was dramatically lower in HPAF-II compared to all other tested cell lines.

PDAC cell lines express wild-type LDLR

Currently, more than a thousand different types of mutations have been found in the LDLR protein (Marais, 2004). Many damaging LDLR mutations affect LDLR total

expression level, maturation, surface localization and LDL uptake (Marais, 2004). If present, such mutations could be responsible for the observed lower levels of LDLR expression, LDL uptake and/or VSV attachment in HPAF-II cells. To directly examine this possibility, total RNA was isolated from HPAF-II, Hs766T, MIA PaCa-2, and Suit2 cells, cDNA was synthesized, PCR-amplified by five pairs of LDLR specific primers, and the overlapping PCR products, covering the entire LDLR ORF, were sequenced. Although several silent mutations were detected (Fig. 19), the sequence analysis did not detect a single mutation affecting LDLR amino acid sequence in HPAF-II or any other tested PDAC cell line. Therefore, all tested PDAC cell lines produce WT LDLR. In addition, PCR fragments were analyzed by high-resolution gel electrophoresis to detect alternatively spliced variants of LDLR, exactly as this method was previously described (Tveten et al., 2006). As shown in Figure 20, we did not observe any unusual PCR products, which would suggest the presence of alternatively spliced variants of LDLR in HPAF-II cells. Together, our data show that the lower LDLR expression and LDL uptake in HPAF-II cells were not due to LDLR mutations.

### LDLR upregulation does not improve LDL uptake or VSV attachment in HPAF-II cells

The ELISA (Fig. 15), western blot (Fig. 16) and FACS (Fig. 17) analyses suggested potential abnormalities in the level of LDLR expression, which could explain lower LDL uptake and VSV attachment. Thus, we next examined whether an upregulation of LDLR expression would improve VSV attachment and/or LDL uptake in HPAF-II.

Two different drug types were tested to increase LDLR expression levels, statins and a proprotein convertase subtilisin/kexin type 9 (PCSK9) inhibitor. Statins are competitive inhibitors of hydroxymethylglutaryl-CoA (HMG-CoA) reductase, which is the key rate-

limiting enzyme of cholesterol synthesis. Statins inhibit cholesterol synthesis in the liver and some other cell types, including cancer cells (Pahan, 2006). One consequence of the decreased cholesterol production is that cells compensate for it by upregulating expression of LDLR to increase cholesterol uptake from the medium (Vaziri and Liang, 2004). PCSK9 is a secretory serine protease that binds surface LDLR, induces its internalization and lysosomal degradation, thus inhibiting LDLR recycling to the surface (Santos and Watts, 2015). PCSK9 inhibitors bind to PCSK9 and increase LDLR receptor cycling, thus increasing surface LDLR levels and improving LDL uptake (Santos and Watts, 2015). Therefore, we decided to use various statins and a PCSK9 inhibitor to increase LDLR expression and test whether this approach could improve VSV attachment and LDL uptake in HPAF-II cells.

To increase LDLR levels prior to VSV attachment assay, HPAF-II cells were pretreated for 24 h with 4 widely used FDA-approved statins, atorvastatin (“Lipitor”), rosuvastatin (“Crestor”), simvastatin (“Zocor”), or fluvastatin (“Lescol”), or with a PCSK9 antagonist SBC-110576 (McNutt et al., 2009). Other tested conditions were cell starvation (0% FBS medium), which could increase LDLR levels (Wu et al., 2012), and unlabeled LDL addition that could decrease LDLR levels (Chen et al., 2007; Russell et al., 1983; Ye et al., 2014). After 24 h treatment, cell monolayers were incubated with VSV for 1 h at 4°C to examine VSV attachment using western blotting. As shown in Figure 21, LDLR expression (including the upper mature LDLR band) was strongly improved by each of the tested statins, however VSV attachment levels were not improved. SBC-110576 and addition of LDL did not have an effect on LDLR expression (the upper mature LDLR band) or VSV attachment. However, disappearance of the lower

LDLR band can be observed after SBC-110576 treatment, suggesting expected improvement in LDLR maturation (Fig. 21). Interestingly, starvation did improve VSV attachment, however this was likely not due to LDLR, as LDLR level were not affected by starvation (Fig. 21). Overall, our data demonstrate that increasing LDLR expression does not improve VSV attachment in HPAF-II cells, suggesting that lower LDLR expression was not a main factor determining inefficient VSV attachment to HPAF-II.

As VSV attachment was not improved by statins, we determined whether the statin-mediated increase in LDLR expression could improve LDL uptake in HPAF-II. Cells were pretreated for 24 hours with the same statins as in the previous experiment and then incubated with LDL for 4 h and then analyzed by FACS analysis. Our data show only marginal increase in LDL uptake after statin treatment (Fig. 22), especially when compared to untreated Suit2 cells, indicating that the lower levels of both VSV attachment and LDL uptake in HPAF-II cells were independent of low LDLR expression in this cell line.

### Type I IFN signaling and soluble LDLR do not play a role in the inefficient attachment of VSV to HPAF-II cells

Our previous studies demonstrated that upregulated type I IFN signaling plays an important role in resistance of PDAC cell lines to VSV (Cataldi et al., 2015; Hastie et al., 2016; Moerdyk-Schauwecker et al., 2013; Murphy et al., 2012) and that the treatment of resistant PDAC cell lines with ruxolitinib (a specific JAK1/2 inhibitor) dramatically inhibits antiviral signaling and improves VSV replication in all resistant PDAC cell lines (Cataldi et al., 2015; Hastie et al., 2016). To examine whether the observed inefficient binding of VSV to HPAF-II cells is a result of the type I IFN pathway upregulation, HPAF-II and Suit2 (as a negative control) cells were pretreated with ruxolitinib for 24 h

before performing VSV attachment to cell monolayer assay. In agreement with our previous studies (Cataldi et al., 2015; Hastie et al., 2016), ruxolitinib treatment downregulated IFN-stimulated gene (ISG) Mx1 in HPAF-II cells (Fig. 23). However, the treatment did not improve VSV attachment (Fig. 23). This suggests that the defect of HPAF-II in VSV attachment is type I IFN independent, and that the inefficient attachment and upregulated antiviral signaling independently contribute to resistance of HPAF-II to VSV. In agreement with this, another resistant PDAC cell line, Hs766T, does not display a defect in VSV attachment, although it has the same upregulation of type I IFN signaling as HPAF-II (Cataldi et al., 2015; Hastie et al., 2016; Moerdyk-Schauwecker et al., 2013; Murphy et al., 2012).

Previous studies have shown that soluble LDLR (sLDLR) secretion by cells can be type I IFN induced, and that sLDLR can inhibit VSV infection in WISH cells (this cell line has been recently shown to be misidentified and identical to HeLa cells) (Fischer et al., 1994; Fischer et al., 1993; Kniss and Summerfield, 2014). Here, we wanted to test a hypothesis that HPAF-II cells secrete an excessive amount of sLDLR, which could inhibit VSV attachment. First, to test whether sLDLR can inhibit VSV infectivity in PDACs, sLDLR and VSV or VSV alone were added to the cells and incubated for 30 min at 37°C [the assay was conducted as described previously (Fischer et al., 1994; Fischer et al., 1993; Kniss and Summerfield, 2014). Cells were then washed to remove any unbound virus and overlaid with agar to prevent secondary infections. VSV plaques were counted to determine the effect of sLDLR on VSV infectivity. As shown in Fig. 24, the presence of the exogenous sLDLR led to a 10-fold decrease in VSV infectivity, confirming that sLDLR secretion can inhibit VSV attachment in PDAC cell lines. To examine the levels

of secreted sLDLR produced by different PDAC cell lines, cells were incubated for 24 h in a medium without FBS, the medium then was collected and analyzed by ELISA for sLDLR. As shown in Figure 25, the tested PDAC cell lines produced different amount of sLDLR, but no association between VSV attachment efficiency and sLDLR levels in the media could be observed. In addition, the effects of type I IFN on sLDLR secretion or total LDLR levels in PDAC cells were examined. PDAC cell lines were treated either with IFN-α (to stimulate type I IFN signaling) or ruxolitinib (to inhibit it) or both, and sLDLR (Fig. 26) and cell-associated LDLR (Fig. 27) levels were analyzed using ELISA assay. In contrast to previous studies with WISH cells (Fischer et al., 1994; Fischer et al., 1993), the treatments had either no or negligible effects on sLDLR production and cell-associated LDLR. Furthermore, when HPAF-II were treated with ruxolitinib (to inhibit type I IFN signaling), LDL uptake was not improved (Fig. 28). Together, our data demonstrate that sLDLR secretion is not responsible for the inefficient attachment of VSV to HPAF-II cells, and that LDLR expression, LDL uptake and VSV attachment in PDAC cells are controlled independently of type I IFN signaling.

Polycations improve VSV attachment to HPAF-II cells

Our data show that inefficient VSV attachment to HPAF-II cells, as well as defective LDL uptake, could not be improved in HPAF-II cells even when LDLR expression was markedly increased by treating cells with statins (Fig. 21 and 22). While future studies are needed to identify specific defects of LDLR in VSV attachment and LDL uptake, here we decided to use an alternative approach to improve VSV attachment by targeting LDLR-independent VSV attachment. Previous studies have suggested that phosphatidylserine (Carneiro et al., 2006; Coil and Miller, 2004; Schlegel et al., 1983),

sialoglycolipids (Schloemer and Wagner, 1975), heparan sulfate (Guibinga et al., 2002), or electrostatic interactions between VSV and cell membrane (Bailey et al., 1984; Conti et al., 1991) could play an important role in VSV attachment. As none of these studies examined PDAC cell lines, we want to conform that LDLR-independent attachment also occurs in PDAC cell lines. Cells were treated with 0.05% trypsin in PBS for 30 min at 37°C to digest surface LDLR, then used for FACS analysis of VSV attachment to cells in suspension (Fig. 29). To confirm successful digestion of LDLR by trypsin, total protein was isolated from trypsin-treated cells and analyzed by western blotting for LDLR (Fig. 30). Despite the lack of any detectable LDLR in trypsin-treated HPAF-II, MIA PaCa-2, and Suit2 cell lines, and a significant decrease of the mature LDLR (upper band) in Hs766T cells (Fig. 30), VSV attachment occurred in all cell lines (Fig. 29). Again, HPAF-II showed the lowest level of VSV attachment, as they are defective in VSV attachment even in the presence of LDLR, when the analyzed cells were detached using EDTA (Fig. 11). These data suggest that VSV particles can attach to PDAC cells in an LDLR-independent manner.

There are several approaches to improve LDLR-independent VSV attachment to cells. Several early studies demonstrated that different pH conditions or the addition of positively-charged polycations, such as polybrene or DEAE-dextran, can significantly improve VSV attachment to various cell membrane components via nonspecific electrostatic interactions (Bailey et al., 1984; Conti et al., 1991; Matlin et al., 1982). Moreover, polybrene and other polycations are routinely used to improve transduction of target cells with replication-defective lentiviral particles that are pseudotyped with VSV-G (Denning et al., 2013; Reiser et al., 1996; Yee et al., 1994). To examine whether pH or

polycations can improve VSV infection of HPAF-II cells, cells were pretreated for 30 min with various concentrations of protons (pH levels), polybrene or DEAE-dextran, then incubated with VSV for 1 h at 37°C in the presence of each test condition (Fig. 31). Virus and chemical reagents then were removed and cells were placed back at 37°C for 46 h, and VSV infection driven GFP fluorescence was measured. As different pH conditions or polycations were present only for 1 h 30 min and removed after virus incubation, the differences in VSV-associated GFP fluorescence identified in this original screening were likely reflecting the efficacy of VSV initial infection. None of the pH conditions improved VSV infection in HPAF-II (Fig. 31, each condition is compared to GFP fluorescence in HPAF-II cells treated with VSV only). However, among all tested conditions, the two highest tested concentrations (10 μg/ml and 50 μg/ml) of polybrene and DEAE-dextran showed a clear increase in VSV infectivity (Fig. 31). To examine whether the improved VSV infectivity under these treatment conditions results in increased oncolysis, an MTT cell viability assay was performed 5 days p.i. Compared to VSV alone, the 2 highest concentrations (10 and 50 μg/ml) of polybrene and all 3 concentrations of DEAE-dextran significantly decreased cell viability (Fig. 32).

To examine whether the observed improvement in VSV infectivity was due to an improvement in VSV attachment, cells were pretreated for 30 min with 10 μg/ml of polybrene or DEAE-dextran, then incubated with VSV for 1 h at 4°C (to prevent virus entry) in the presence of these polycations. Cells were washed to remove any unbound virus, then protein was isolated and analyzed by western blotting. Both polybrene and DEAE-dextran treatments did show a clear improvement in VSV attachment, even though the improvement with DEAE-dextran was markedly stronger (Fig. 33).

We then tested whether the improved VSV attachment to HPAF-II was possibly due to an increased LDLR expression or functionality as a result of the treatments of cells with polycations. Pretreatment of cells for 30 min with 10 μg/ml of polybrene or DEAE-dextran, followed by incubation with VSV for 1 h at 4°C in the presence of these polycations did not improve LDLR expression (Fig. 33). Furthermore, when cells were pretreated for 30 min with 10 μg/ml of polybrene or DEAE-dextran then incubated with LDL for 4 h at 37 °C in the presence of these polycations, no improvement in LDL uptake was observed when cells were analyzed by FACS analysis (Fig. 34). Taken together, these data indicate that polybrene and DEAE-dextran improve VSV attachment to HPAF-II cells via an LDLR-independent mechanism.

### Combining polybrene or DEAE-dextran with ruxolitinib breaks resistance of HPAF-II to VSV

We have shown previously that the treatment of HPAF-II and other resistant PDAC cell lines with JAK1/2 inhibitors significantly improve their permissiveness to VSV (Cataldi et al., 2015; Hastie et al., 2016; Moerdyk-Schauwecker et al., 2013). However, JAK Inhibitor I treatment only moderately improves susceptibility of resistant cells to VSV initial infection (Moerdyk-Schauwecker et al., 2013), and pre-treatment of cells with ruxolitinib (compared to post-treatment only) did not change the kinetics of VSV replication, with a significant increase in VSV replication that could be seen only after 48 h p.i even in cells pretreated with ruxolitinib for up to 48 h, suggesting that ruxolitinib did not improve the rate of initial infection but rather facilitated secondary infection via inhibition of antiviral signaling in PDAC cells (Cataldi et al., 2015; Hastie et al., 2016; Moerdyk-Schauwecker et al., 2013). As polybrene and DEAE-dextran improve VSV attachment and primary infection and ruxolitinib improves VSV replication, we

hypothesized that combining these two treatments would improve overall VSV infection and oncolysis in HPAF-II cells. Cells were pretreated with 10 µg/ml polybrene or DEAE-dextran or mock-treated for 30 min, then VSV was added in the presence of polycations (or mock treatment) for 1 h at 37 °C, followed by media removal and washes with PBS, and then cells were incubated in the presence of 2.5 µM ruxolitinib or mock treatment. VSV infection-associated GFP fluorescence was monitored for 71 h. In agreement with our previous study (Cataldi et al., 2015), ruxolitininb alone significantly improved VSV replication starting at 48 h p.i., however the polycation/ruxolitinib combinations showed even stronger improvement (Fig. 35). Importantly, the polycation/ruxolitinib combinations did not only result in higher VSV replication (Fig. 35), but also the significant increase in VSV replication was already seen at 24 h p.i. versus 48 h p.i. for ruxolitinib treatment only (Fig. 35), likely due to polybrene and DEAE-dextran improving the rate of initial infections, as these polycations were present only during 1 h incubation of HPAF-II cells with VSV. Figure 36 shows representative pictures of the treated cells at 22 and 48 h p.i., and it confirms that an important improvement in VSV replication can already be seen at 22 h p.i. for the polycation/ruxolitinib combinations. To examine whether the improved VSV infectivity under these treatment conditions results in increased oncolysis, an MTT cell viability assay was performed 71 h p.i. Ruxolitinib did improve oncolysis significantly, however the polycation/ruxolitinib combinations induced even more oncolysis (Fig. 37).

To confirm that polybrene and DEAE-dextran improve initial infections, HPAF-II cells were treated as in the previous experiment, however cells were analyzed by FACS for the number of infected cells at an earlier time point (18 h p.i.), when for HPAF-II we

generally observe only initially infected cells (Fig. 38). Polybrene and DEAE-dextran treatments resulted in many more GFP-positive cells (55.7% and 55.9%, respectively, versus 1.1% for VSV only) than the ruxolitinib condition (27%), confirming that these polycations improved initial infection. When the polycations were combined with ruxolitinib, almost all cells were infected (90.3% and 83.6% for polybrene/ruxolitinib and DEAE-dextran /ruxolitinib, respectively), likely because the initial infections were improved by polybrene or DEAE-dextran, and secondary infections were improved by ruxolitinib via enhancement of VSV replication in the initially infected cells and inhibition of antiviral responses in the secondary-infected cells. Taken together, polycations and ruxolitinib complement each other when combined and break the multiple mechanisms of resistance of HPAF-II to VSV.

## 3.4 Conclusion

A dramatically weaker attachment of VSV in the most resistant tested PDAC cell line, HPAF-II, was shown. Although sequence analysis of the VSV receptor, LDLR, did not reveal any mutations in PDAC cell lines, HPAF-II cells displayed the lowest level of LDLR expression and dramatically lower LDLR activity. Treatment of cells with statins strongly increased LDLR expression levels, but did not improve VSV attachment. However, LDLR-independent attachment of VSV to HPAF-II cells was dramatically improved by treating cells with polybrene or DEAE-dextran. Moreover, we successfully used a novel triple combination treatment to break the resistance of HPAF-II to VSV by combining the virus with ruxolitinib and polybrene or DEAE-dextran, thus simultaneously improving VSV attachment and replication. These results are summarized in Figure 39 and will be further discussed in the dissertation summary (Chapter 4).

3.5 Figures

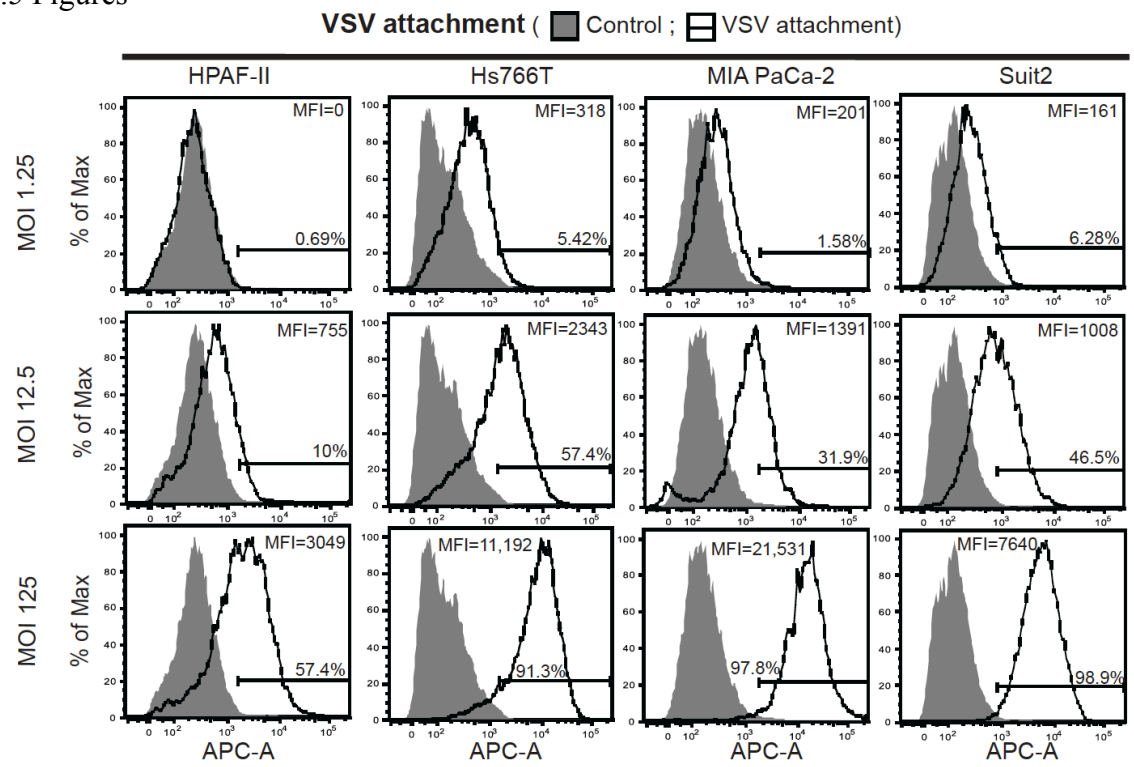


Figure 11: VSV attachment in PDAC cell lines (suspension). For VSV attachment to cells in suspension, cells were detached with PBS with 0.2% EDTA and incubated for 1h at 4°C with VSV-ΔM51-eqFP650. After incubation with VSV-G primary antibody and APC-conjugated secondary antibody, cells were analyzed by FACS. "Control" cells were mock-treated (without VSV), and primary and secondary antibodies were used. "VSV attachment" cells were incubated with various amounts of VSV (the indicated MOIs are based on virus titration on MiaPaCa-2). Gated populations are positive for VSV attachment (% of VSV-positive cells is indicated above the gate line). MFI stands for "Mean Fluorescent Intensity" of each population and was calculated by FlowJo software (Treestar).

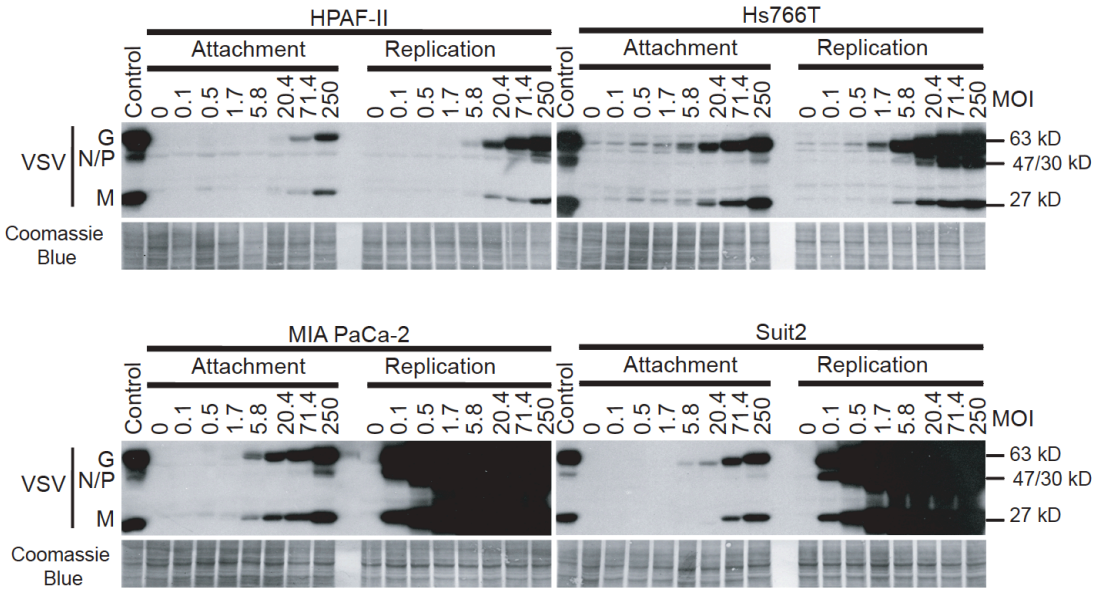


Figure 12: VSV attachment in PDAC cell lines (monolayer). For VSV attachment to cells in monolayer, cell monolayers were incubated for 1h at 4°C ("Attachment") or for additional 8h at 37°C ("Replication") with VSV-ΔM51-eqFP650. Protein was isolated and analyzed by western blotting. MOI is indicated on top and is based on MiaPaCa-2. Protein (kDa) product sizes are indicated on the right. Coomassie blue stain was used to indicate equal loading.

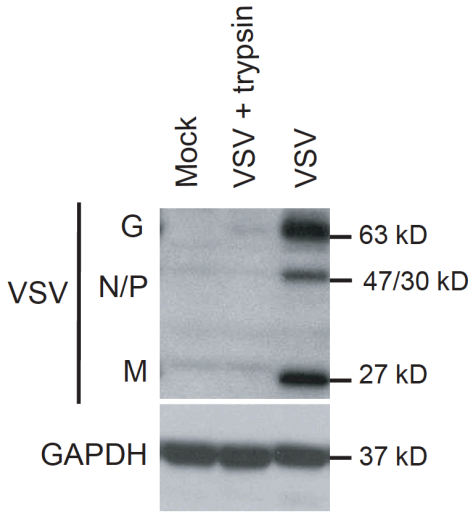


Figure 13: Trypsin treatment after VSV attachment. For VSV attachment to cells in monolayer, cell monolayers were incubated for 1h at 4°C ("VSV") with VSV-ΔM51-eqFP650. To confirm that VSV only attached to cells at 4°C and did not enter, cells were treated with 0.05% trypsin for 15 minutes after VSV-ΔM51-eqFP650 was incubated for 1h at 4°C ("VSV+trypsin"). Protein was isolated and analyzed by western blotting. This experiment was done on Suit2 at an MOI of 50 (based on MIA PaCa-2). Protein (kDa) product sizes are indicated on the right. GAPDH was used to indicate equal loading.

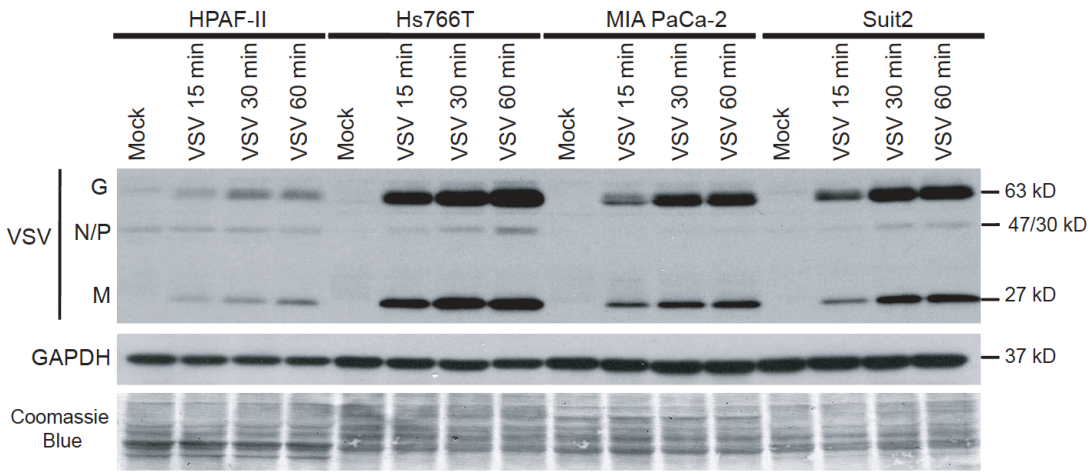


Figure 14: VSV attachment kinetics in PDAC cell lines. Cells in monolayer were incubated for 1h at 4°C ("Attachment") with VSV-ΔM51-eqFP650 or mock-treated ("Mock"). MOI used is 50 based on MiaPaCa-2. Protein (kDa) product sizes are indicated on the right. GAPDH and Coomassie blue stain were used to confirm equal loading.

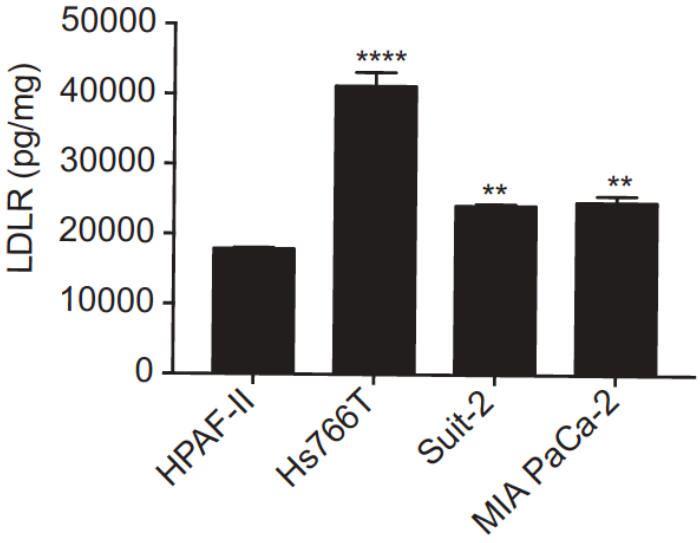


Figure 15: Analysis of LDLR protein expression in PDAC cell lines by ELISA. Total protein lysates were isolated from untreated cells and analyzed by ELISA for LDLR levels. LDLR levels were normalized to total protein levels. Assay was done in triplicate and data represent the mean ± standard error of mean. Cell lines were compared using a 1-way ANOVA followed by the Dunnett posttest for comparison to HPAF-II. **, $P<0.01$; ****, $p<0.0001$.

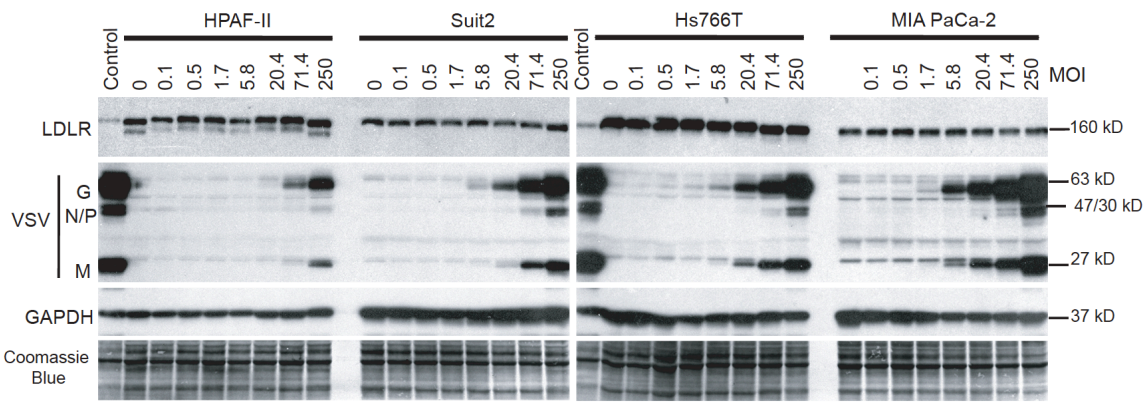


Figure 16: Analysis of LDLR protein expression in PDAC cell lines by western blot. Cell monolayers were incubated for 1h at 4°C with various amounts of VSV-ΔM51-eqFP650 (the indicated MOIs are based on virus titration on MiaPaCa-2). Protein lysates were analyzed for LDLR and VSV proteins by western blot. Protein (kDa) product sizes are indicated on the right. GAPDH and Coomassie blue stain were used to confirm equal loading.

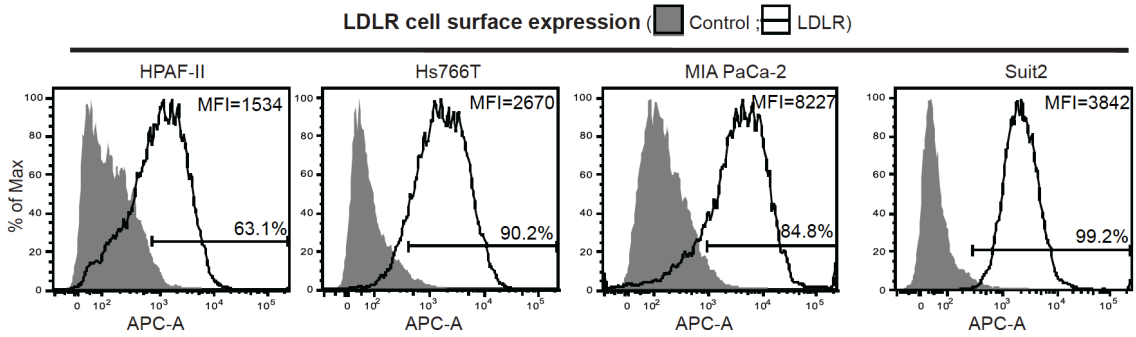


Figure 17: LDLR cell surface expression in PDAC cell lines. For LDLR cell surface expression, cells were kept on ice and not permeabilized and not fixed. After incubation with anti-LDLR primary antibody and APC-conjugated secondary antibody cells were analyzed by FACS using the APC-A channel. “Control” - cells were incubated with secondary antibody only. “LDLR” - cells were incubated with primary and secondary antibody. Gated populations are positive for LDLR (% of LDLR-positive cells is indicated above the gate line). MFI stands for “Mean Fluorescent Intensity” of each population and was calculated by FlowJo software (Treestar). Data are representative of 3 independent experiments.

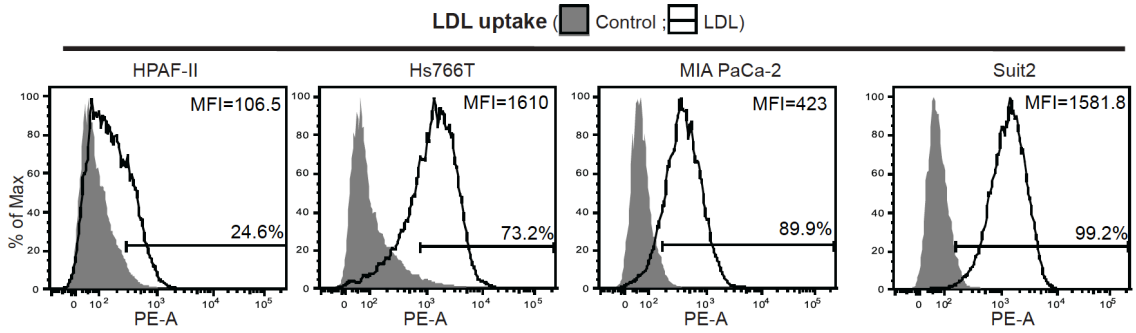


Figure 18: LDL uptake in PDAC cell lines. For the LDL uptake assay, cells were incubated for 4 h with fluorescently labeled LDL and then analyzed by FACS using the PE-A channel. "Control": fluorescently labeled LDL was not added; "LDL": fluorescently labeled LDL was added. Gated populations are positive for LDL uptake (% of LDL-positive cells is indicated above the gate line). MFI stands for "Mean Fluorescent Intensity" for each population and was calculated by FlowJo software (Treestar). Data are representative of 3 independent experiments.

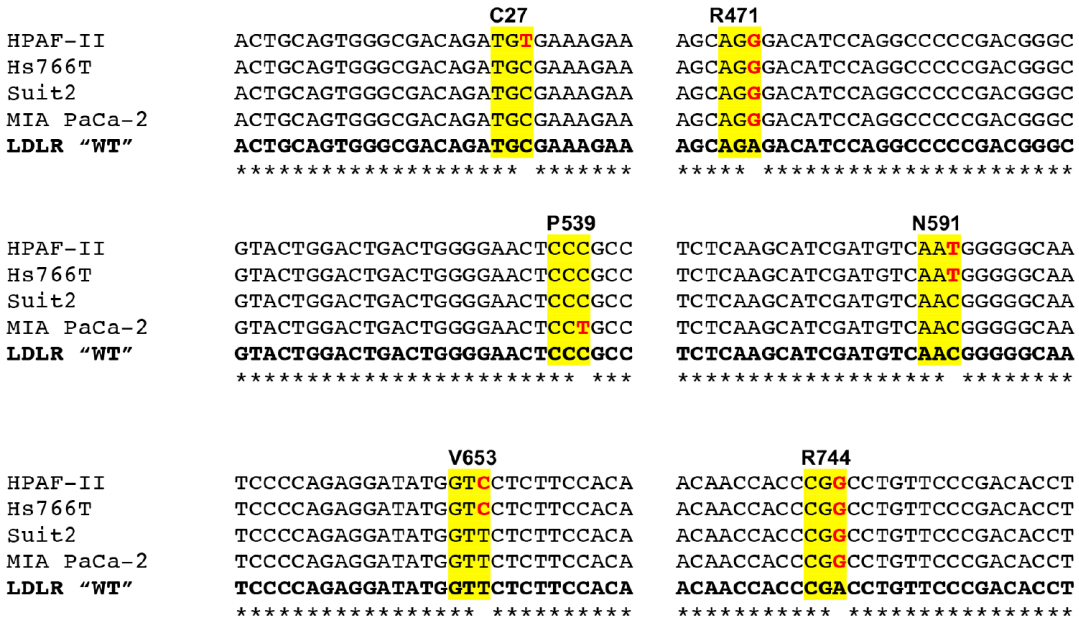


Figure 19: Sequence alignment of LDLR cDNA sequences for four tested human PDAC cell lines. Only selected regions are shown where nucleotide substitutions were detected when compared to the "WT" LDLR ORF (NCBI Reference Sequence: NM_000527.3). All other not shown LDLR cDNA sequences are identical between cell lines and the reference LDLR sequence.

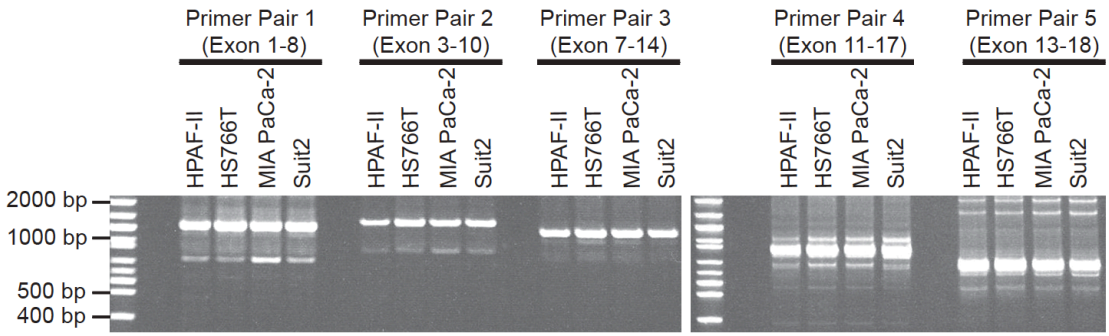


Figure 20: LDLR RNA analysis in PDAC cell lines. Total RNA was isolated from PDAC cells lines, cDNA was synthesized using random hexamer primers, and PCR was carried out on cDNA using human LDLR specific primers. DNA samples were analyzed on Criterion 5% TBE gels (BIO-RAD), which were stained with ethidium bromide. The Quick-Load® 2-Log DNA Ladder (0.1-10.0 kb) was used.

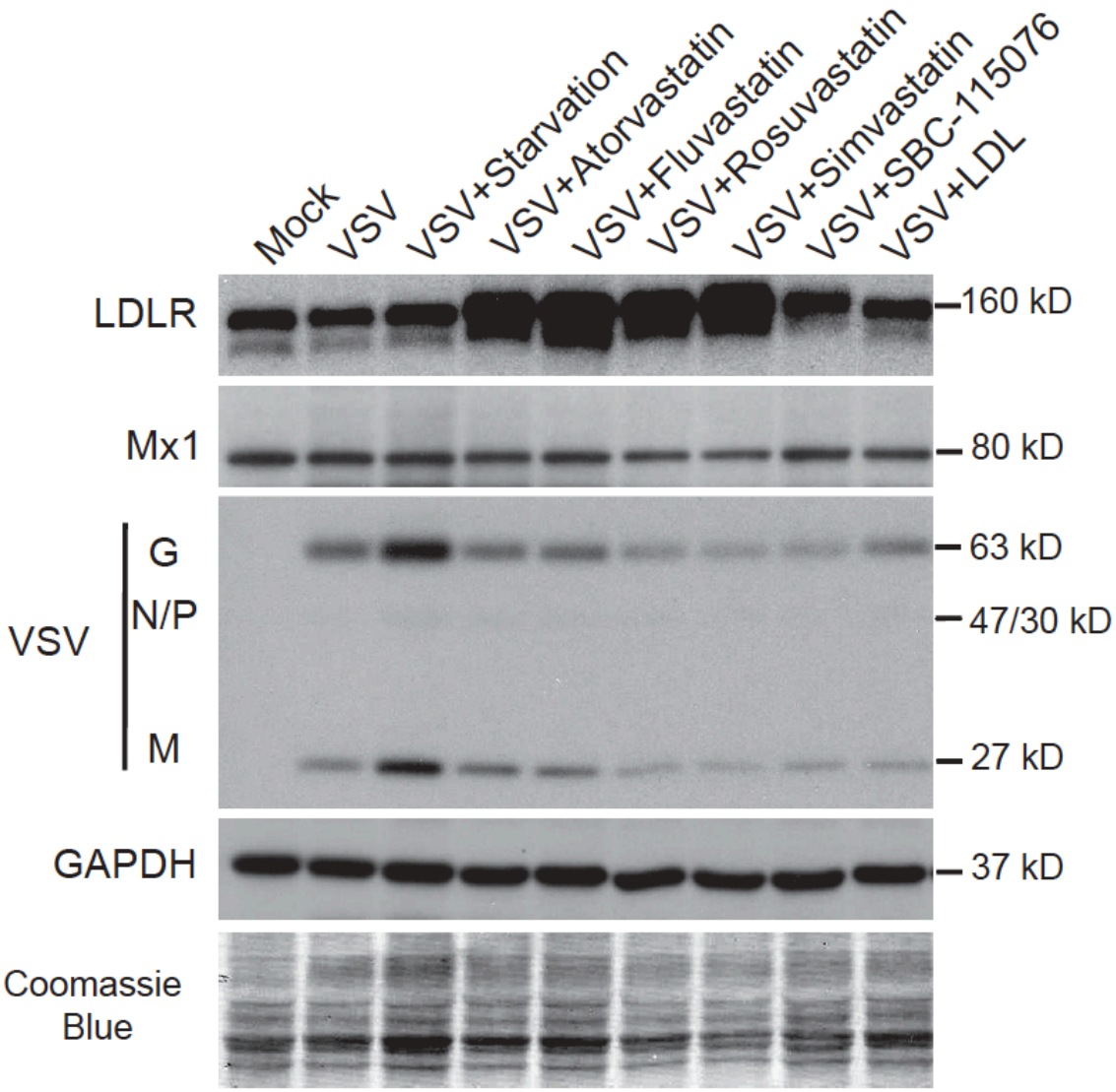


Figure 21: Effect of statins on LDLR expression and VSV attachment in PDAC cell lines. Cells were pretreated with statins (10 µM) or SBC-115076 (10 µM) or LDL (25 µg/ml) for 24 h and were then incubated for 1h at 4°C with VSV-ΔM51-eqFP650. MOI was 250 based on MiaPaCa-2. Protein isolates were used for western blot analyzes. Protein (kDa) product sizes are indicated on the right. GAPDH and Coomassie blue stain were used to indicate equal loading.

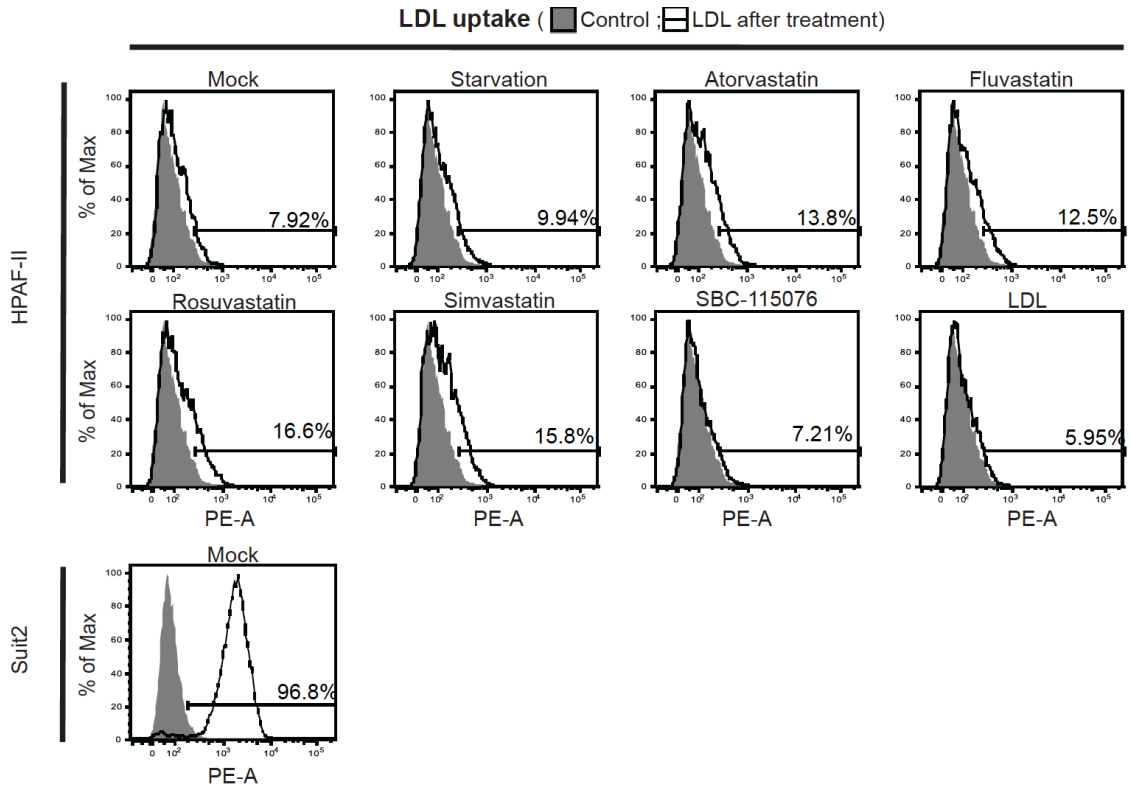


Figure 22: Effect of statins on LDL uptake in PDAC cell lines. Cells were pretreated with statins (10 µM) or SBC-115076 (10 µM) or LDL (25 µg/ml) for 24 h and then incubated for 4 h at 37°C with fluorescently labeled LDL. Samples were analyzed by FACS using the PE-A channel. "Control": fluorescently labeled LDL was not added; "LDL": fluorescently labeled LDL was added. Treatments are indicated on top of each histogram. Gated populations are positive for LDL uptake (% of LDL-positive cells is indicated above the gate line). MFI stands for "Mean Fluorescent Intensity" for each population and was calculated by FlowJo software (Treestar).

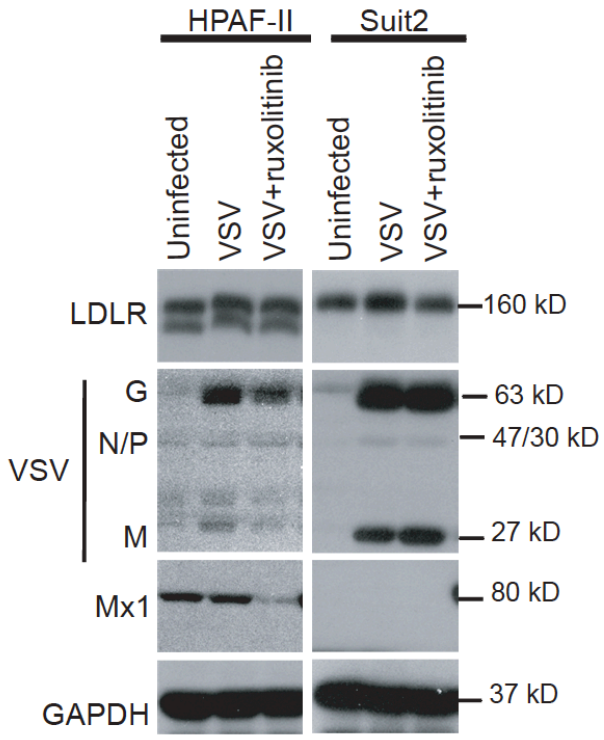


Figure 23: Effect of type I IFN on VSV attachment in PDAC cell lines. Cells were pretreated with ruxolitinib (2.5 μM) for 24h and then incubated for 1h at 4°C with VSV-ΔM51-eqFP650. MOI used was 20 based on MiaPaCa-2. Protein was isolated and analyzed by western blot. Protein (kDa) product sizes are indicated on the right. GAPDH was used to indicate equal loading.

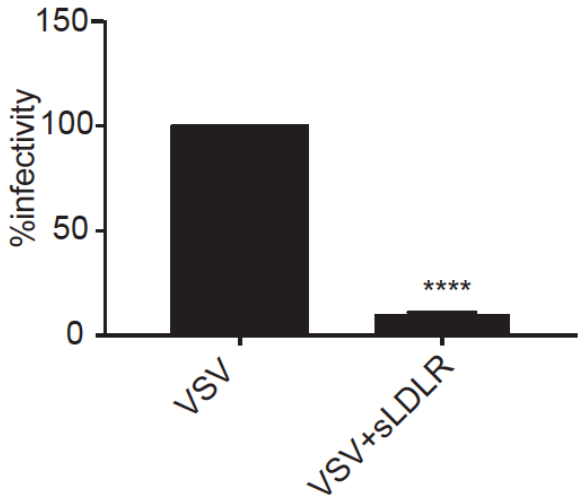


Figure 24: Effect of sLDLR on VSV infectivity in PDAC cell lines. VSV-ΔM51-eqFP650 alone or VSV-ΔM51-eqFP650 with soluble LDLR (1 μg/ml) was added on PDAC cell line and plaques were counted the next day to determine effect on infectivity. Data are representative of 3 independent experiments and shows the mean ± standard error of mean. Conditions were compared using an unpaired t-test. ****, $p<0.0001$.

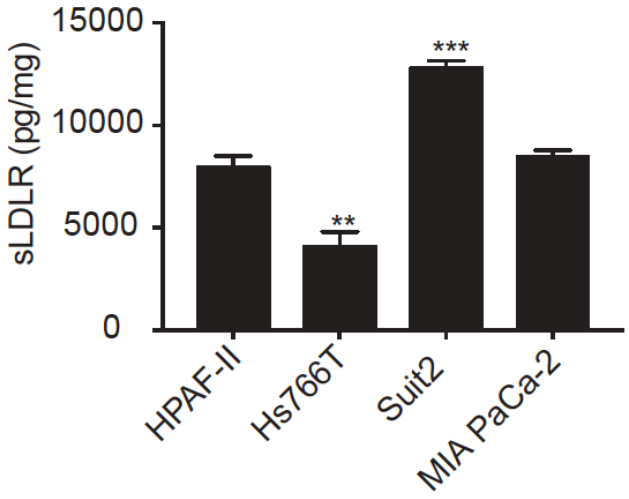


Figure 25: sLDLR secretion in PDAC cell lines. Cells were grown in culture for 24 h and then media were used to determine sLDLR levels by ELISA. Soluble LDLR levels were normalized by total protein. Assay was done in triplicate and data represent the mean ± standard error of mean. Conditions were compared using a 1-way ANOVA followed by the Dunnett posttest for comparison to HPAF-II. **, $P<0.01$; ***, $p<0.001$.

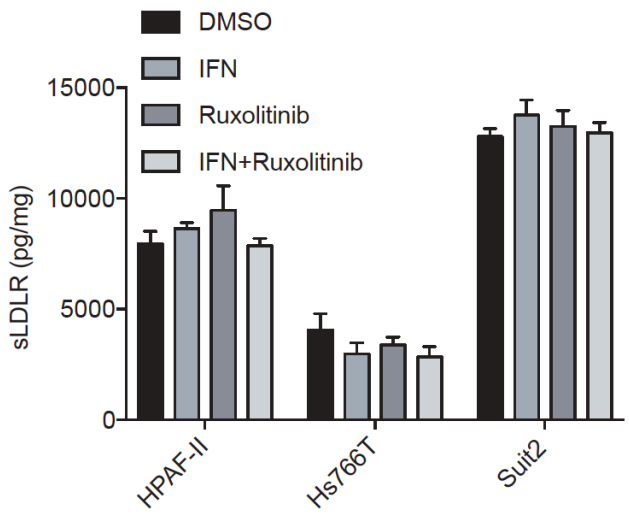


Figure 26: Effect of type I IFN on sLDLR in PDAC cell lines. Cells were treated with IFN (5000 U/ml), ruxolitinib (2.5 µM) or IFN (5000 U/ml)/ruxolitinib (2.5 µM) for 24 h. Medium isolates were then used to determine effect on sLDLR levels by ELISA. sLDLR levels were normalized by total protein. Assay was done in triplicate and data represent the mean ± standard error of mean. Conditions were compared using a 1-way ANOVA followed by the Dunnett posttest for comparison to the control.

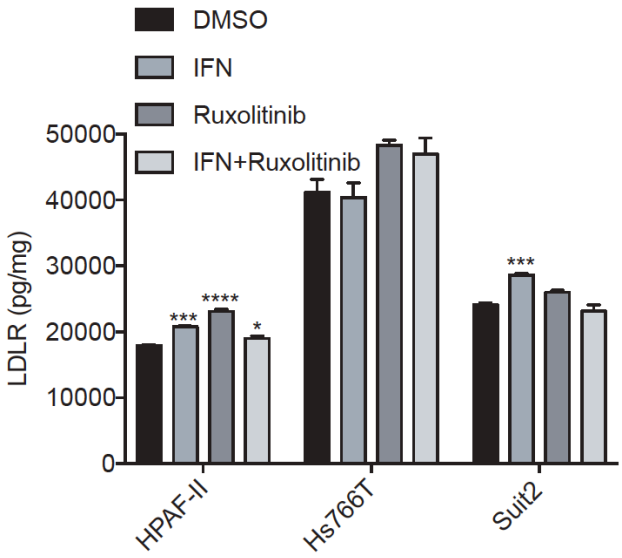


Figure 27: Effect of type I IFN on LDLR in PDAC cell lines. Cells were treated with IFN (5000 U/ml), ruxolitinib (2.5 μM) or IFN (5000 U/ml)/ruxolitinib (2.5 μM) for 24 h. Protein isolates were then used to determine effect on LDLR levels by ELISA. LDLR levels were normalized by total protein. Assay was done in triplicate and data represent the mean ± standard error of mean. Conditions were compared using a 1-way ANOVA followed by the Dunnett posttest for comparison to the control. *, $p<0.05$; ***, $p<0.001$; ****, $p<0.0001$.

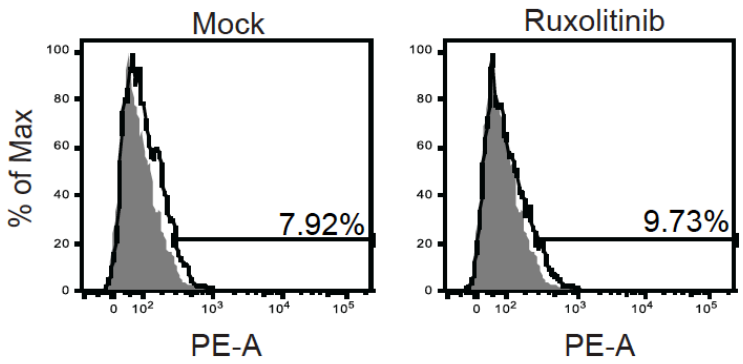


Figure 28: Effect of type I IFN on LDL uptake in HPAF-II. Cells were pretreated with ruxolitininb (2.5 μM) for 24h and then incubated for 4 h at 37°C with fluorescently labeled LDL. Samples were analyzed by FACS using the PE-A channel. "Control": fluorescently labeled LDL was not added; "LDL": fluorescently labeled LDL was added. Treatments are indicated on top of each histogram. The "Mock" sample is the same as in Fig. 22. Gated populations are positive for LDL uptake (% of LDL-positive cells is indicated above the gate line). MFI stands for "Mean Fluorescent Intensity" for each population and was calculated by FlowJo software (Treestar).

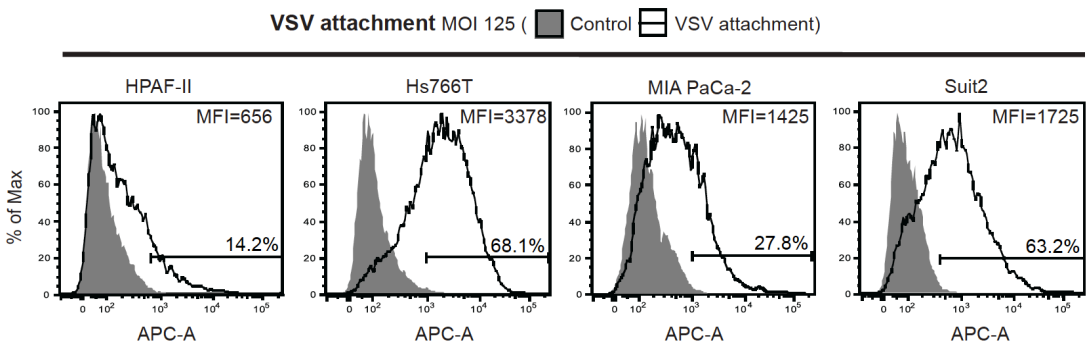


Figure 29: Effect of LDLR digestion on VSV attachment in PDAC cell lines. Cells were treated with PBS with 0.05% trypsin and then were used for VSV-ΔM51-eqFP650 attachment analysis. For the attachment assay, after a 1 h incubation at 4°C with VSV-ΔM51-eqFP650 (MOI 125 based on MiaPaC-2), cells were incubated with anti-VSV-G antibody and APC-conjugated secondary antibody and analyzed by FACS using the APC-A channel. "Control" - cells were mock-treated (without VSV-ΔM51-eqFP650), and primary and secondary antibodies were used. "VSV attachment" - cells were incubated with VSV-ΔM51-eqFP650. Gated populations are positive for VSV attachment (% of VSV-positive cells is indicated above the gate line). MFI stands for "Mean Fluorescent Intensity" of each population and was calculated by FlowJo software (Treestar).

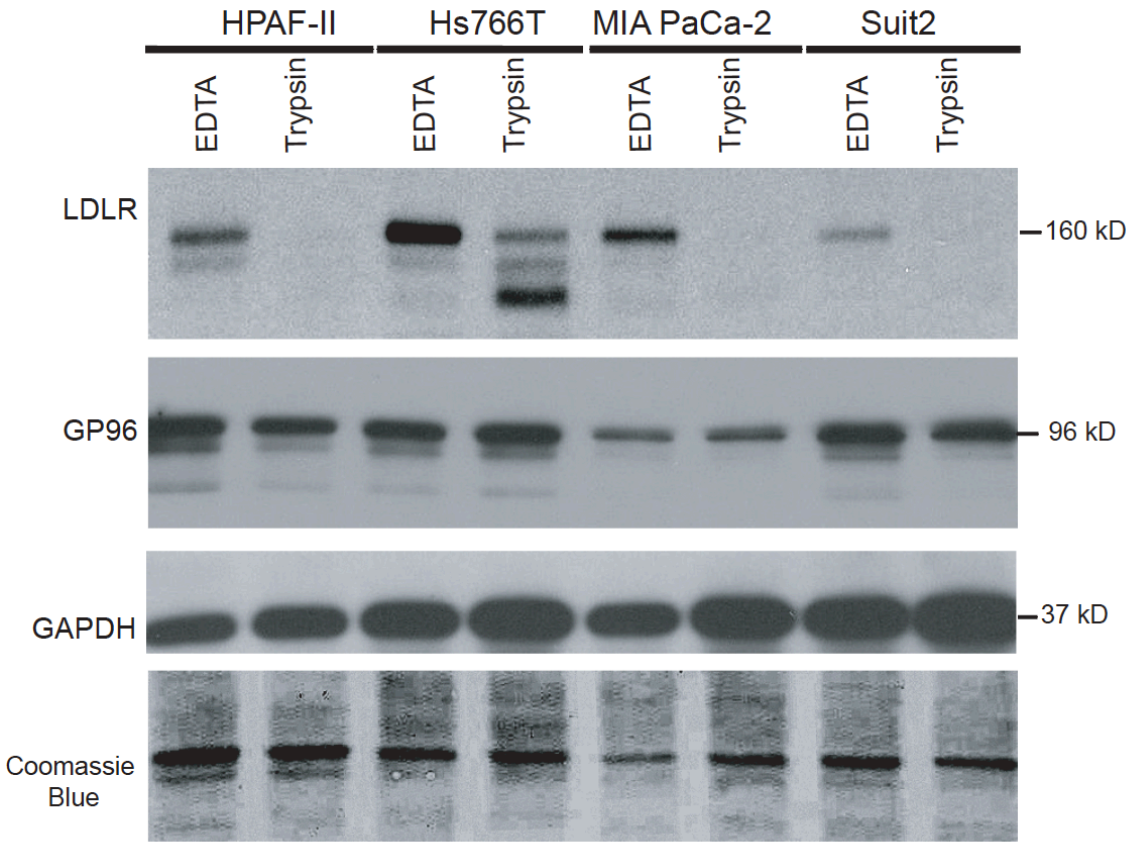


Figure 30: LDLR digestion by trypsin in PDAC cell lines. Cells were treated with PBS with 0.05% trypsin and then protein was isolated to confirm LDLR digestion. Protein was isolated and analyzed by western blot. Protein (kDa) product sizes are indicated on the right. GAPDH and Coomassie blue stain were used to indicate equal loading.

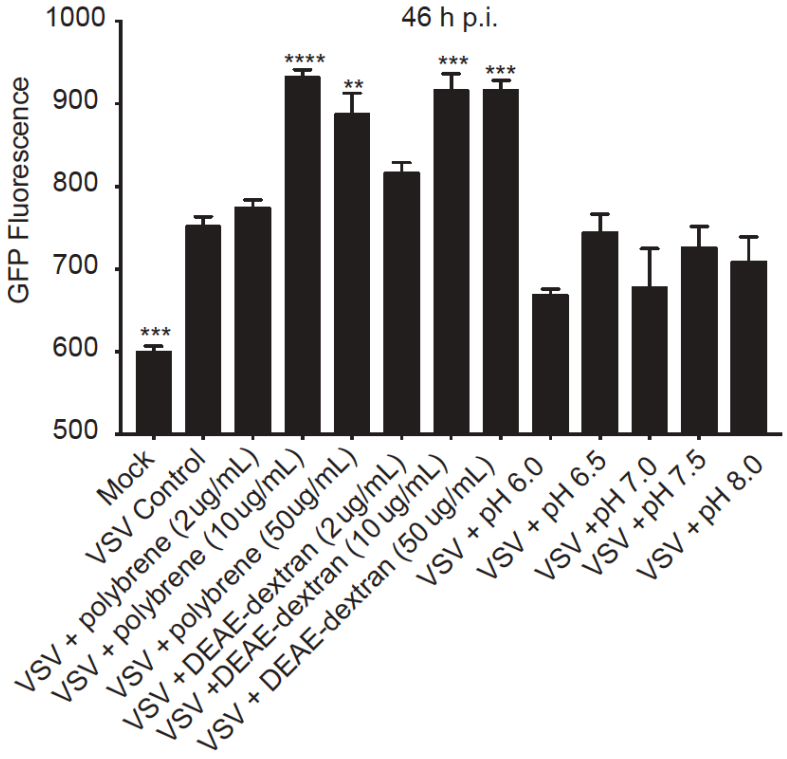


Figure 31: Effect of polycation treatment on VSV infectivity (GFP fluorescence) in HPAF-II. Cells were treated with polybrene, DEAE dextran or different pH at the indicated concentrations and then incubated for 1 h at 37°C with VSV-ΔM51-GFP at the indicated MOI (based on HPAF-II). GFP fluorescence was analyzed at 46 h p.i. Assay was done in triplicate and data represent the mean ± standard error of mean. Conditions were compared using a 1-way ANOVA followed by the Dunnett posttest for comparison to "+VSV Control". *, $p<0.05$; **, $P<0.01$; ***, $p<0.001$; ****, $p<0.0001$.

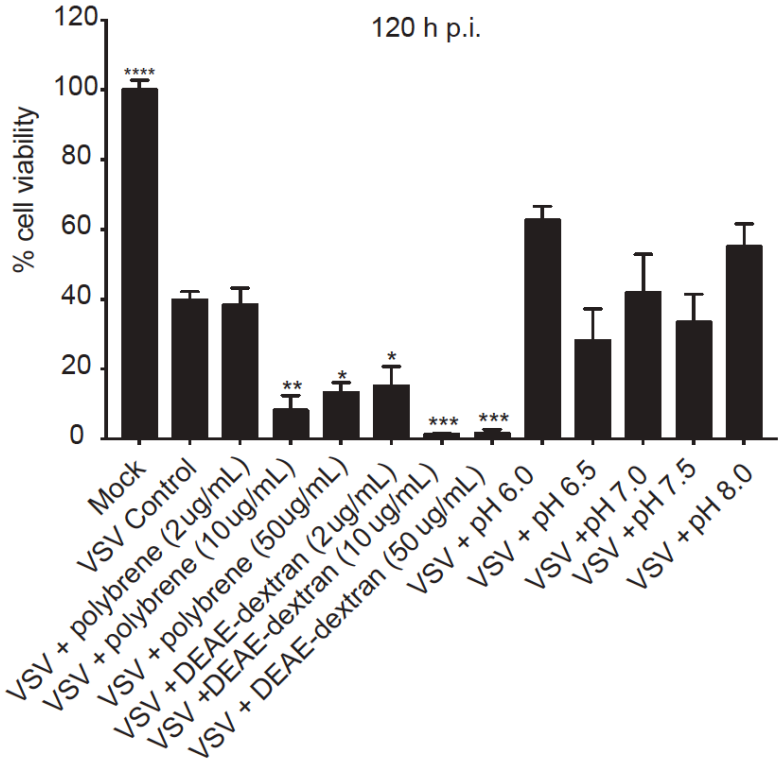


Figure 32: Effect of polycation treatment on VSV-mediated oncolysis in HPAF-II. Cells were treated with polybrene, DEAE dextran or different pH at the indicated concentrations and then incubated for 1 h at 37°C with VSV-ΔM51-GFP at the indicated MOI (based on HPAF-II). 5 days p.i. cells were analyzed for viability by MTT. Assay was done in triplicate and data represent the mean ± standard error of mean. Conditions were compared using a 1-way ANOVA followed by the Dunnett posttest for comparison to "+VSV Control". *, $p<0.05$; **, $P<0.01$; ***, $p<0.001$; ****, $p<0.0001$.

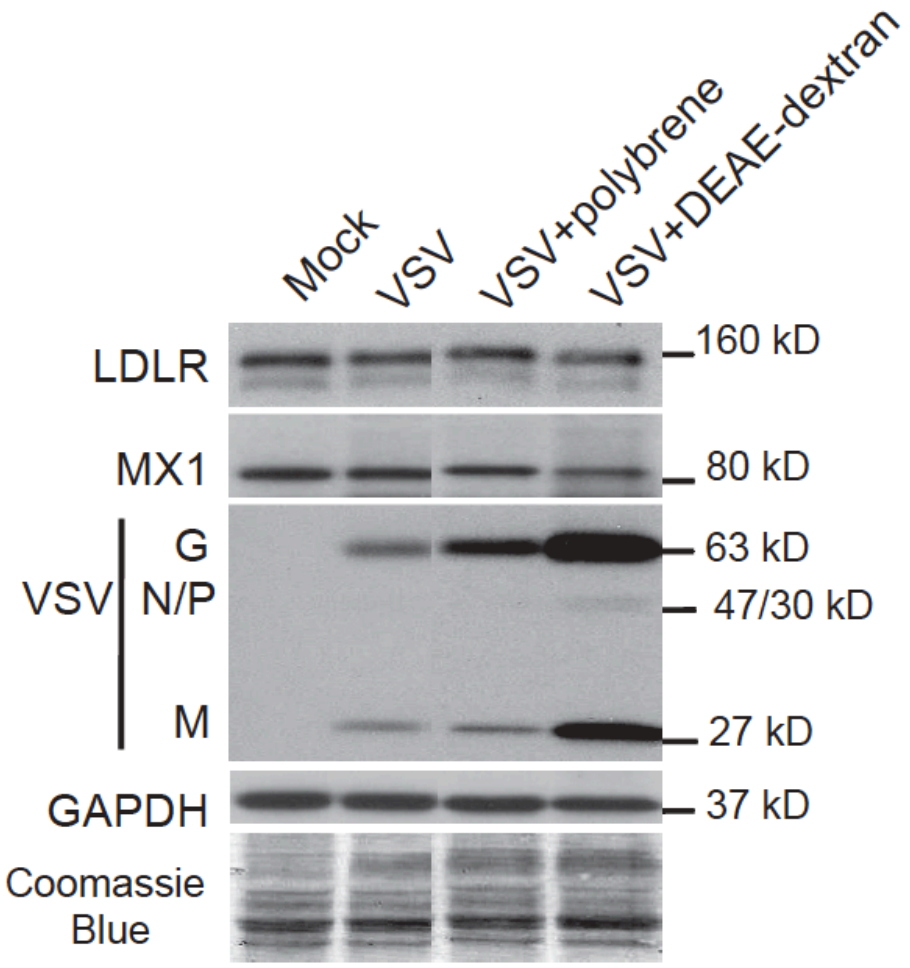


Figure 33: Effect of polycation treatment on LDLR expression and VSV attachment in HPAF-II. Cells were pretreated with polybrene (10 µg/ml) and DEAE-dextran (10 µg/ml) and were then incubated for 1h at 4°C with VSV-ΔM51-eqFP650. MOI was 250 based on MiaPaCa-2. Protein isolates were used for western blot analyzes. Protein (kDa) product sizes are indicated on the right. GAPDH and Coomassie blue stain were used to indicate equal loading.

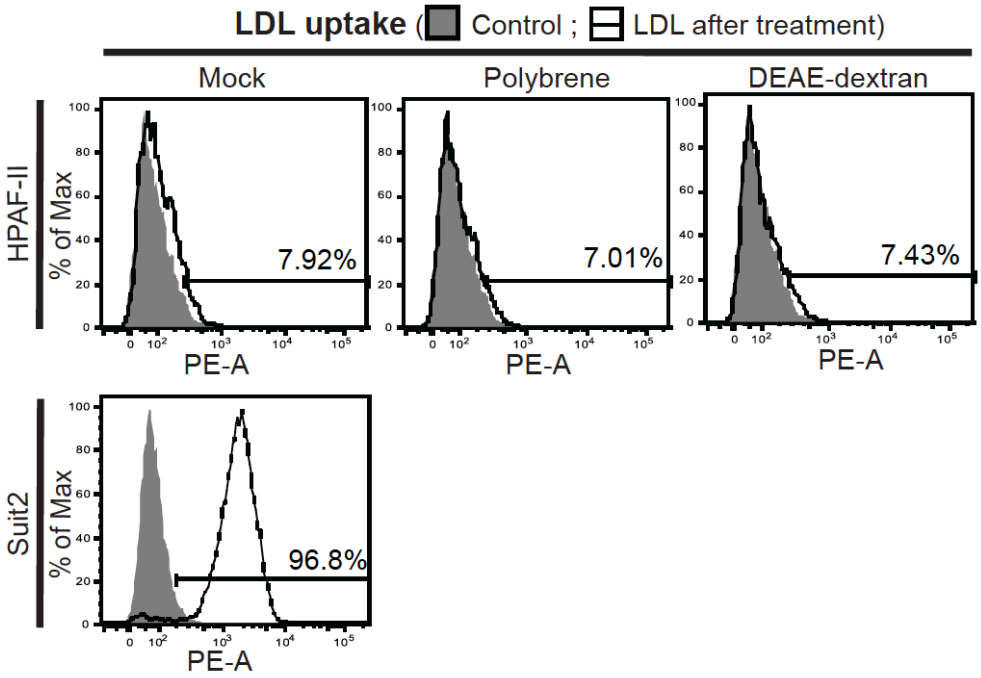


Figure 34: Effect of polycation treatment on LDL uptake in HPAF-II. Cells were pretreated with polybrene (10 µg/ml) and DEAE-dextran (10 µg/ml) and then incubated for 4 h at 37°C with fluorescently labeled LDL. Samples were analyzed by FACS using the PE-A channel. "Control": fluorescently labeled LDL was not added; "LDL": fluorescently labeled LDL was added. Treatments are indicated on top of each histogram. The "Mock" samples are the same than in Fig. 22. Gated populations are positive for LDL uptake (% of LDL-positive cells is indicated above the gate line). MFI stands for "Mean Fluorescent Intensity" for each population and was calculated by FlowJo software (Treestar).

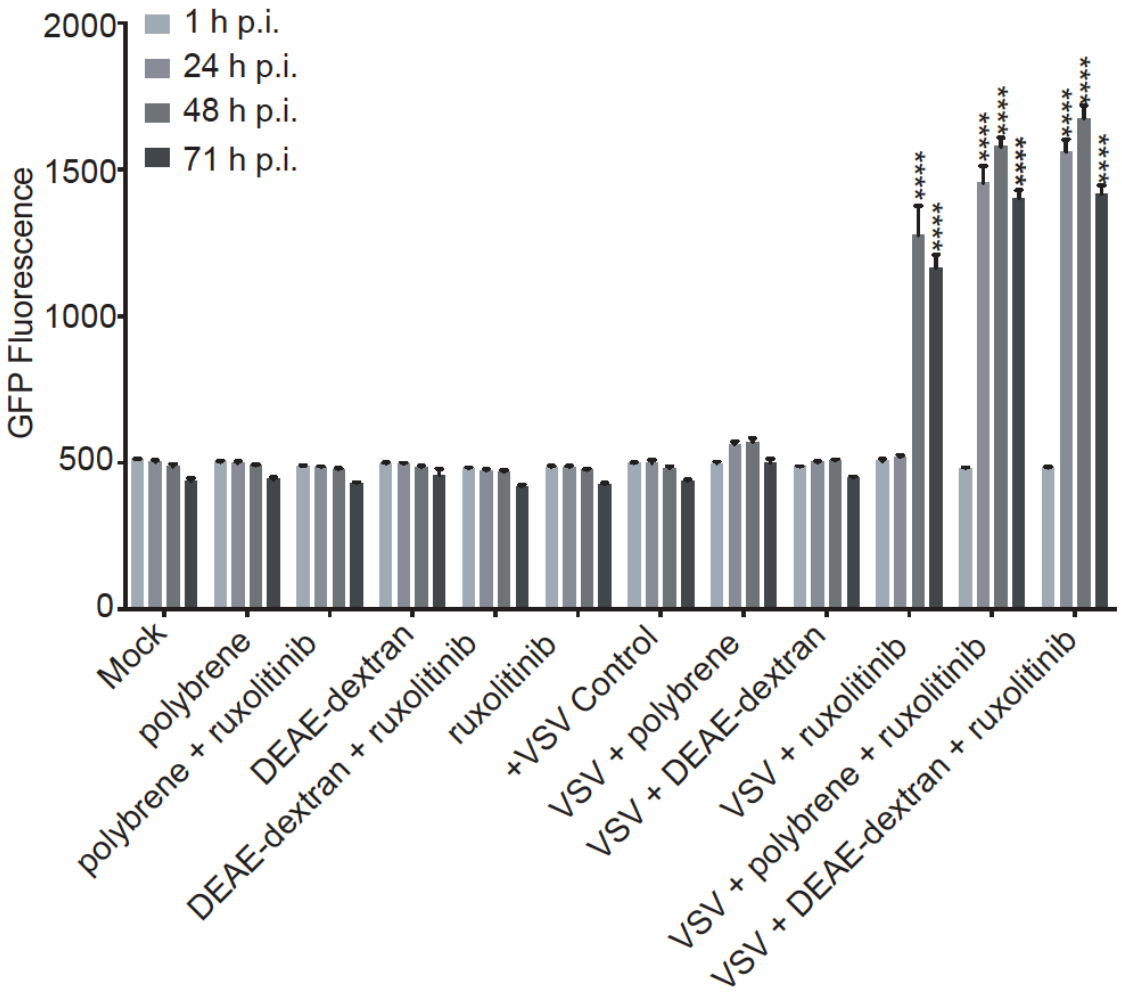


Figure 35: Effect of combining polycations with ruxolitinib on VSV infectivity (GFP fluorescence) in HPAF-II. Cells were pretreated with 10 µg/ml polybrene or DEAE-dextran or mock-treated for 30 min, then VSV-ΔM51-GFP at the indicate MOI (based on HPAF-II) was added in the presence of polycations (or mock treated) for 1 h at 37 °C, followed by media removal and washes with PBS, and then cells were incubated in the presence of 2.5 µM ruxolitinib or mock treatment. VSV infection-associated GFP fluorescence was monitored for 71 h. Assay was done in triplicate and data represent the mean ± standard error of mean. For GFP fluorescence conditions were compared using a 2-way ANOVA followed by the Dunnett posttest for comparison to Mock. ****, $p<0.0001$.

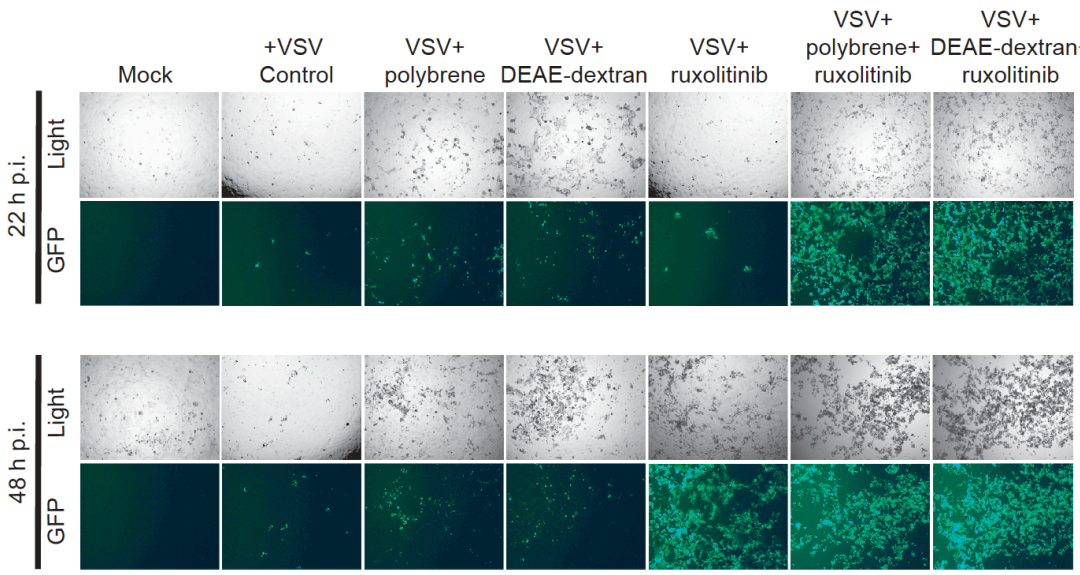


Figure 36: Effect of combining polycations with ruxolitinib on VSV infectivity (microscopy pictures) in HPAF-II. Cells were pretreated with 10 µg/ml polybrene or DEAE-dextran or mock-treated for 30 min, then VSV-ΔM51-GFP at the indicate MOI (based on HPAF-II) was added in the presence of polycations (or mock treated) for 1 h at 37 °C, followed by media removal and washes with PBS, and then cells were incubated in the presence of 2.5 µM ruxolitinib or mock treatment. Pictures were taken at 22 and 48 h p.i.

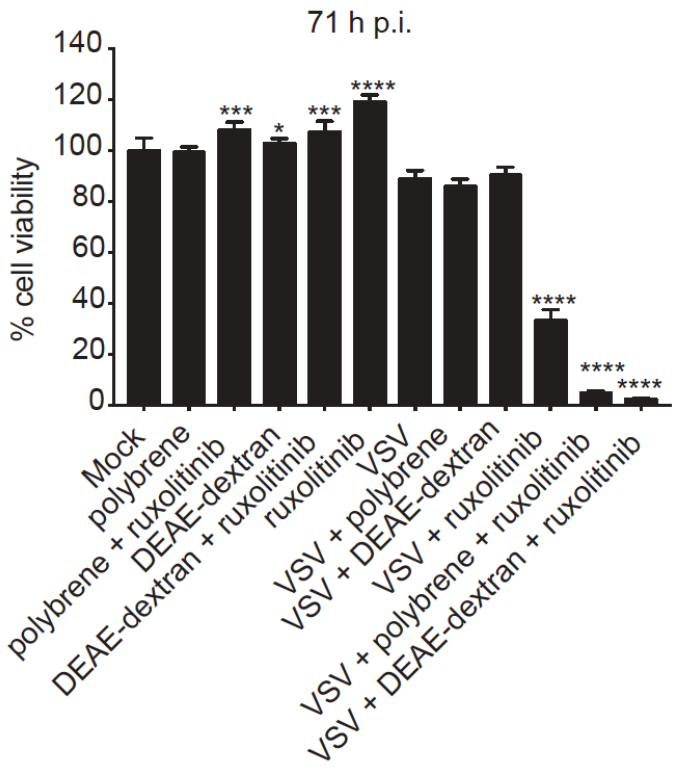


Figure 37: Effect of combining polycations with ruxolitinib on VSV-mediated oncolysis in HPAF-II. Cells were pretreated with 10 µg/ml polybrene or DEAE-dextran or mock-treated for 30 min, then VSV-ΔM51-GFP at the indicate MOI (based on HPAF-II) was added in the presence of polycations (or mock treated) for 1 h at 37 °C, followed by media removal and washes with PBS, and then cells were incubated in the presence of 2.5 µM ruxolitinib or mock treatment. MTT assay was performed at 71 h to determine cell viability. Assay was done in triplicate and data represent the mean ± standard error of mean. Conditions were compared using a 1-way ANOVA followed by the Dunnett posttest for comparison to Mock. *, $p<0.05$; ***, $p<0.001$; ****, $p<0.0001$.

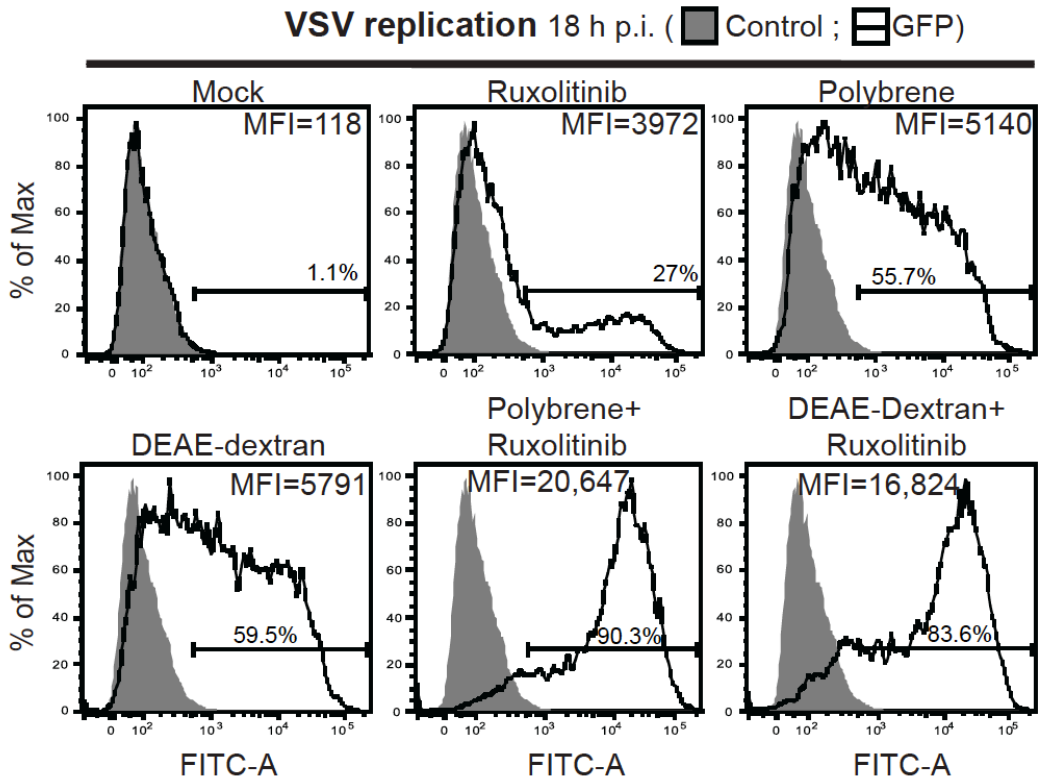


Figure 38: Effect of combining polycations with ruxolitinib on initial infection in HPAF-II. Cells were pretreated with 10 µg/ml polybrene or DEAE-dextran or mock-treated for 30 min, then VSV-ΔM51-GFP (cell specific MOI 0.001 on HPAF-II) was added in the presence of polycations (or mock treated) for 1 h at 37 °C, followed by media removal and washes with PBS, and then cells were incubated in the presence of 2.5 µM ruxolitinib or mock treatment for 18 h. Percentage of GFP positive cells was determined by flow cytometry at 18 h p.i using the FITC-A channel. Gated populations are positive for GFP. "Control" represents cells alone and "GFP" represents GFP positive cells in which VSV replication occurred. Gated populations are positive for VSV replication. MFI stands for "Mean Fluorescent Intensity" for each population and was calculated by FlowJo software (Treestar).

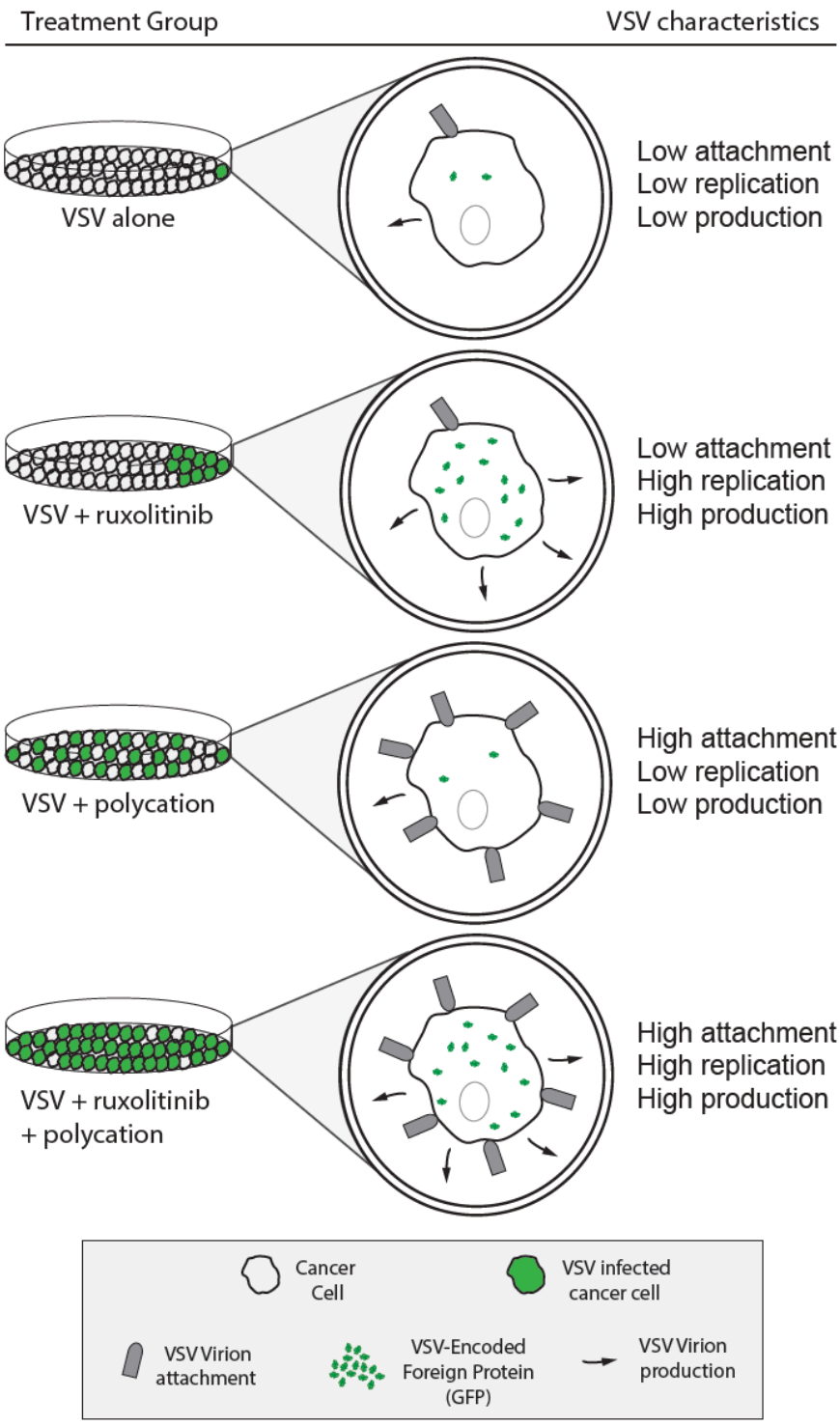


Figure 39: Summary figure of treatment groups and their effect on VSV characteristics. Treatment conditions are indicated underneath each well (on the left). Green cells represent infected cancer cells. On the right, the effect of these treatments on VSV characteristics (attachment, replication and production) is represented. This illustration was created by Sébastien Alexandre Felt.

# CHAPTER 4: DISSERTATION SUMMARY

In chapter 2, we investigated apoptosis activation in human PDAC cells in response to three different VSV recombinants expressing ΔM51 or wild type M protein. We demonstrated that VSV-ΔM51 is a more potent inducer of apoptosis in the majority of PDAC cells than VSV with WT M, and that it activates apoptosis mainly via the type II extrinsic pathway. We also showed that resistance of some PDAC cell lines to VSV-mediated oncolysis is not due only to type I IFN responses that limit virus replication (Moerdyk-Schauwecker et al., 2013; Murphy et al., 2012), but also to cellular defects in apoptosis.

Our study examined VSV-mediated apoptosis in pancreatic cancer cells for the first time. Previous studies in other systems showed VSV-M51R mutation activated apoptosis mainly via the caspase 8 dependent extrinsic pathway (Cary et al., 2011; Gaddy DF and and Lyles, 2005; Gaddy DF, 2007), while VSV encoding WT M protein typically activated apoptosis through the caspase 9 dependent intrinsic pathway (Balachandran et al., 2001; Balachandran et al., 2000; Gaddy DF and and Lyles, 2005)**.** However, this distinction is not absolute as either or both pathways can be activated during infection with either variant (Balachandran et al., 2001; Cary et al., 2011). Our data show a similar situation in PDAC cells. Despite similar levels of replication in most cell lines (except for Hs766T and HPAF-II which are highly resistant to VSV), VSV-GFP virus induced both intrinsic and extrinsic pathways in most PDAC cell lines, but only the intrinsic pathway

in Capan-2 and AsPC-1 cell lines. This suggests that cellular factors can determine the mechanism of apoptosis mediated by the same virus. However, viral factors can also determine the mechanism of apoptosis. For example, compared to VSV-GFP, VSV-ΔM51-GFP caused significantly stronger apoptosis in Suit2, Capan-2, T3M4 and AsPC-1 cells, even though both viruses replicated to similar levels in these 4 cell lines.

The role of type I IFN signaling and ISGs in apoptosis induction in PDAC cells is not well understood. Consistent with the anti-proliferative and pro-apoptotic effects generally associated with type I IFN responses, treatment with exogenous type I IFN has been shown to induce apoptosis in at least some PDAC cell lines, although induction efficiency varied considerably across cell lines (Booy et al., 2014). Many ISGs including Fas ligand, TRAIL and several IRFs, have known pro-apoptotic effects (Chawla-Sarkar et al., 2003; Cheon et al., 2014). Some antiviral ISGs, including OAS-RNase L and PKR, have also been shown to have pro-apoptotic roles (Clemens, 2003). However, other ISGs (for example, IFI6, also known as G1P3 or ISG6-16) are known to be anti-apoptotic (Cheriyath et al., 2007; Cheriyath et al., 2011).

The role of ISGs in VSV-mediated apoptosis is also complex. PKR in particular has been shown to be important for efficient induction of apoptosis by VSV-M51R mutation in mouse fibrosarcoma cells (Gaddy DF, 2007). In contrast, PKR does not appear to be important for induction of apoptosis by VSV with WT M protein (Balachandran et al., 2000). Moreover, cellular PKR expression was associated with resistance to WT VSV infection, apoptosis induction and killing (Balachandran et al., 2000). Together, these studies suggest that ISG expression is beneficial for apoptosis induction by VSV-M51

mutants (due to PKR and other factors), but negatively impacts apoptosis induction by VSV expressing WT M due to inhibitory effects on viral replication.

Our results are consistent with induction/enhancement of apoptosis by ISGs in PDAC cell lines permissive to VSV and showing VSV inducible type I IFN signaling (Figure 5 and Table 1) (Moerdyk-Schauwecker et al., 2013). In these cell lines, VSV-ΔM51-GFP was a more effective apoptosis inducer than VSV recombinants expressing WT M. Unlike WT M protein, M protein with an M51 mutation is unable to block type I IFN mediated antiviral responses in infected cells (Stojdl DF et al., 2003) and allows for expression of ISGs, including pro-apoptotic ISGs, in response to infection.

In contrast to PDACs with VSV inducible ISG expression, it is likely that constitutive high-level expression of ISGs in VSV-resistant PDAC cell lines negatively impacts VSV-mediated apoptosis by dramatically inhibiting virus replication (regardless of M protein variant). Furthermore, the pattern of ISG expression differs in response to acute virus infection or IFN treatment as compared to chronic virus infection (Li et al., 2014; Wilson et al., 2013) or diseases involving chronic type I IFN production, including some cancers (Cheon et al., 2014). Thus, the role of ISGs in apoptosis induction in response to VSV infection may be different in cancers with constitutive versus inducible expression of ISGs.

Importantly, our data also show that type I IFN responses are not required for robust VSV induced apoptosis in PDAC cells. Two PDAC cell lines defective in type I IFN signaling in response to VSV, MIA PaCa-2 and Capan-1, supported the highest levels of caspase cleavage in response to VSV infection regardless of M protein status. In this

instance, the absence of the pro-apoptotic effect of type I IFN responses is likely compensated for by the uninhibited replication of virus.

Overall, VSV-ΔM51-GFP is a potent inducer of apoptosis in the majority of PDAC cell lines. This is significant, as PDACs are known to be highly resistant to a variety of chemotherapies in part because of defects in apoptosis (Hamacher et al., 2008; Neesse et al., 2012; Roder et al., 2011). This result not only speaks to the potential of VSV-ΔM51-GFP as an oncolytic agent but also suggests it may also be useful as a sensitizer to chemotherapy. In several cancers, VSV-M51R infection improved doxorubicin treatment by facilitating degradation of the anti-apoptotic protein Mcl-1 (Schache et al., 2009), while another study showed that WT VSV in combination with gemcitabine increased apoptosis and increased killing of lung cancer cell lines *in vitro* and *in vivo* (Li et al., 2004). If successful, such combination therapies could allow for equal or greater efficacy at lower doses of chemotherapeutic drug, reducing side effects in patients.

Furthermore, while VSV-ΔM51-GFP was a potent inducer of apoptosis in most PDAC cells, apoptosis had little or no antiviral effect on VSV-ΔM51-GFP replication in PDAC cells. This was also previously demonstrated for VSV in several other systems (Balachandran et al., 2001; Hobbs et al., 2003; Hobbs et al., 2001; Sharif-Askari et al., 2007) and is most likely due to VSV's relatively fast replication cycle in most cells, allowing the virus to complete its replication cycle prior to cell death. Interestingly, other studies have shown that inhibition of apoptosis can increase VSV replication (Chattopadhyay et al., 2011; Desforges et al., 2002; Sharif-Askari et al., 2007), indicating that small variations in viral replication or apoptosis kinetics likely determine whether or not an apoptotic response negatively impacts VSV replication. Given this, while cancer

related apoptosis defects can be a therapeutic barrier, they may actually benefit VSV oncolytic therapy in many cases by allowing VSV to "win" the race against this antiviral mechanism. Apoptosis defects may also be another mechanism increasing VSV specificity for cancerous versus normal tissue as has been shown for other oncolytic viruses (Liu and Kirn, 2005). In general, induction of apoptosis does not seriously impact VSVs ability to replicate in cancer cells, making it a promising oncolytic virus and suggesting that cotherapy with agents that induce and/or enhance apoptosis should be feasible.

While VSV-ΔM51-GFP was a potent inducer of apoptosis and subsequent cell death in most PDAC cells, this was not the case in some PDAC cell lines. Three PDAC cell lines, Hs766T, HPAC and HPAF-II, with the strongest resistance to VSV-ΔM51-GFP mediated apoptosis were known from our previous studies to have constitutive expression of some antiviral IFN-stimulated genes (Moerdyk-Schauwecker et al., 2013; Murphy et al., 2012). At least in case of HPAC cells, failure to undergo apoptosis was not due to low VSV replication levels. The inability of Hs766T and HPAF-II cells to undergo apoptosis could be due to limited VSV-ΔM51-GFP replication. However, increasing viral replication via inhibition of constitutive type I IFN responses did not improve induction of apoptosis. It should be noted that we cannot rule out that stimulation of VSV replication using JAK Inh. I was counteracted by simultaneous inhibition of the potentially pro-apoptotic effects of type I IFN signaling. In particular, this case is distinct from that of MIA PaCa-2 and Capan-1, as while JAK Inh. I facilitates virus replication and spread, initiation of infection in resistant cell lines remains relatively inefficient (Moerdyk-Schauwecker et al., 2013).

In addition to resisting apoptosis induction by VSV, Hs766T and HPAF-II were also resistant to apoptosis when treated with Fas activating antibody. Therefore, our data indicate two separate mechanisms behind resistance of PDAC cells to VSV-ΔM51-GFP mediated apoptosis: (1) virus-specific defects in apoptosis, as seen with HPAC, where Fas activating antibody can induce apoptosis but virus-induced apoptosis is significantly inhibited, or (2) general defects in Fas receptor mediated apoptosis, as seen with the Hs766T and HPAF-II cells, where apoptosis cannot be induced effectively by virus or Fas activating antibody.

As PDAC cell lines that evaded VSV-ΔM51-GFP mediated apoptosis activation showed no or low levels of cleaved caspase 8 and 9, it is likely that cellular factors upstream of these initiator caspases are involved in this resistance (Hanahan and Weinberg, 2011; Kelly and Strasser, 2011). As TRAIL was relatively effective in inducing apoptosis in all these cell lines, the defect(s) may primarily impact the Fas receptor mediated pathway. Fas receptor was expressed at lower levels in Hs766T cells than in many other cell lines, which may contribute to its apoptosis resistance. Evasion of apoptosis by PDACs is commonly impacted by overexpression of Fas decoy receptors (DcR3), Fas associated phosphatase-1 (FAP-1), and/or FLICE-inhibitory protein c-FLIP (Hamacher et al., 2008; Neesse et al., 2012; Roder et al., 2011), all of which target events upstream of caspase 8. Our future studies will examine these factors.

Although we did not find a relationship between expression of Bcl-2 proteins and resistance of PDAC cell lines to VSV-ΔM51-mediated oncolysis, further studies are also needed to determine the influence of these or other regulators downstream of caspase 8 and 9 such as inhibitors of apoptosis (IAPs) (Hamacher et al., 2008). Our future studies

will also examine the role of other types of cell death in VSV infected PDACs, particularly autophagy as VSV has already been reported to induce autophagy in different types of cancer cells (Schache et al., 2009).

In Chapter 3, we examined a possible role of virus attachment in the resistance of some human PDAC cell lines to VSV, as it is the first critical stage for a successful viral infection. We demonstrated that HPAF-II, the most resistant PDAC cell line, in addition to an upregulated type I IFN signaling and a constitutive expression of ISGs, also shows impaired VSV attachment. This result was surprising as VSV is known for its pantropism and the ability to infect virtually any cell line (of vertebrate or invertebrate origin) in the lab (Hastie et al., 2013b). Pretreating HPAF-II cells with ruxolitinib did not improve VSV attachment indicating that type I IFN signaling does not play a major role in VSV attachment. This is consistent with the fact that another VSV-resistant PDAC cell line Hs766T, which also constitutively expresses a similar subset of ISGs (Hastie et al., 2016), did not show a defect in VSV attachment. In general, these results suggest that HPAF-II cells are highly resistant to VSV because they are not only non-permissive to VSV replication due to their constitutive antiviral state, but also non-susceptible to VSV due to impaired virus attachment, which is type I IFN independent.

LDLR has been shown to be one of the receptors for VSV (Amirache et al., 2014; Ammayappan et al., 2013; Finkelshtein et al., 2013a) and other viruses, such as hepatitis C virus, rhinovirus, and Rous sarcoma virus (Agnello et al., 1999; Bates et al., 1993; Hofer et al., 1994). Therefore, our study examined if HPAF-II cells have a defect in LDLR expression or functionality, which could explain ineffective VSV attachment. In

agreement with our hypothesis, HPAF-II did show lower LDLR expression and dramatically lower LDL uptake.

As of today, more than a thousand different types of mutations have been found in the LDLR protein, which were categorized into 6 classes (Marais, 2004). Class 1 mutations lead to no LDLR expression. Class 2 mutations retard the maturation of the LDL receptor by glycosylation. Class 3 mutations lead to LDLR not being able to bind its ligand. Class 4 mutations lead to LDLR not being able to internalize. Class 5 mutations lead to LDL receptor degradation that prevents it from reaching the cell surface and from recycling to the cell surface. Class 6 mutations lead to the failure of directing LDL receptors to the basolateral surface of polarized cells (Marais, 2004). With mutations being so common in LDLR, we hypothesized that HPAF-II could have a mutation in LDLR, which would explain its defects in LDL uptake and VSV attachment. However, our sequence analysis of LDLR mRNA showed no mutations affecting LDLR amino acid sequence in HPAF-II (or other 3 tested PDAC cell lines), suggesting that other factor(s) are responsible for lower activities of LDLR in HPAF-II cells.

As HPAF-II showed lower LDLR expression and LDL uptake, cells were pretreated with statins to improve the LDLR expression and LDL uptake. Statins block the pathway for synthesizing cholesterol in the liver and some other cell types, including cancer cells (Pahan, 2006). One consequence of the decrease in the produced cholesterol is that cells compensate for it by increasing expression of LDLR to uptake cholesterol from the plasma (Vaziri and Liang, 2004). Although all four tested statins strongly increased LDLR expression, this increase did not improve VSV attachment in HPAF-II. Moreover,

statins also did not improve LDL uptake. These results indicate that LDLR is dysfunctional or at least less functional in this cell line.

Taken together, the impaired VSV attachment and defective uptake of LDL in HPAF-II, were not determined by mutations or a relatively lower LDLR expression levels in this cell line, but via some other mechanism(s). Dysfunctionality of the LDLR receptor could be due to the absence or catalytic inactivity of GP96, an important chaperone of LDLR (Weekes et al., 2012). GP96 is required for normal cell binding of VSV (Bloor et al., 2010) and human herpesvirus 6A (HHV-6) binding (Prusty et al., 2014), likely because of its function as an LDLR chaperone. However, our analysis showed that HPAF-II cells express normal levels of full-length GP96 (Fig. 30), indicating that there must be another factor determining LDLR dysfunctionality.

Many factors could inhibit LDLR functionality (LDL uptake). HPAF-II cells show a mature LDLR band on the western blot but also a lower-weight LDLR band that could indicate an immature LDLR-precursor or LDLR degradation. Overexpression of PCSK9, a secretory serine protease that interacts with LDLR, has been shown to accelerate the degradation of LDLR (Maxwell et al., 2005). Interestingly, when HPAF-II was treated with SBC-115076, a potent PCSK9 antagonist, the lower band in HPAF-II disappeared indicating that PCSK9 could be overexpressed in HPAF-II. However, this mechanism cannot explain LDLR dysfunctionality in HPAF-II cells, as the SBC-115076 treatment did not improve LDL uptake or VSV attachment. It can also cannot be ruled out that the LDLR functionality could be affected by some abnormalities in posttranslational modifications of LDLR in HPAF-II cells, which is consistent with the lower LDLR band seen only in cell lysates from HPAF-II, but not other tested PDAC cell lines. Previous

studies have shown that *O*-glycosylation in the stem region of LDLR is important for cell surface expression and stability of this receptor. Absence of *O*-glycosylation in the stem region can lead to proteolytic cleavage and the release into the medium of the bulk of the N-terminal extracellular domain of the receptor (Kingsley et al., 1986; Kozarsky et al., 1988). It is possible that HPAF-II is lacking *O*-glycosylation, however it is important to note that HPAF-II did not release the most sLDLR into the medium, compared to other tested PDAC cells. It has also been suggested that the N-terminal segment of LDLR also has *O*-glycans (Davis et al., 1986). The same group also demonstrated that *O*-glycosylation at the N-terminal segment of LDLR did not affect LDLR cell surface expression and LDL binding/internalization (Davis et al., 1986). However, another group has shown in another cell line that N-terminal *O*-glycosylation is important for LDLR function as it showed an effect on LDL binding (Yoshimura et al., 1987). They also determined that the molecular mass of a mature LDLR in SDS-polyacrylamide gels was reduced about 5000 Daltons when the N-terminal segment of LDLR was not *O*-glycosylated (Yoshimura et al., 1987). We did not see such a large shift on our gels, however we used 10% gel, whereas in that study a 6% gel was used.

It is also possible that a negative factor on the cell surface of HPAF-II interferes with LDL uptake and VSV attachment, and even with LDLR antibody binding in our FACS assay. Interestingly, MUC1 mucin overexpression in some PDAC cell lines, including HPAF-II, have been shown to limit the uptake of anticancer drugs by tumor cells (Kalra and Campbell, 2007, 2009). It is possible that MUC1 masks LDLR and prevents both VSV attachment and LDL uptake. Future studies will examine all these possibilities.

Finally, previous studies have shown that sLDLR secretion can inhibit VSV (Fischer et al., 1994; Fischer et al., 1993) and also HCV (Albecka et al., 2012) infection. Furthermore, other soluble LDLR family members, like soluble Very-Low-Density Lipoprotein Receptor, have been shown to inhibit rhinovirus (Marlovits et al., 1998). We confirmed that sLDLR has also an inhibitory effect on VSV infection in PDAC cell lines, however HPAF-II did not secrete higher levels of sLDLR, compared to other tested PDAC cell lines. Our data did not suggest any link between sLDLR secretion and VSV attachment levels indicating that sLDLR does not play a major role at inhibiting VSV attachment.

As statin-mediated increase in LDLR expression did not improve VSV attachment or LDLR functionality, we evaluated LDLR independent mechanisms to improve VSV attachment. While LDLR is suggested as one of the receptors for VSV (Finkelshtein et al., 2013a), previous studies have also suggested that phosphatidylserine (Carneiro et al., 2006; Coil and Miller, 2004; Schlegel et al., 1983), sialoglycolipids (Schloemer and Wagner, 1975), heparan sulfate (Guibinga et al., 2002) and virus/cell membrane electrostatic interactions (Bailey et al., 1984; Conti et al., 1991) may play an important role in VSV attachment. We employed a cell surface "shaving" technique with trypsin to remove surface LDLR, and our data showed that VSV can indeed attach to PDAC cells in an LDLR-independent VSV manner. We then decided to test two commonly used polycations, polybrene or DEAE-dextran, which previously have shown to improve VSV attachment (Bailey et al., 1984; Conti et al., 1991), and also used in various application using VSV-G pseudotyped lentiviruses (Denning et al., 2013; Reiser et al., 1996; Yee et al., 1994). Adding these polycations strongly improved VSV attachment, VSV infection

and VSV induced cell death. These improvements in VSV attachment were LDLR independent as the polycations had no effect on LDL uptake or LDLR expression.

As the cell and virus lipid membrane both possess net-negative charges, it is suggested that polycations act by counteracting repulsive electrostatic effects and thus improving attachment. Early studies have shown that treatment of HeLa cells with polybrene has to be done before the infection and/or during the infection but not after the infection with VSV (Conti et al., 1991; Matlin et al., 1982). The study concluded that polybrene must have an effect on VSV binding to cells potentially by improving virus/receptor interaction. Studies on DEAE-dextran made similar observations and concluded that alterations in cell surface charge distribution enhance VSV attachment (Bailey et al., 1984; Conti et al., 1991). More recent studies using retroviruses observed that polybrene increased their attachment by 10-fold (Davis et al., 2002). Interestingly, this enhancement was receptor and virus envelope independent, as retrovirus adsorption occurred equivalently on receptor positive and negative cells, as well as with envelope positive and negative ("bald") virus particles. The study concluded that electrostatic interactions play an important role in mediating early virus-cell interactions (Davis et al., 2002).

Our data not only show that polycations strongly improve VSV attachment to HPAF-II cells, but we also successfully used a novel triple combination treatment to break multiple mechanisms of resistance of HPAF-II cells to VSV. We have previously shown that adding pre-treatment of cells with ruxolitinib (compared to post-treatment only) did not change the kinetics of VSV replication, suggesting that ruxolitinib had a modest effect on the initial infection but mainly facilitated secondary infection via inhibition of

antiviral signaling in PDAC cells (Cataldi et al., 2015; Hastie et al., 2016). Here, combining polycations (improving initial infection) with ruxolitinib (improving viral replication) did not only improve overall VSV replication and oncolysis but also accelerated VSV replication kinetics by 24 h, compared to ruxolitinib only treatment.

The primary goal of this study was to determine if VSV attachment could be a limiting factor in VSV-based oncolytic virotherapy against PDAC. We demonstrated that VSV attaches significantly less to most resistant PDAC cell line HPAF-II, and this mechanism contributes to the resistance of HPAF-II to VSV infection. Also, for the first time, we show that combining a polycation with a JAK inhibitor can improve the outcome of oncolytic virus treatment *in vitro*. Future experiments will test at least some of these combinations *in vivo* in a clinically-relevant PDAC animal model. Previous studies examining polycations were done in the context of gene therapy to improve viral as well as non-viral gene delivery (Tiera et al., 2011), as inefficient gene delivery is often a major limitation in the success of gene therapy (Aied et al., 2013). The effects of polycations *in vitro* and *in vivo* have been extensively studied for adenovirus-based gene therapy vectors. Several studies in different mouse models have shown that combining adenovirus with different polycations (including DEAE-dextran) can improve adenovirus-mediated gene transfer without any additional toxicity (Gregory et al., 2003; Kaplan et al., 1998; Kushwah et al., 2007; McKay et al., 2000). As polycations improve adenovirus-mediated gene transfer, less virus would have to be used, which would improve the therapeutic index by reducing unwanted responses associated with high doses of virus. On the other hand, multiple reports indicate that polycations could exhibit nonspecific cytotoxicity *in vivo* as well as *in vitro* (Monnery et al., 2017; Zarogoulidis et

al., 2013), with some studies demonstrating unacceptable cytotoxicity for DEAE-dextran (Simmons et al., 1981; Zarogoulidis et al., 2013) and polybrene (Lin et al., 2011; Seitz et al., 1998), at least under some experimental conditions. Therefore, while our study conceptually demonstrates the feasibility of the polycation-mediated improvement of VSV-based OV therapy *in vitro*, future studies are needed to compare polybrene and DEAE-dextran to other polycations that could be used safely and effectively *in vivo* in combination with VSV and ruxolitinib. For instance, the non-specific cytotoxicity of polycations is already being addressed currently through development of biodegradable polycations (Park et al., 2006). We envision that polycations would be particularly useful during initial infection, especially in context of intratumoral injection, in maximizing the number of initially infected cells, while ruxolitinib would stimulate replication and spread of the virus within tumors.

In regard to ruxolitinib, this drug was recently approved by the FDA for the treatment of patients with intermediate or high-risk myelofibrosis (Vaddi et al., 2012). It is important to be aware that inhibition of innate antiviral responses by ruxolitinib or other inhibitors of antiviral response could potentially result in increase of VSV virulence in normal tissues. However, it has recently been shown that ruxolitinib enhanced VSV oncolytic virus treatment *in vivo*, both in subcutaneous as well as orthotopic xenograft mouse models of ovarian cancer, without causing significant additional toxicity (Dold et al., 2016). Moreover, other combined treatments of VSV with inhibitors of antiviral responses were examined *in vivo* and also were shown to be effective and safe. For example, VSV in combination with rapamycin, the inhibitor of mammalian target of rapamycin (mTOR, stimulates type I IFN production via phosphorylation of its effectors)

selectively killed tumor, but not normal cells and increased the survival of immunocompetent rats bearing malignant gliomas. In addition, histone deacetylase (HDAC) inhibitors MS-275 or SAHA reversibly compromised host antiviral responses and enhanced spread of VSV in various cancer types, with no detection of VSV in normal tissues (Nguyên TL, 2008; Shestakova et al., 2001; Shulak et al., 2014). Our future *in vivo* experiments will address the efficacy and safety of the triple combination treatment of VSV with ruxolitinib and a polycation. To fully examine the anticancer abilities and safety of this treatment, it will need to be tested in an immunocompetent *in vivo* system. Unfortunately, our current *in vitro* system, based on clinically-relevant human PDAC, complicates this task, as HPAF-II and other human PDAC cell lines cannot be tested in immunocompetent mice. Also, in our previous study all tested mouse PDAC cell lines had defective type I IFN signaling and were highly permissive to VSV (Hastie et al., 2013a). Currently, we are examining several other mouse PDAC cell lines for their type I IFN status and susceptibility/permissiveness to VSV. Based on this study, we expect to identify VSV-permissive and VSV-resistant mouse PDAC cells lines that could be tested with VSV/ruxolitinib/polycation combinations in immunocompetent mouse model of PDAC. We envision that this novel triple combination (VSV/ruxolitinib/polycation) approach could be used in the future to treat PDAC tumors highly resistant to OV therapy.

# REFERENCES

Aghi, M., Martuza, R.L., 2005. Oncolytic viral therapies - the clinical experience. Oncogene 24, 7802-7816.

Agnello, V., Abel, G., Elfahal, M., Knight, G.B., Zhang, Q.X., 1999. Hepatitis C virus and other flaviviridae viruses enter cells via low density lipoprotein receptor. Proceedings of the National Academy of Sciences of the United States of America 96, 12766-12771.

Ahmed, M., McKenzie, M.O., Puckett, S., Hojnacki, M., Poliquin, L., Lyles, D.S., 2003. Ability of the matrix protein of vesicular stomatitis virus to suppress beta interferon gene expression is genetically correlated with the inhibition of host RNA and protein synthesis. J Virol 77, 4646-4657.

Aied, A., Greiser, U., Pandit, A., Wang, W., 2013. Polymer gene delivery: overcoming the obstacles. Drug Discov Today 18, 1090-1098.

Albecka, A., Belouzard, S., Op de Beeck, A., Descamps, V., Goueslain, L., Bertrand-Michel, J., Terce, F., Duverlie, G., Rouille, Y., Dubuisson, J., 2012. Role of low-density lipoprotein receptor in the hepatitis C virus life cycle. Hepatology 55, 998-1007.

Amirache, F., Levy, C., Costa, C., Mangeot, P.E., Torbett, B.E., Wang, C.X., Negre, D., Cosset, F.L., Verhoeyen, E., 2014. Mystery solved: VSV-G-LVs do not allow efficient gene transfer into unstimulated T cells, B cells, and HSCs because they lack the LDL receptor. Blood 123, 1422-1424.

Ammayappan, A., Peng, K.W., Russell, S.J., 2013. Characteristics of oncolytic vesicular stomatitis virus displaying tumor-targeting ligands. J Virol 87, 13543-13555.

Bailey, C.A., Miller, D.K., Lenard, J., 1984. Effects of DEAE-dextran on infection and hemolysis by VSV. Evidence that nonspecific electrostatic interactions mediate effective binding of VSV to cells. Virology 133, 111-118.

Balachandran, S., Porosnicu, M., Barber, G.N., 2001. Oncolytic activity of vesicular stomatitis virus is effective against tumors exhibiting aberrant p53, Ras, or myc function and involves the induction of apoptosis. J Virol 75, 3474-3479.

Balachandran, S., Roberts, P.C., Brown, L.E., Truong, H., Pattnaik, A.K., Archer, D.R., Barber, G.N., 2000. Essential role for the dsRNA-dependent protein kinase PKR in innate immunity to viral infection. Immunity 13, 129-141.

Baltimore, D., 1971. Expression of animal virus genomes. Bacteriol Rev 35, 235-241.

Barber, G.N., 2004. Vesicular stomatitis virus as an oncolytic vector. Viral Immunol 17, 516-527.

Barnhart, B.C., Alappat, E.C., Peter, M.E., 2003. The CD95 type I/type II model. Semin Immunol 15, 185-193.

Bates, P., Young, J.A., Varmus, H.E., 1993. A receptor for subgroup A Rous sarcoma virus is related to the low density lipoprotein receptor. Cell 74, 1043-1051.

Beisiegel, U., Schneider, W.J., Brown, M.S., Goldstein, J.L., 1982. Immunoblot analysis of low density lipoprotein receptors in fibroblasts from subjects with familial hypercholesterolemia. The Journal of biological chemistry 257, 13150-13156.

Bell, J., McFadden, G., 2014. Viruses for tumor therapy. Cell Host Microbe 15, 260-265.

Birrell, M.A., Hardaker, E., Wong, S., McCluskie, K., Catley, M., De Alba, J., Newton, R., Haj-Yahia, S., Pun, K.T., Watts, C.J., Shaw, R.J., Savage, T.J., Belvisi, M.G., 2005. Ikappa-B kinase-2 inhibitor blocks inflammation in human airway smooth muscle and a rat model of asthma. Am J Respir Crit Care Med 172, 962-971.

Birrell, M.A., Wong, S., Hardaker, E.L., Catley, M.C., McCluskie, K., Collins, M., Haj-Yahia, S., Belvisi, M.G., 2006. IkappaB kinase-2-independent and -dependent inflammation in airway disease models: relevance of IKK-2 inhibition to the clinic. Mol Pharmacol 69, 1791-1800.

Bloor, S., Maelfait, J., Krumbach, R., Beyaert, R., Randow, F., 2010. Endoplasmic reticulum chaperone gp96 is essential for infection with vesicular stomatitis virus. Proceedings of the National Academy of Sciences of the United States of America 107, 6970-6975.

Booy, S., van Eijck, C.H., Dogan, F., van Koetsveld, P.M., Hofland, L.J., 2014. Influence of type-I Interferon receptor expression level on the response to type-I Interferons in human pancreatic cancer cells. Journal of cellular and molecular medicine 18, 492-502.

Brown, C.W., Stephenson, K.B., Hanson, S., Kucharczyk, M., Duncan, R., Bell, J.C., Lichty, B.D., 2009. The p14 FAST protein of reptilian reovirus increases vesicular stomatitis virus neuropathogenesis. J Virol 83, 552-561.

Bukreyev, A., Skiadopoulos, M.H., Murphy, B.R., Collins, P.L., 2006. Nonsegmented negative-strand viruses as vaccine vectors. J Virol 80, 10293-10306.

Carneiro, F.A., Lapido-Loureiro, P.A., Cordo, S.M., Stauffer, F., Weissmuller, G., Bianconi, M.L., Juliano, M.A., Juliano, L., Bisch, P.M., Da Poian, A.T., 2006. Probing the interaction between vesicular stomatitis virus and phosphatidylserine. Eur Biophys J 35, 145-154.

Cary, Z.D., Willingham, M.C., Lyles, D.S., 2011. Oncolytic Vesicular Stomatitis Virus Induces Apoptosis in U87 Glioblastoma Cells by a Type II Death Receptor Mechanism and Induces Cell Death and Tumor Clearance In Vivo. J Virol 85, 5708-5717.

Cataldi, M., Shah, N.R., Felt, S.A., Grdzelishvili, V.Z., 2015. Breaking resistance of pancreatic cancer cells to an attenuated vesicular stomatitis virus through a novel activity of IKK inhibitor TPCA-1. Virology 485, 340-354.

Chattopadhyay, S., Yamashita, M., Zhang, Y., Sen, G.C., 2011. The IRF-3/Bax-mediated apoptotic pathway, activated by viral cytoplasmic RNA and DNA, inhibits virus replication. J Virol 85, 3708-3716.

Chawla-Sarkar, M., Lindner, D.J., Liu, Y.F., Williams, B.R., Sen, G.C., Silverman, R.H., Borden, E.C., 2003. Apoptosis and interferons: role of interferon-stimulated genes as mediators of apoptosis. Apoptosis 8, 237-249.

Chen, Y., Ruan, X.Z., Li, Q., Huang, A., Moorhead, J.F., Powis, S.H., Varghese, Z., 2007. Inflammatory cytokines disrupt LDL-receptor feedback regulation and cause statin resistance: a comparative study in human hepatic cells and mesangial cells. Am J Physiol Renal Physiol 293, F680-687.

Cheon, H., Borden, E.C., Stark, G.R., 2014. Interferons and their stimulated genes in the tumor microenvironment. Semin Oncol 41, 156-173.

Cheriyath, V., Glaser, K.B., Waring, J.F., Baz, R., Hussein, M.A., Borden, E.C., 2007. G1P3, an IFN-induced survival factor, antagonizes TRAIL-induced apoptosis in human myeloma cells. The Journal of clinical investigation 117, 3107-3117.

Cheriyath, V., Leaman, D.W., Borden, E.C., 2011. Emerging roles of FAM14 family members (G1P3/ISG 6-16 and ISG12/IFI27) in innate immunity and cancer. J Interferon Cytokine Res 31, 173-181.

Clarke DK, N.F., Lee M, Johnson JE, Wright K, Calderon P, Guo M, Natuk R, Cooper D, Hendry RM, Udem SA., 2007. Synergistic attenuation of vesicular stomatitis virus by combination of specific G gene truncations and N gene translocations. J Virol 81, 2056-2064.

Clemens, M.J., 2003. Interferons and apoptosis. J Interferon Cytokine Res 23, 277-292.

Coil, D.A., Miller, A.D., 2004. Phosphatidylserine is not the cell surface receptor for vesicular stomatitis virus. J Virol 78, 10920-10926.

Conti, C., Mastromarino, P., Riccioli, A., Orsi, N., 1991. Electrostatic interactions in the early events of VSV infection. Res Virol 142, 17-24.

Das, S.C., Nayak, D., Zhou, Y., Pattnaik, A.K., 2006. Visualization of intracellular transport of vesicular stomatitis virus nucleocapsids in living cells. J Virol 80, 6368-6377.

Davis, C.G., Elhammer, A., Russell, D.W., Schneider, W.J., Kornfeld, S., Brown, M.S., Goldstein, J.L., 1986. Deletion of clustered O-linked carbohydrates does not impair

function of low density lipoprotein receptor in transfected fibroblasts. The Journal of biological chemistry 261, 2828-2838.

Davis, H.E., Morgan, J.R., Yarmush, M.L., 2002. Polybrene increases retrovirus gene transfer efficiency by enhancing receptor-independent virus adsorption on target cell membranes. Biophys Chem 97, 159-172.

Denning, W., Das, S., Guo, S., Xu, J., Kappes, J.C., Hel, Z., 2013. Optimization of the transductional efficiency of lentiviral vectors: effect of sera and polycations. Mol Biotechnol 53, 308-314.

Desforges, M., Despars, G., Berard, S., Gosselin, M., McKenzie, M.O., Lyles, D.S., Talbot, P.J., Poliquin, L., 2002. Matrix protein mutations contribute to inefficient induction of apoptosis leading to persistent infection of human neural cells by vesicular stomatitis virus. Virology 295, 63-73.

Dold, C., Rodriguez Urbiola, C., Wollmann, G., Egerer, L., Muik, A., Bellmann, L., Fiegl, H., Marth, C., Kimpel, J., von Laer, D., 2016. Application of interferon modulators to overcome partial resistance of human ovarian cancers to VSV-GP oncolytic viral therapy. Mol Ther Oncolytics 3, 16021.

Donina, S., Strele, I., Proboka, G., Auzins, J., Alberts, P., Jonsson, B., Venskus, D., Muceniece, A., 2015. Adapted ECHO-7 virus Rigvir immunotherapy (oncolytic virotherapy) prolongs survival in melanoma patients after surgical excision of the tumour in a retrospective study. Melanoma Res 25, 421-426.

Draper, S.J., Heeney, J.L., 2010. Viruses as vaccine vectors for infectious diseases and cancer. Nat Rev Microbiol 8, 62-73.

Ebert O, Harbaran S, Shinozaki K, and Woo, S.L., 2005. Systemic therapy of experimental breast cancer metastases by mutant vesicular stomatitis virus in immune-competent mice. Cancer Gene Therapy 12, 350-358.

Felt, S.A., Moerdyk-Schauwecker, M.J., Grdzelishvili, V.Z., 2015. Induction of apoptosis in pancreatic cancer cells by vesicular stomatitis virus. Virology 474, 163-173.

Finke, S., Conzelmann, K.K., 2005. Recombinant rhabdoviruses: vectors for vaccine development and gene therapy. Curr Top Microbiol Immunol 292, 165-200.

Finkelshtein, D., Werman, A., Novick, D., Barak, S., Rubinstein, M., 2013a. LDL receptor and its family members serve as the cellular receptors for vesicular stomatitis virus. Proc Natl Acad Sci U S A 110, 7306-7311.

Finkelshtein, D., Werman, A., Novick, D., Barak, S., Rubinstein, M., 2013b. LDL receptor and its family members serve as the cellular receptors for vesicular stomatitis virus. Proc Natl Acad Sci USA 110, 7306-7311.

Fischer, D.G., Novick, D., Cohen, B., Rubinstein, M., 1994. Isolation and characterization of a soluble form of the LDL receptor, an interferon-induced antiviral protein. Proc Soc Exp Biol Med 206, 228-232.

Fischer, D.G., Tal, N., Novick, D., Barak, S., Rubinstein, M., 1993. An antiviral soluble form of the LDL receptor induced by interferon. Science 262, 250-253.

Frenzel, A., Grespi, F., Chmelewskij, W., Villunger, A., 2009. Bcl2 family proteins in carcinogenesis and the treatment of cancer. Apoptosis 14, 584-596.

Gadaleta, P., Perfetti, X., Mersich, S., Coulombie, F., 2005. Early activation of the mitochondrial apoptotic pathway in Vesicular Stomatitis virus-infected cells. Virus research 109, 65-69.

Gaddy DF, and Lyles, D.S., 2005. Vesicular stomatitis viruses expressing wild-type or mutant M proteins activate apoptosis through distinct pathways. J Virol 79, 4170-4179.

Gaddy DF, L., D.S., 2007. Oncolytic vesicular stomatitis virus induces apoptosis via signaling through PKR, Fas, and Daxx. J Virol 81, 2792-2804.

Galluzzi, L., Brenner, C., Morselli, E., Touat, Z., Kroemer, G., 2008. Viral control of mitochondrial apoptosis. PLoS Pathog 4, e1000018.

Garber, K., 2006. China approves world's first oncolytic virus therapy for cancer treatment. J Natl Cancer Inst 98, 298-300.

Gregory, L.G., Harbottle, R.P., Lawrence, L., Knapton, H.J., Themis, M., Coutelle, C., 2003. Enhancement of adenovirus-mediated gene transfer to the airways by DEAE dextran and sodium caprate in vivo. Mol Ther 7, 19-26.

Guibinga, G.H., Miyanohara, A., Esko, J.D., Friedmann, T., 2002. Cell surface heparan sulfate is a receptor for attachment of envelope protein-free retrovirus-like particles and VSV-G pseudotyped MLV-derived retrovirus vectors to target cells. Mol Ther 5, 538-546.

Guillaumond, F., Bidaut, G., Ouaissi, M., Servais, S., Gouirand, V., Olivares, O., Lac, S., Borge, L., Roques, J., Gayet, O., Pinault, M., Guimaraes, C., Nigri, J., Loncle, C., Lavaut, M.N., Garcia, S., Tailleux, A., Staels, B., Calvo, E., Tomasini, R., Iovanna, J.L., Vasseur, S., 2015. Cholesterol uptake disruption, in association with chemotherapy, is a promising combined metabolic therapy for pancreatic adenocarcinoma. Proceedings of the National Academy of Sciences of the United States of America 112, 2473-2478.

Hamacher, R., Schmid, R.M., Saur, D., Schneider, G., 2008. Apoptotic pathways in pancreatic ductal adenocarcinoma. Mol Cancer 7, 64.

Hammill, A.M., Conner, J., Cripe, T.P., 2010. Oncolytic virotherapy reaches adolescence. Pediatric blood & cancer 55, 1253-1263.

Hanahan, D., Weinberg, R.A., 2011. Hallmarks of cancer: the next generation. Cell 144, 646-674.

Hastie, E., Besmer, D.M., Shah, N.R., Murphy, A.M., Moerdyk-Schauwecker, M., Molestina, C., Roy, L.D., Curry, J.M., Mukherjee, P., Grdzelishvili, V.Z., 2013a. Oncolytic Vesicular Stomatitis Virus in an Immunocompetent Model of MUC1-Positive or MUC1-Null Pancreatic Ductal Adenocarcinoma. J Virol 87, 10283-10294.

Hastie, E., Cataldi, M., Marriott, I., Grdzelishvili, V.Z., 2013b. Understanding and altering cell tropism of vesicular stomatitis virus. Virus research 176, 16-32.

Hastie, E., Cataldi, M., Moerdyk-Schauwecker, M.J., Felt, S.A., Steuerwald, N., Grdzelishvili, V.Z., 2016. Novel biomarkers of resistance of pancreatic cancer cells to oncolytic vesicular stomatitis virus. Oncotarget 7, 61601-61618.

Hastie, E., Cataldi, M., Steuerwald, N., Grdzelishvili, V.Z., 2015. An unexpected inhibition of antiviral signaling by virus-encoded tumor suppressor p53 in pancreatic cancer cells. Virology 483, 126-140.

Hastie, E., Grdzelishvili, V.Z., 2012. Vesicular stomatitis virus as a flexible platform for oncolytic virotherapy against cancer. J Gen Virol 93, 2529-2545.

Hinz, S., Trauzold, A., Boenicke, L., Sandberg, C., Beckmann, S., Bayer, E., Walczak, H., Kalthoff, H., Ungefroren, H., 2000. Bcl-XL protects pancreatic adenocarcinoma cells against CD95- and TRAIL-receptor-mediated apoptosis. Oncogene 19, 5477-5486.

Hobbs, J.A., Hommel-Berrey, G., Brahmi, Z., 2003. Requirement of caspase-3 for efficient apoptosis induction and caspase-7 activation but not viral replication or cell rounding in cells infected with vesicular stomatitis virus. Hum Immunol 64, 82-92.

Hobbs, J.A., Schloemer, R.H., Hommel-Berrey, G., Brahmi, Z., 2001. Caspase-3-like proteases are activated by infection but are not required for replication of vesicular stomatitis virus. Virus research 80, 53-65.

Hofer, F., Gruenberger, M., Kowalski, H., Machat, H., Huettinger, M., Kuechler, E., Blaas, D., 1994. Members of the low density lipoprotein receptor family mediate cell entry of a minor-group common cold virus. Proceedings of the National Academy of Sciences of the United States of America 91, 1839-1842.

Iwamura T, Katsuki T, K., I., 1987. Establishment and characterization of a human pancreatic cancer cell line (SUIT-2) producing carcinoembryonic antigen and carbohydrate antigen 19-9. Jpn J Cancer Res. 78, 54-62.

Jianrong Li and Yu Zhang (2012). Messenger RNA Cap Methylation in Vesicular Stomatitis Virus, a Prototype of Non‐Segmented Negative‐Sense RNA Virus, Methylation - From DNA, RNA and Histones to Diseases and Treatment, Prof. Anica Dricu (Ed.), InTech, DOI: 10.5772/54598. Available from: https://www.intechopen.com/books/methylation-from-dna-rna-and-histones-to-diseases-

and-treatment/messenger-rna-cap-methylation-in-vesicular-stomatitis-virus-a-prototype-of-non-segmented-negative-se

Johnson JE, Nasar F, Coleman JW, Price RE, Javadian A, Draper K, Lee M, Reilly PA, Clarke DK, Hendry RM, Udem, S.A., 2007. Neurovirulence properties of recombinant vesicular stomatitis virus vectors in non-human primates. Virology 360, 36-49.

Kalra, A.V., Campbell, R.B., 2007. Mucin impedes cytotoxic effect of 5-FU against growth of human pancreatic cancer cells: overcoming cellular barriers for therapeutic gain. Br J Cancer 97, 910-918.

Kalra, A.V., Campbell, R.B., 2009. Mucin overexpression limits the effectiveness of 5-FU by reducing intracellular drug uptake and antineoplastic drug effects in pancreatic tumours. Eur J Cancer 45, 164-173.

Kamisawa, T., Wood, L.D., Itoi, T., Takaori, K., 2016. Pancreatic cancer. Lancet.

Kaplan, J.M., Pennington, S.E., St George, J.A., Woodworth, L.A., Fasbender, A., Marshall, J., Cheng, S.H., Wadsworth, S.C., Gregory, R.J., Smith, A.E., 1998. Potentiation of gene transfer to the mouse lung by complexes of adenovirus vector and polycations improves therapeutic potential. Hum Gene Ther 9, 1469-1479.

Kelly, E., Russell, S.J., 2007. History of oncolytic viruses: genesis to genetic engineering. Molecular therapy : the journal of the American Society of Gene Therapy 15, 651-659.

Kelly, G.L., Strasser, A., 2011. The essential role of evasion from cell death in cancer. Adv Cancer Res 111, 39-96.

Kingsley, D.M., Kozarsky, K.F., Hobbie, L., Krieger, M., 1986. Reversible defects in O-linked glycosylation and LDL receptor expression in a UDP-Gal/UDP-GalNAc 4-epimerase deficient mutant. Cell 44, 749-759.

Kniss, D.A., Summerfield, T.L., 2014. Discovery of HeLa Cell Contamination in HES Cells: Call for Cell Line Authentication in Reproductive Biology Research. Reprod Sci 21, 1015-1019.

Kopecky, S.A., Lyles, D.S., 2003. Contrasting effects of matrix protein on apoptosis in HeLa and BHK cells infected with vesicular stomatitis virus are due to inhibition of host gene expression. J Virol 77, 4658-4669.

Kopecky, S.A., Willingham, M.C., Lyles, D.S., 2001. Matrix protein and another viral component contribute to induction of apoptosis in cells infected with vesicular stomatitis virus. J Virol 75, 12169-12181.

Koyama, A.H., 1995. Induction of apoptotic DNA fragmentation by the infection of vesicular stomatitis virus. Virus research 37, 285-290.

Kozarsky, K., Kingsley, D., Krieger, M., 1988. Use of a mutant cell line to study the kinetics and function of O-linked glycosylation of low density lipoprotein receptors. Proceedings of the National Academy of Sciences of the United States of America 85, 4335-4339.

Kushwah, R., Oliver, J.R., Cao, H., Hu, J., 2007. Nacystelyn enhances adenoviral vector-mediated gene delivery to mouse airways. Gene therapy 14, 1243-1248.

Lawson, N.D., Stillman, E.A., Whitt, M.A., Rose, J.K., 1995. Recombinant vesicular stomatitis viruses from DNA. Proc Natl Acad Sci USA 92, 4477-4481.

Li, Q., Wei, Y.Q., Wen, Y.J., Zhao, X., Tian, L., Yang, L., Mao, Y.Q., Kan, B., Wu, Y., Ding, Z.Y., Deng, H.X., Li, J., Luo, Y., Li, H.L., He, Q.M., Su, J.M., Xiao, F., Zou, C.H., Fu, C.H., Xie, X.J., Yi, T., Tan, G.H., Wang, L., Chen, J., Liu, J., Gao, Z.N., 2004. Induction of apoptosis and tumor regression by vesicular stomatitis virus in the presence of gemcitabine in lung cancer. Int J Cancer 112, 143-149.

Li, Y., Li, S., Duan, X., Liu, B., Yang, C., Zeng, P., McGilvray, I., Chen, L., 2014. Activation of endogenous type I IFN signaling contributes to persistent HCV infection. Reviews in medical virology.

Lichty BD, Power AT, Stojdl DF, and Bell, J.C., 2004. Vesicular stomatitis virus: re-inventing the bullet. Trends in molecular medicine 10, 210-216.

Lin, P., Correa, D., Lin, Y., Caplan, A.I., 2011. Polybrene inhibits human mesenchymal stem cell proliferation during lentiviral transduction. Plos One 6, e23891.

Liu, J., Uematsu, H., Tsuchida, N., Ikeda, M.A., 2011. Essential role of caspase-8 in p53/p73-dependent apoptosis induced by etoposide in head and neck carcinoma cells. Mol Cancer 10, 95.

Liu TC, Galanis E, and Kirn, D., 2007. Clinical trial results with oncolytic virotherapy: a century of promise, a decade of progress. Nature Clinical Practice: Oncology 4, 101-117.

Liu, T.C., Kirn, D., 2005. Viruses with deletions in antiapoptotic genes as potential oncolytic agents. Oncogene 24, 6069-6079.

Lowery, M.A., O'Reilly, E.M., 2015. Novel Therapeutics for Pancreatic Adenocarcinoma. Hematology/oncology clinics of North America 29, 777-787.

Lyles DS, R., CE, 2007. Rhabdoviridae, in: In: DM Knipe and PM Howley, e. (Ed.), Fields Virology. Lippincott Williams & Wilkins, Philadelphia, 5th edition., pp. 1363-1408.

Marais, A.D., 2004. Familial hypercholesterolaemia. Clin Biochem Rev 25, 49-68.

Marlovits, T.C., Abrahamsberg, C., Blaas, D., 1998. Very-low-density lipoprotein receptor fragment shed from HeLa cells inhibits human rhinovirus infection. J Virol 72, 10246-10250.

Matlin, K.S., Reggio, H., Helenius, A., Simons, K., 1982. Pathway of vesicular stomatitis virus entry leading to infection. J Mol Biol 156, 609-631.

Maxwell, K.N., Fisher, E.A., Breslow, J.L., 2005. Overexpression of PCSK9 accelerates the degradation of the LDLR in a post-endoplasmic reticulum compartment. Proceedings of the National Academy of Sciences of the United States of America 102, 2069-2074.

McKay, T.R., MacVinish, L.J., Carpenter, B., Themis, M., Jezzard, S., Goldin, R., Pavirani, A., Hickman, M.E., Cuthbert, A.W., Coutelle, C., 2000. Selective in vivo transfection of murine biliary epithelia using polycation-enhanced adenovirus. Gene therapy 7, 644-652.

McNutt, M.C., Kwon, H.J., Chen, C., Chen, J.R., Horton, J.D., Lagace, T.A., 2009. Antagonism of secreted PCSK9 increases low density lipoprotein receptor expression in HepG2 cells. The Journal of biological chemistry 284, 10561-10570.

Moerdyk-Schauwecker, M., Hwang, S.I., Grdzelishvili, V.Z., 2014. Cellular proteins associated with the interior and exterior of vesicular stomatitis virus virions. Plos One 9, e104688.

Moerdyk-Schauwecker, M., Shah, N.R., Murphy, A.M., Hastie, E., Mukherjee, P., Grdzelishvili, V.Z., 2013. Resistance of pancreatic cancer cells to oncolytic vesicular stomatitis virus: role of type I interferon signaling. Virology 436, 221-234.

Monnery, B.D., Wright, M., Cavill, R., Hoogenboom, R., Shaunak, S., Steinke, J.H., Thanou, M., 2017. Cytotoxicity of polycations: Relationship of molecular weight and the hydrolytic theory of the mechanism of toxicity. Int J Pharm 521, 249-258.

Moyer, S.A., Baker, S.C., Lessard, J.L., 1986. Tubulin: a factor necessary for the synthesis of both Sendai virus and vesicular stomatitis virus RNAs. Proc Natl Acad Sci USA 83, 5405-5409.

Murphy, A.M., Besmer, D.M., Moerdyk-Schauwecker, M., Moestl, N., Ornelles, D.A., Mukherjee, P., Grdzelishvili, V.Z., 2012. Vesicular stomatitis virus as an oncolytic agent against pancreatic ductal adenocarcinoma. J Virol 86, 3073-3087.

Naik, S., Russell, S.J., 2009. Engineering oncolytic viruses to exploit tumor specific defects in innate immune signaling pathways. Expert Opin Biol Ther 9, 1163-1176.

Neesse, A., Gress, T.M., Michl, P., 2012. Therapeutic targeting of apoptotic pathways: novel aspects in pancreatic cancer. Curr Pharm Biotechnol 13, 2273-2282.

Nguyen, A.T., Hirama, T., Chauhan, V., Mackenzie, R., Milne, R., 2006. Binding characteristics of a panel of monoclonal antibodies against the ligand binding domain of the human LDLr. J Lipid Res 47, 1399-1405.

Nguyên TL, A.H., Arguello M, Breitbach C, Leveille S, Diallo JS, Yasmeen A, Bismar TA, Kirn D, Falls T, Snoulten VE, Vanderhyden BC, Werier J, Atkins H, Vähä-Koskela MJ, Stojdl DF, Bell JC, Hiscott J., 2008. Chemical targeting of the innate antiviral response by histone deacetylase inhibitors renders refractory cancers sensitive to viral oncolysis. Proceedings of the National Academy of Sciences 105, 14981-14986.

O'Brien, V., 1998. Viruses and apoptosis. J Gen Virol 79 ( Pt 8), 1833-1845.

Orloff, M., 2016. Spotlight on talimogene laherparepvec for the treatment of melanoma lesions in the skin and lymph nodes. Oncolytic Virother 5, 91-98.

Pahan, K., 2006. Lipid-lowering drugs. Cell Mol Life Sci 63, 1165-1178.

Park, T.G., Jeong, J.H., Kim, S.W., 2006. Current status of polymeric gene delivery systems. Adv Drug Deliv Rev 58, 467-486.

Pearson, A.S., Koch, P.E., Atkinson, N., Xiong, M., Finberg, R.W., Roth, J.A., Fang, B., 1999. Factors limiting adenovirus-mediated gene transfer into human lung and pancreatic cancer cell lines. Clinical cancer research : an official journal of the American Association for Cancer Research 5, 4208-4213.

Petersen, J.M., Her, L.S., Varvel, V., Lund, E., Dahlberg, J.E., 2000. The matrix protein of vesicular stomatitis virus inhibits nucleocytoplasmic transport when it is in the nucleus and associated with nuclear pore complexes. Molecular and cellular biology 20, 8590-8601.

Podolin, P.L., Callahan, J.F., Bolognese, B.J., Li, Y.H., Carlson, K., Davis, T.G., Mellor, G.W., Evans, C., Roshak, A.K., 2005. Attenuation of murine collagen-induced arthritis by a novel, potent, selective small molecule inhibitor of IkappaB Kinase 2, TPCA-1 (2-[(aminocarbonyl)amino]-5-(4-fluorophenyl)-3-thiophenecarboxamide), occurs via reduction of proinflammatory cytokines and antigen-induced T cell Proliferation. J Pharmacol Exp Ther 312, 373-381.

Prusty, B.K., Siegl, C., Gulve, N., Mori, Y., Rudel, T., 2014. GP96 interacts with HHV-6 during viral entry and directs it for cellular degradation. Plos One 9, e113962.

Quiroz E, Moreno N, Peralta PH, and Tesh, R.B., 1988. A human case of encephalitis associated with vesicular stomatitis virus (Indiana serotype) infection. Am J Trop Med Hyg 39, 312-314.

Rahib, L., Smith, B.D., Aizenberg, R., Rosenzweig, A.B., Fleshman, J.M., Matrisian, L.M., 2014. Projecting cancer incidence and deaths to 2030: the unexpected burden of thyroid, liver, and pancreas cancers in the United States. Cancer research 74, 2913-2921.

Ramsburg, E., Publicover, J., Buonocore, L., Poholek, A., Robek, M., Palin, A., Rose, J.K., 2005. A vesicular stomatitis virus recombinant expressing granulocyte-macrophage colony-stimulating factor induces enhanced T-cell responses and is highly attenuated for replication in animals. J Virol 79, 15043-15053.

Rehman, H., Silk, A.W., Kane, M.P., Kaufman, H.L., 2016. Into the clinic: Talimogene laherparepvec (T-VEC), a first-in-class intratumoral oncolytic viral therapy. J Immunother Cancer 4, 53.

Reiser, J., Harmison, G., Kluepfel-Stahl, S., Brady, R.O., Karlsson, S., Schubert, M., 1996. Transduction of nondividing cells using pseudotyped defective high-titer HIV type 1 particles. Proceedings of the National Academy of Sciences of the United States of America 93, 15266-15271.

Roder, C., Trauzold, A., Kalthoff, H., 2011. Impact of death receptor signaling on the malignancy of pancreatic ductal adenocarcinoma. Eur J Cell Biol 90, 450-455.

Russell, D.W., Yamamoto, T., Schneider, W.J., Slaughter, C.J., Brown, M.S., Goldstein, J.L., 1983. cDNA cloning of the bovine low density lipoprotein receptor: feedback regulation of a receptor mRNA. Proceedings of the National Academy of Sciences of the United States of America 80, 7501-7505.

Russell, S.J., Peng, K.W., Bell, J.C., 2012. Oncolytic virotherapy. Nat Biotechnol 30, 658-670.

Santos, R.D., Watts, G.F., 2015. Familial hypercholesterolaemia: PCSK9 inhibitors are coming. Lancet 385, 307-310.

Scaffidi, C., Fulda, S., Srinivasan, A., Friesen, C., Li, F., Tomaselli, K.J., Debatin, K.M., Krammer, P.H., Peter, M.E., 1998. Two CD95 (APO-1/Fas) signaling pathways. The EMBO journal 17, 1675-1687.

Schache, P., Gurlevik, E., Struver, N., Woller, N., Malek, N., Zender, L., Manns, M., Wirth, T., Kuhnel, F., Kubicka, S., 2009. VSV virotherapy improves chemotherapy by triggering apoptosis due to proteasomal degradation of Mcl-1. Gene therapy 16, 849-861.

Schlegel, R., Tralka, T.S., Willingham, M.C., Pastan, I., 1983. Inhibition of VSV binding and infectivity by phosphatidylserine: is phosphatidylserine a VSV-binding site? Cell 32, 639-646.

Schloemer, R.H., Wagner, R.R., 1975. Cellular adsorption function of the sialoglycoprotein of vesicular stomatitis virus and its neuraminic acid. J Virol 15, 882-893.

Seitz, B., Baktanian, E., Gordon, E.M., Anderson, W.F., LaBree, L., McDonnell, P.J., 1998. Retroviral vector-mediated gene transfer into keratocytes: in vitro effects of polybrene and protamine sulfate. Graefes Arch Clin Exp Ophthalmol 236, 602-612.

Sharif-Askari, E., Nakhaei, P., Oliere, S., Tumilasci, V., Hernandez, E., Wilkinson, P., Lin, R., Bell, J., Hiscott, J., 2007. Bax-dependent mitochondrial membrane permeabilization enhances IRF3-mediated innate immune response during VSV infection. Virology 365, 20-33.

Shestakova, E., Bandu, M.T., Doly, J., Bonnefoy, E., 2001. Inhibition of histone deacetylation induces constitutive derepression of the beta interferon promoter and confers antiviral activity. J Virol 75, 3444-3452.

Shulak, L., Beljanski, V., Chiang, C., Dutta, S.M., Van Grevenynghe, J., Belgnaoui, S.M., Nguyen, T.L., Di Lenardo, T., Semmes, O.J., Lin, R., Hiscott, J., 2014. Histone deacetylase inhibitors potentiate vesicular stomatitis virus oncolysis in prostate cancer cells by modulating NF-kappaB-dependent autophagy. J Virol 88, 2927-2940.

Simmons, C.F., Jr., Rennke, H.G., Humes, H.D., 1981. Acute renal failure induced by diethylaminoethyl dextran: importance of cationic charge. Kidney Int 19, 424-430.

Stathis A, Moore, M.J., 2010. Advanced pancreatic carcinoma: current treatment and future challenges. Nat Rev Clin Oncol 7, 163-172.

Stojdl DF, Lichty BD, tenOever BR, Paterson JM, Power AT, Knowles S, Marius R, Reynard J, Poliquin L, Atkins H, Brown EG, Durbin RK, Durbin JE, Hiscott J, JC, B., 2003. VSV strains with defects in their ability to shutdown innate immunity are potent systemic anti-cancer agents. Cancer cell 4, 263-275.

Stojdl, D.F., Lichty, B.D., Knowles, S., Marius, R., Atkins, H., Sonenberg, N., Bell, J.C., 2000. Exploiting tumor-specific defects in the interferon pathway with a previously unknown oncolytic virus. Nat Med 6, 821-825.

Tiera, M.J., Shi, Q., Winnik, F.M., Fernandes, J.C., 2011. Polycation-based gene therapy: current knowledge and new perspectives. Curr Gene Ther 11, 288-306.

Timm, A., Yin, J., 2012. Kinetics of virus production from single cells. Virology 424, 11-17.

Tolleshaug, H., Goldstein, J.L., Schneider, W.J., Brown, M.S., 1982. Posttranslational processing of the LDL receptor and its genetic disruption in familial hypercholesterolemia. Cell 30, 715-724.

Tolleshaug, H., Hobgood, K.K., Brown, M.S., Goldstein, J.L., 1983. The LDL receptor locus in familial hypercholesterolemia: multiple mutations disrupt transport and processing of a membrane receptor. Cell 32, 941-951.

Turnbull, S., West, E.J., Scott, K.J., Appleton, E., Melcher, A., Ralph, C., 2015. Evidence for Oncolytic Virotherapy: Where Have We Got to and Where Are We Going? Viruses 7, 6291-6312.

Tveten, K., Ranheim, T., Berge, K.E., Leren, T.P., Kulseth, M.A., 2006. Analysis of alternatively spliced isoforms of human LDL receptor mRNA. Clin Chim Acta 373, 151-157.

Vaddi, K., Sarlis, N.J., Gupta, V., 2012. Ruxolitinib, an oral JAK1 and JAK2 inhibitor, in myelofibrosis. Expert Opin Pharmacother 13, 2397-2407.

van Driel, I.R., Goldstein, J.L., Sudhof, T.C., Brown, M.S., 1987. First cysteine-rich repeat in ligand-binding domain of low density lipoprotein receptor binds Ca2+ and monoclonal antibodies, but not lipoproteins. The Journal of biological chemistry 262, 17443-17449.

Vaziri, N.D., Liang, K., 2004. Effects of HMG-CoA reductase inhibition on hepatic expression of key cholesterol-regulatory enzymes and receptors in nephrotic syndrome. Am J Nephrol 24, 606-613.

Verma, I.M., Weitzman, M.D., 2005. Gene therapy: twenty-first century medicine. Annu Rev Biochem 74, 711-738.

von Messling V, Cattaneo, R., 2004. Toward novel vaccines and therapies based on negative-strand RNA viruses. Current Topics in Microbiology and Immunology 283.

Wang, B.X., Rahbar, R., Fish, E.N., 2011. Interferon: current status and future prospects in cancer therapy. J Interferon Cytokine Res 31, 545-552.

Weekes, M.P., Antrobus, R., Talbot, S., Hor, S., Simecek, N., Smith, D.L., Bloor, S., Randow, F., Lehner, P.J., 2012. Proteomic plasma membrane profiling reveals an essential role for gp96 in the cell surface expression of LDLR family members, including the LDL receptor and LRP6. J Proteome Res 11, 1475-1484.

Wennier, S., Li, S., McFadden, G., 2011. Oncolytic virotherapy for pancreatic cancer. Expert Rev Mol Med 13, e18.

Westphal, S., Kalthoff, H., 2003. Apoptosis: targets in pancreatic cancer. Mol Cancer 2, 6.

Wilson, E.B., Yamada, D.H., Elsaesser, H., Herskovitz, J., Deng, J., Cheng, G., Aronow, B.J., Karp, C.L., Brooks, D.G., 2013. Blockade of chronic type I interferon signaling to control persistent LCMV infection. Science 340, 202-207.

Wollmann G, Rogulin V, Simon I, Rose JK, AN, v.d.P., 2010. Some attenuated variants of vesicular stomatitis virus show enhanced oncolytic activity against human glioblastoma cells relative to normal brain cells. J Virol 84, 1563-1573.

Wong, R.S., 2011. Apoptosis in cancer: from pathogenesis to treatment. J Exp Clin Cancer Res 30, 87.

Wu, M., Dong, B., Cao, A., Li, H., Liu, J., 2012. Delineation of molecular pathways that regulate hepatic PCSK9 and LDL receptor expression during fasting in normolipidemic hamsters. Atherosclerosis 224, 401-410.

Ye, Q., Lei, H., Fan, Z., Zheng, W., Zheng, S., 2014. Difference in LDL receptor feedback regulation in macrophages and vascular smooth muscle cells: foam cell transformation under inflammatory stress. Inflammation 37, 555-565.

Yee, J.K., Friedmann, T., Burns, J.C., 1994. Generation of high-titer pseudotyped retroviral vectors with very broad host range. Methods Cell Biol 43 Pt A, 99-112.

Yoshimura, A., Yoshida, T., Seguchi, T., Waki, M., Ono, M., Kuwano, M., 1987. Low binding capacity and altered O-linked glycosylation of low density lipoprotein receptor in a monensin-resistant mutant of Chinese hamster ovary cells. The Journal of biological chemistry 262, 13299-13308.

Zarogoulidis, P., Hohenforst-Schmidt, W., Darwiche, K., Krauss, L., Sparopoulou, D., Sakkas, L., Gschwendtner, A., Huang, H., Turner, F.J., Freitag, L., Zarogoulidis, K., 2013. 2-diethylaminoethyl-dextran methyl methacrylate copolymer nonviral vector: still a long way toward the safety of aerosol gene therapy. Gene therapy 20, 1022-1028.